

AN ABSTRACT OF THE THESIS OF

Christopher K. H. Guay for the degree of Master of Science in Oceanography presented on February 13, 1997. Title: Barium as a Tracer of Arctic Halocline and River Waters.

Redacted for Privacy

Abstract approved: _____

Kelly Kenison Falkner

Dissolved Ba concentrations were determined for water samples obtained from major Arctic river estuaries and adjacent regions of Arctic seas between 1993 and 1996. Complex behavior was observed in the mixing zones between fluvial and oceanic waters, where riverine Ba signals were altered by mixing with different shelf water masses and by non-conservative processes such as biological uptake and desorption from suspended riverine particles. Despite this complexity, Ba concentrations observed in the Mackenzie River ($138\text{--}574\text{ nmol Ba L}^{-1}$) were clearly much higher than those observed in the Eurasian Arctic rivers ($12\text{--}175\text{ nmol Ba L}^{-1}$); while the Ba signatures of Arctic rivers are subject to temporal and seasonal variability, such variability is much smaller than the overall difference between Ba concentrations in the Mackenzie and Eurasian Arctic rivers. These results suggest that Ba can be used to distinguish between North American and Eurasian sources of fluvial discharge to the Arctic and thus provide information not available from other tracers of oceanic circulation in the Arctic.

Barium concentrations were determined for water samples collected during six oceanographic cruises to the Arctic in 1993 and during the 1994 Arctic Ocean Section. Upper Arctic ($< 200\text{ m}$) values ranged widely ($19\text{ to }168\text{ nmol Ba L}^{-1}$) in a manner geographically consistent with identified sources and sinks. The highest values ($\geq 75\text{ nmol Ba L}^{-1}$) observed in the surface mixed layer of the Arctic interior (i.e., beyond the 200 m

isobath) occurred in the Canada Basin. The biological removal of Ba from surface waters of the Chukchi Sea and the tendency of Bering inflow to enter the Arctic interior at depths below the relatively fresher mixed layer suggest that the Mackenzie River is the dominant source of the high Ba observed in the surface waters of the Canada Basin.

Features characterized by local salinity minima and Ba maxima in surface waters down to depths of 30-50 m were observed over the Arlis Plateau and Mendeleyev Ridge in both 1993 and 1994, and over the Makarov Basin and Lomonosov Ridge in 1994. The physical and chemical properties of these waters suggest that they have been significantly influenced by fluvial discharge. It could not be determined from the available data whether these features arose from offshore transport of Eurasian river discharge from the Laptev and East Siberian seas or from meanders of the Mackenzie River-influenced Beaufort Gyre.

In both 1993 and 1994, Ba concentrations in the upper halocline layer (as defined by a core salinity of 33.1) ranged between 42 and 77 nmol Ba L⁻¹, with highest values observed in the Canada Basin. These results are consistent with the nutrient maxima and oxygen minimum known to be associated with upper halocline waters in the Canada Basin, providing further evidence that they originate over the Chukchi and Beaufort shelves and that their mechanism of formation is linked with the influx of water through Bering Strait. The Ba distributions for 1993 and 1994 delineate the lateral extent of upper halocline waters with Canada Basin character and show them to be chemically distinct from upper halocline waters in the Eurasian Basin. The front separating these water types ran roughly along the Mendeleyev and Alpha ridges, consistent with reports that the boundary between Atlantic and Pacific water mass assemblies in the Arctic has recently been displaced from its historical position over the Lomonosov Ridge. Lateral gradients in both Ba and the NO parameter were observed within the lower halocline layer (defined by an NO minimum and core salinity of 34.2-34.4) along the 1994 Arctic Ocean Section, indicating that lower halocline waters receive additional inputs as they transit to the Canadian Basin from their region of formation in the Eurasian sector of the Arctic.

©Copyright by Christopher K. H. Guay
February 13, 1997
All Rights Reserved

Barium as a Tracer of Arctic Halocline and River Waters

by

Christopher K. H. Guay

A THESIS

submitted to

Oregon State University

in partial fulfillment of
the requirements for the
degree of

Master of Science

Presented February 13, 1997

Commencement June 1997

Master of Science thesis of Christopher K. H. Guay presented on February 13, 1997

APPROVED:

Redacted for Privacy

Major Professor, representing Oceanography

Redacted for Privacy

Dean of College of Oceanic and Atmospheric Sciences

Redacted for Privacy

Dean of Graduate School

I understand that my thesis will become a part of the permanent collection of Oregon State University libraries. My signature below authorizes release of my thesis to any reader upon request.

Redacted for Privacy

Christopher K. H. Guay, Author

ACKNOWLEDGEMENTS

I would like to thank my major professor, Kelly Falkner, for providing me with first-rate laboratory facilities, exceptional fieldwork opportunities, sound advice and enthusiastic support during this very rigorous and exciting program of research. Thanks also to members of my thesis committee, Bob Collier, Robin Muench, Clayton Paulson and Jeff Ramsey, for contributing valuable insight and suggestions throughout the course of this work.

The following people collected water samples for this research during oceanographic cruises to the Arctic in 1993 and 1994. SCICEX-93: Jamie Morison, Ted DeLaca, personnel from the Arctic Submarine Laboratory, and other members of the scientific party and crew of the *USS Pargo*; HX171: Jackie Grebmeier and other members of the scientific party and crew of the *R/V Alpha Helix*; HX174: Tom Weingartner and other members of the scientific party and crew of the *R/V Alpha Helix*; ARK IX/4: Robin Muench, Ursula Schauer, Marcus Frank, and other members of the scientific party and crew of the *R/V Polarstern*; ARCRAD-93: Lee Cooper and other members of the scientific party and crew of the *USCGC Polar Star*; Larsen-93: Eddy Carmack, Robbie Macdonald, Fiona McLaughlin, and other members of the scientific party and crew of the *CCGS Henry Larsen*; AOS 94: Knut Aagaard, Chris Measures, Jim Swift, Eddy Carmack, and other members of the scientific party and crew of the *CCGS Louis S. St-Laurent*. This work truly would not have been possible without all of their generous cooperation.

Jay Simpkins (OSU), Darren Tuele and Humfrey Melling (IOS, Sydney, B.C.), and Jimmy Jacobsen and the personnel of the Polar Continental Shelf Project in Tuktoyuktuk, N.W.T. contributed stalwart efforts during the 1994 Canada expedition. Dan Adkison, Jim Brooks, Bill Bryant, Tamara Davis, Alexey Ivanov, Paul Stine and others from Texas A&M/GERG allowed me to participate in the fieldwork they organized and implemented in Russia in 1994 and 1995. The captains and crews of the vessels *R/V Yakov Smirnitsky*, *R/V Valerian Al'banov* and *I/B Taymyr* displayed expert seamanship, tenacity and courage

while performing their duties under challenging Arctic conditions, and the generosity and camaraderie they extended towards me will always be remembered; Les Kutny (Aurora College, Inuvik, N.W.T.), Clément Gariépy (UQAM, Montréal, Québec) and Doug Chipertzak (FAO, Inuvik, N.W.T.) collected samples for this research from the Mackenzie River in 1996. I would especially like to acknowledge the late Gera Panteleyev, who obtained samples for this research from the Ob and Yenisey Rivers in 1993. Gera was lost at sea in the Arctic in 1995.

Assistance with sample analyses at the OSU ICPMS facility was provided by Adrian Avram, Pat Collier, Sandy Moore, Andy Ungerer and Tim Wagner. Robin Muench (ESR, Seattle, WA) provided CTD data from the 1993 cruise of the *R/V Dmitry Mendeleev* in the Kara Sea. Invaluable cooperation also came from Russian colleagues at the Research Institute for Nature Conservation of the Arctic and the North, the Arctic and Antarctic Research Institute, the VNIIOkeangeologiya Institute, and the VICAAR agency in St. Petersburg, and at the hydrobase in Arkhangelsk. Thanks to Laurie Padman, Pat Wheeler, Tim Boyd, Carolyn Viscosi-Shirley and others in the OSU Arctic seminar group, Gary Klinkhammer, Jack Dymond, Jim McManus, Peter Jones and two anonymous reviewers, whose comments led to significant improvement of this thesis. This research was supported by ONR Young Investigator Program Grant N00014-9310318 and ONR AASERT Grant N00014-9311093.

TABLE OF CONTENTS

	<u>Page</u>
1. INTRODUCTION	1
2. BACKGROUND	5
2.1 Arctic rivers and their drainage basins	5
2.1.1 Mackenzie River	9
2.1.2 Eurasian Arctic rivers	11
2.2 Freshwater budget of the Arctic Ocean	17
2.3 Physical and chemical tracers of Arctic circulation	19
2.4 Marine geochemical behavior of barium	23
3. SURVEY OF BARIUM IN ESTUARIES OF MAJOR ARCTIC RIVERS	25
3.1 Experimental design	28
3.1.1 Sample collection	28
3.1.2 Analytical procedure	31
3.2 Results	32
3.2.1 Mixing in Arctic river estuaries and adjacent shelf regions	32
3.2.2 Behavior of Ba in mixing zones	35
3.3 Discussion	45
3.3.1 Elevated Ba in Mackenzie River relative to Eurasian rivers	45
3.3.2 Interannual and seasonal variability in riverine Ba signals	47
4. BARIUM DISTRIBUTIONS IN THE SURFACE MIXED LAYER AND HALOCLINE OF THE ARCTIC OCEAN	49
4.1 Field program	49
4.2 Results	49
4.2.1 Surface mixed layer in 1993	49
4.2.2 Upper halocline in 1993	57
4.2.3 1994 Arctic Ocean Section	60

TABLE OF CONTENTS (Continued)

	<u>Page</u>
4.3 Discussion	64
4.3.1 Surface mixed layer	65
4.3.2 Upper halocline layer	72
4.3.3 Lower halocline layer	73
5. CONCLUSIONS	75
BIBLIOGRAPHY	76

LIST OF FIGURES

<u>Figure</u>	<u>Page</u>
1. Bathymetry and major rivers of the Arctic	2
2. Mean annual discharge ($\text{km}^3 \text{ yr}^{-1}$) of the ten largest rivers flowing directly into the Arctic Ocean (values taken from Treshnikov, 1985)	6
3. Mean monthly discharge of the four largest Arctic rivers: (a) Yenisey River, (b) Ob River, (c) Lena River, and (d) Mackenzie River	7
4. Drainage basin of the Mackenzie River	10
5. Drainage basins of rivers flowing into the White, Barents and Kara seas	12
6. Drainage basins of rivers flowing into the Laptev and East Siberian seas	15
7. Locations of samples obtained in 1993-1995 from the estuaries of major Eurasian Arctic rivers and adjacent shelf areas (Barents and Kara seas)	26
8. Locations of samples obtained in 1995 from the estuaries of major Eurasian Arctic rivers and adjacent shelf areas (Laptev and East Siberian seas)	28
9. Locations of samples obtained in 1994 and 1996 from the estuaries of the Mackenzie River	30
10. T-S plots of CTD data collected in (a) the Barents Sea in 1994-1995, (b) the Kara Sea in 1994-1995, (c) the Laptev Sea in 1995, and (d) the East Siberian Sea in 1995	33
11. Dissolved Ba in the estuary of the Mackenzie River in 1994 and 1996	35
12. Dissolved Ba in the estuary of the Pechora River in 1994 and 1995	37
13. Dissolved Ba in the estuary of the Ob River in (a) 1993, (b) 1994, and (c) 1995	38
14. Dissolved Ba in the estuary of the Yenisey River in (a) 1993, (b) 1994, and (c) 1995	39
15. Dissolved Ba in the estuary of the Pyasina River in 1994 and 1995	41
16. Dissolved Ba in the estuary of the Lena River 1995	41
17. Dissolved Ba in the estuaries of the Khatanga and Yana rivers in 1995	43
18. Dissolved Ba in the estuary of the Indigirka River in 1995	43
19. Dissolved Ba in the estuary of the Kolyma River in 1995	44

LIST OF FIGURES (Continued)

<u>Figure</u>	<u>Page</u>
20. Composite plot of dissolved Ba versus salinity for 311 water samples collected between 1993 and 1996 from the estuaries of the ten largest rivers discharging directly into the Arctic Ocean	45
21. Stations occupied during six oceanographic cruises to the Arctic in 1993 and during the 1994 Arctic Ocean Section	50
22. Profiles of salinity, temperature and dissolved Ba at (a) ARCRAD-93 Station 40 north of the Chukchi shelf break in the vicinity of the Chukchi Cap (74.50° N, 166.50° W), occupied on 10 August 1993; (b) HX174 Station 73 between Wrangel Island and the Siberian coast (69.90° N, 177.93°E), occupied on 4 October 1993; and (c) ARK IX/4 Station 51 north of the Laptev shelf break (77.86° N, 125.59° E), occupied on 10 September 1993	53
23. Distribution of salinity in the surface mixed layer in 1993 (the following parameter values were used for the Barnes objective analysis: horizontal and vertical grid spacing (G_x and G_y) = 10 nautical miles, numerical convergence parameter (γ) = 0.2, number of iterations (i) = 2, horizontal data spacing (Δn_x) = 100 nautical miles, vertical data spacing (Δn_y) = 70 nautical miles)	54
24. Distribution of Ba in the surface mixed layer in 1993 (G_x and G_y = 10 nautical miles, γ = 0.2, i = 2, Δn_x = 100 nautical miles, Δn_y = 70 nautical miles). Black dots show the locations of all 1993 stations included in the surface mixed layer Ba data	56
25. Distribution of Ba in the upper halocline (i.e. the layer of water with salinity between 32.5-33.5) in 1993 (G_x and G_y = 10 nautical miles, γ = 0.2, i = 2, Δn_x = 70 nautical miles, Δn_y = 100 nautical miles)	59
26. Distribution of salinity along the 1994 Arctic Ocean Section (G_x = 25 nautical miles, G_y = 5 m, γ = 0.2, i = 2, Δn_x = 25 nautical miles, Δn_y = 10 m)	61
27. Distribution of Ba along the 1994 Arctic Ocean Section (G_x = 25 nautical miles, G_y = 5 m, γ = 0.2, i = 2, Δn_x = 25 nautical miles, Δn_y = 10 m)	62
28. NO versus dissolved Ba for 117 samples taken within the lower halocline (taken to be the layer of water with salinity 34.0-34.5) during the 1994 Arctic Ocean Section	64

LIST OF TABLES

<u>Table</u>	<u>Page</u>
1. Discharge, sediment load, and drainage basin area of the ten largest rivers flowing directly into the Arctic (discharge data from UNESCO (1978); sediment load data from Milliman and Meade (1983) and Milliman and Syvitski (1992))	8
2. Oceanographic cruises to the Arctic in 1993 and 1994. At all of the stations occupied, a CTD profiler was deployed to obtain continuous profiles of salinity and temperature. Samples for Ba analyses were not collected at every station	51
3a. Table 3a: Salinity and Ba concentrations of source waters to the upper Arctic	71
3b. Salinity and Ba concentrations in the surface features observed in 1993 and 1994	71

Dedicated to
my parents, Peter and Rachael
and
my brother, Andy

In inquiries respecting the laws of the world and the frame of things, the highest reason is always truest. That which seems faintly possible--it is so refined, is often faint and dim because it is deepest seated in the mind among the eternal verities. Empirical science is apt to cloud the sight, and, by the very knowledge of functions and processes, to bereave the student of the manly contemplation of the whole. The savant becomes unpoetic. But the best read naturalist who lends an entire and devout attention to truth, will see that there remains much to learn of his relation to the world, and that it is not to be learned by any addition or subtraction of other comparison of known quantities, but is arrived at by untaught sallies of the spirit, by a continual self-recovery, and by entire humility. He will perceive that there are far more excellent qualities in the student than preciseness and infallibility; that a guess is often more fruitful than an indisputable affirmation, and that a dream may let us deeper into the secret of nature than a hundred concerted experiments.

--Ralph Waldo Emerson

O sweet spontaneous
earth how often have
the
doting

fingers of
purient philosophers pinched
and
poked

thee
, has the naughty thumb
of science prodded
thy

beauty . how
often have religions taken
thee upon their scraggy knees
squeezing and

buffeting thee that thou mightest conceive
gods
(but
true

to the incomparable
couch of death thy
rhythmic
lover

thou answerest

them only with

spring)

--E. E. Cummings

Barium as a Tracer of Arctic Halocline and River Waters

1. INTRODUCTION

Roughly ten percent of the world's river water flows into the Arctic Ocean (Figure 1), strongly influencing its circulation and hydrologic structure. The large fluvial discharge, along with ice formation and melting processes, net precipitation over evaporation, and the inflow of relatively fresh seawater through Bering Strait, results in intense, salinity-dominated stratification of the upper (< 200 m) Arctic Ocean. Included in the strongly stratified upper water column is the Arctic halocline (the layer of water between the near-freezing, fresh surface mixed layer and the relatively warm, saline Atlantic layer), which insulates the perennial sea ice cover from the heat contained in the underlying Atlantic water (Aagaard et al. 1981); since the high albedo of the ice cover in the polar regions makes it a strong determinant of the Earth's heat budget, this provides one example of how the Arctic Ocean is linked to global climate. Relatively fresh surface waters exported from the Arctic through Fram Strait, of which fluvial discharge is an important component, affect the stability of the water column in the Greenland, Iceland, Norwegian and Labrador Seas and thus influence the convective deep water formation which drives global thermohaline circulation (Aagaard and Carmack 1989). In addition, recent work has highlighted problems associated with radioactive and industrial pollutants in the Arctic, many of which are dumped in rivers or on shelves that are strongly influenced by river waters (Select Committee on Intelligence 1993; Macdonald and Bowers 1996). Thus the ability to track the riverine waters entering the Arctic is necessary for understanding oceanic circulation in the Arctic and its links to global climate, and for assessing the transport and fate of pollutants released in the Arctic.

Several physical and chemical tracers, including temperature, salinity, alkalinity, ^3He , tritium, halocarbons, SiO_2 , and $\delta^{18}\text{O}$, have been applied to studying oceanic circulation in

the Arctic and have been used to estimate ages, residence times and ventilation rates for its different water masses (Östlund and Hut 1984; Jones et al. 1991; Wallace et al. 1992; Schlosser et al. 1994; Bauch et al. 1995). Such tracers have also been used with simple linear mixing models to distinguish the fluvial component from sea-ice meltwater, Pacific, and Atlantic components of Arctic Ocean waters. None of these tracers, however, can be used to distinguish between waters from different rivers within the Arctic.

The research presented in this thesis is part of a program investigating naturally occurring geochemical tracers that have promise for differentiating components of the total fluvial discharge to the Arctic Ocean. The inorganic composition of Arctic river waters is largely determined by the rock types available to weathering in their drainage basins (Reeder et al. 1972; Gordeev et al. 1995). Individual Arctic rivers have distinct aqueous geochemical signatures (reflecting the unique rock distributions and weathering characteristics of their drainage basins) that in principle can be used to distinguish them from each other. The practical application of such an approach depends on the natural variability of the inorganic signals in Arctic rivers and the extent to which they remain detectable as river waters mix with oceanic waters. The potential of Ba as a tracer of oceanic circulation in the Arctic has been described, along with preliminary findings for Bering Strait, and the eastern Chukchi and southern Beaufort seas (Falkner et al. 1994). Subsequent work has focused on the utility of dissolved Ba for differentiating North American and Eurasian sources of fluvial discharge to the Arctic Ocean.

Background information about Arctic rivers and their drainage basins, tracers of oceanic circulation in the Arctic, and the marine geochemistry of Ba will be given in Chapter 2. Results from a survey of Ba concentrations in major Arctic rivers and their estuaries will be summarized in Chapter 3 (Note: Chapter 3 is part of a manuscript in preparation for submission to *Continental Shelf Research*). In Chapter 4, basin-wide distributions of Ba in the surface mixed layer and halocline of the Arctic Ocean in 1993 and 1994 will be presented, along with a discussion of how these distributions reflect known

sources (especially contributions from different rivers) and sinks of Ba in the Arctic (Note: Chapter 4 is part of a manuscript submitted to the special edition of *Deep Sea Research* devoted to the 1994 Arctic Ocean Section). An assessment of Ba as a tracer of oceanic circulation in the Arctic will be given in Chapter 5.

2. BACKGROUND

2.1 Arctic rivers and their drainage basins

Approximately 10% ($3300 \text{ km}^3 \text{ yr}^{-1}$) of the world's fluvial discharge flows into the Arctic, whose surface area and volume constitute only about 5 and 1.5%, respectively, of the global oceans. A third of this disproportionately large flux is contributed by a combination of the three largest Siberian rivers, the Yenisey ($603 \text{ km}^3 \text{ yr}^{-1}$), Ob ($530 \text{ km}^3 \text{ yr}^{-1}$) and Lena ($520 \text{ km}^3 \text{ yr}^{-1}$), and the largest North American river, the Mackenzie ($340 \text{ km}^3 \text{ yr}^{-1}$). Roughly $590 \text{ km}^3 \text{ yr}^{-1}$ is contributed by the next six largest Arctic rivers, all of which enter from Eurasia (Treshnikov 1985) (Figure 2).

While interannual variability in the discharge of the major Arctic rivers is typically between 5-20% (Carmack 1990), seasonal variability is considerably higher (Figure 3, Table 1). Low flows occur during the winter when freezing occurs in the rivers and their drainage areas, and high flows occur in spring and summer when large amounts of snow and ice melt in the watersheds. In the Yenisey and Lena rivers, the maximum peak flows in June and July are on average about 40 times higher than the minimum monthly flows in winter (Carmack 1990). In the Mackenzie River, the maximum flow in early June is about 6-8 times higher than minimum flows between January and April (Carmack et al. 1989). Three major subarctic lakes (Lake Athabasca, Great Slave Lake, and Great Bear Lake) serve to moderate seasonal fluctuations in flow in the watershed of the Mackenzie River. With the exception of Lake Baikal (the source of the Angara River, a major tributary to the Yenisey River), there are no major natural lakes present in the drainage basins of the large Eurasian Arctic rivers. A number of large artificial reservoirs exist behind dams on major tributaries to the Ob, Yenisey and Lena rivers, but they apparently do not significantly moderate the total discharge of these rivers.

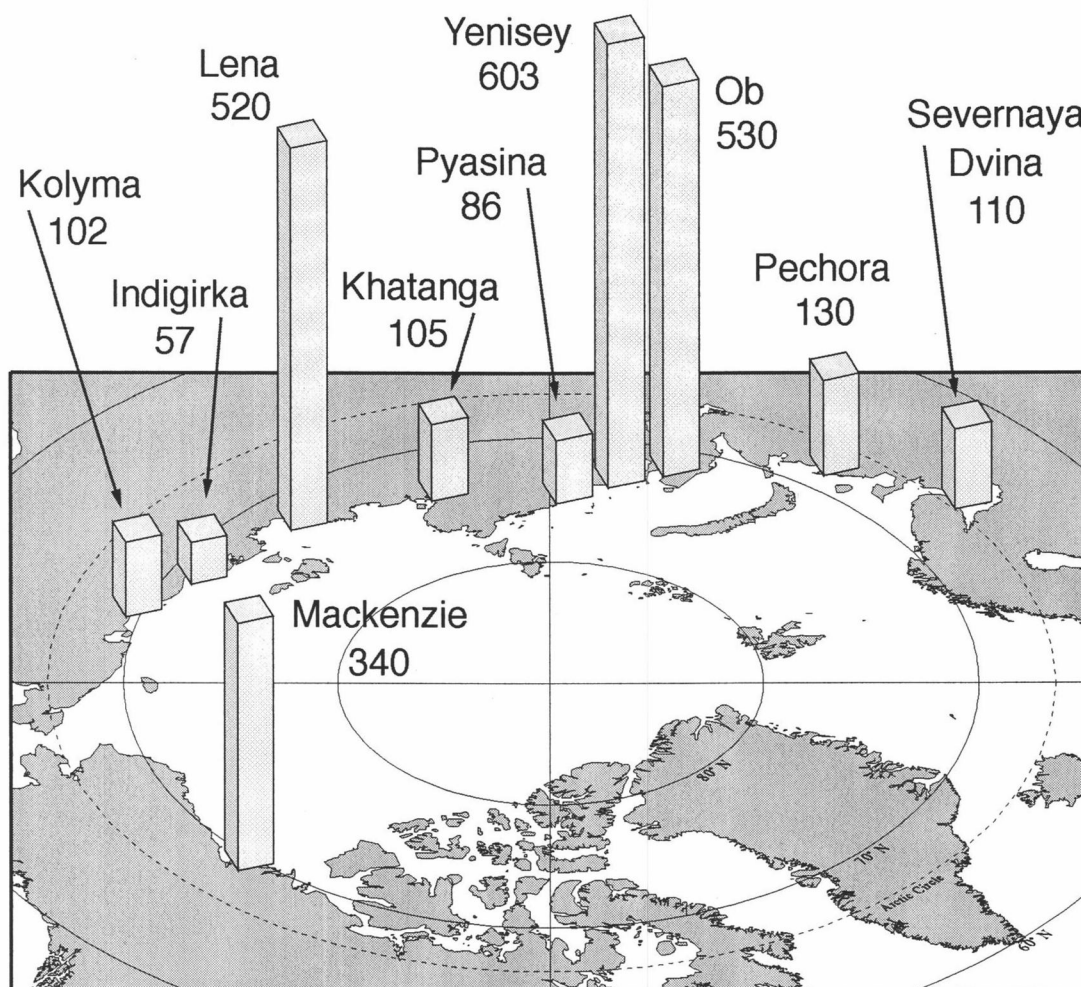
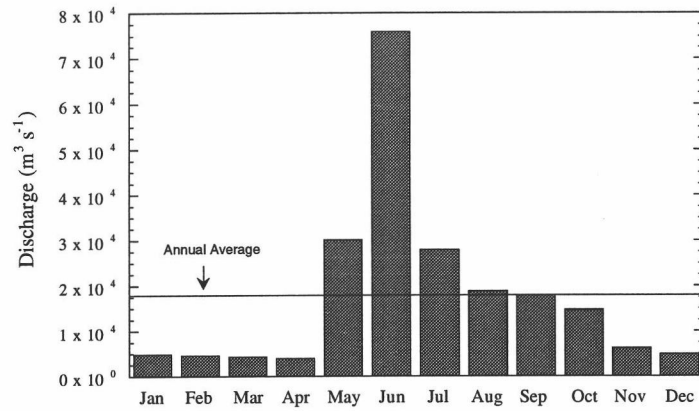
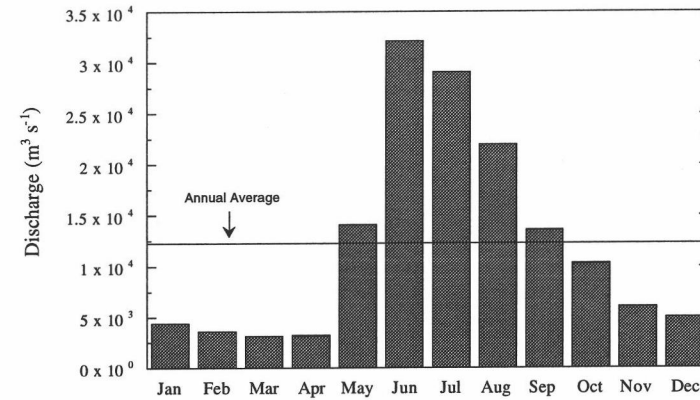


Figure 2: Mean annual discharge ($\text{km}^3 \text{ yr}^{-1}$) of the ten largest rivers flowing directly into the Arctic Ocean (values taken from Treshnikov, 1985).

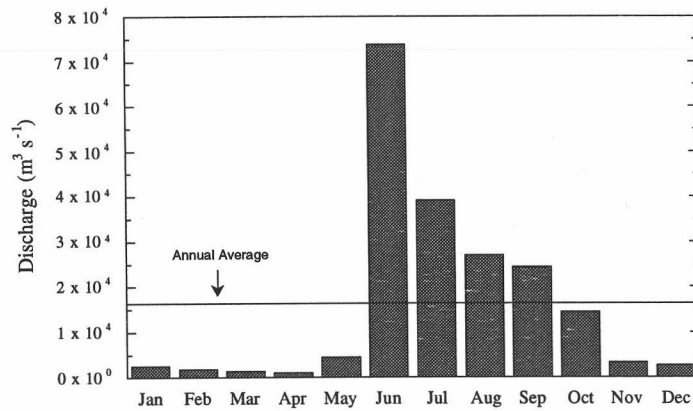
a) Yenisey River (Igarka)



b) Ob River (Salekhard)



c) Lena River (Kysur)



d) Mackenzie River (Arctic Red River)

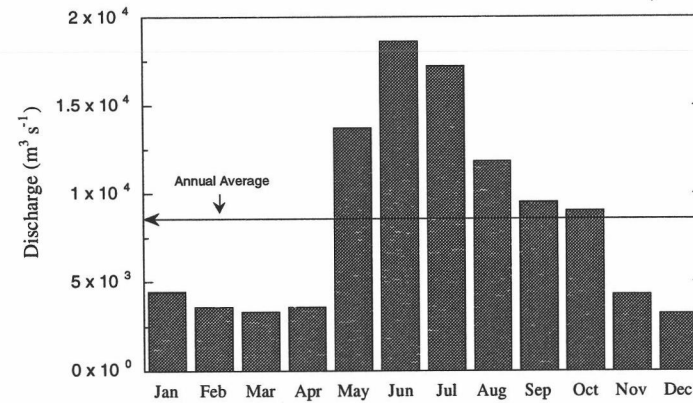


Figure 3: Mean monthly discharge of the four largest Arctic rivers: (a) Yenisey River, (b) Ob River, (c) Lena River, and (d) Mackenzie River.

Table 1: Discharge, sediment load, and drainage basin area of the ten largest rivers flowing directly into the Arctic (discharge data from UNESCO (1978); sediment load data from Milliman and Meade (1983) and Milliman and Syvitski (1992)).

River (Station)	Monthly Average Discharge $10^3 \text{ m}^3 \text{ s}^{-1}$												Annual average discharge $10^3 \text{ m}^3/\text{s}$	Sedi- ment load 10^6 t yr^{-1}	Basin area 10^6 km^2
	Jan	Feb	Mar	Apr	May	Jun	Jul	Aug	Sep	Oct	Nov	Dec			
N. America															
Mackenzie (Arctic Red River)	4.47	3.59	3.33	3.59	13.7	18.6	17.2	11.8	9.52	9.03	4.31	3.22	8.53	127	1.787
Eurasia															
Yenisey (Igarka)	4.84	4.54	4.19	3.98	30.2	76.0	27.9	18.9	17.9	14.7	6.12	4.88	17.8	13	2.44
Ob (Salekhard)	4.37	3.61	3.12	3.21	14.1	32.1	29.1	22.0	13.6	10.3	6.06	4.97	12.3	16	2.95
Lena (Kysur)	2.61	1.90	1.37	1.12	4.49	73.8	39.1	27.0	24.4	14.4	3.27	2.71	16.4	12	2.43
S. Dvina (Ust-Pinega)	1.02	0.82	0.72	2.30	13.9	7.21	3.02	2.26	2.44	3.04	2.45	1.38	3.38	4.5	0.348
Pechora (Ust-Tsilma)	0.65	0.50	0.43	0.81	9.13	13.7	4.34	2.22	2.74	3.27	1.59	0.96	3.36	6.1	0.248
Kolyma (Sredne- Kolymsk)	0.11	0.08	0.06	0.05	2.11	9.79	5.28	4.11	3.29	0.95	0.30	0.20	2.23	6	0.361
Khatanga (Khatanga)	n/a	n/a	n/a	n/a	n/a	n/a	n/a	n/a	n/a	n/a	n/a	n/a	3.32	n/a	0.275
Indigirka (Vorontsovo)	0.04	0.02	0.01	0.01	0.03	5.58	5.68	4.09	2.13	0.48	0.13	0.08	1.55	14	0.305
Pyasina (Ust-Tareya)	n/a	n/a	n/a	n/a	n/a	n/a	n/a	n/a	n/a	n/a	n/a	n/a	2.60	n/a	0.182

2.1.1 Mackenzie River

The Mackenzie River has the second largest drainage basin in North America ($1.787 \times 10^6 \text{ km}^2$, encompassing areas of British Columbia, Alberta, Saskatchewan, the Yukon Territory, and the Northwest Territories between 52° - 70° N latitude (Figure 4). The eastern region of the basin contains part of the Canadian Shield, a complex of Precambrian metamorphic and plutonic rocks (some of the oldest rocks of the earth's crust) exposed over a vast area of subarctic Canada. This region is semi-arid and characterized by rough, rocky, low-relief terrain interspersed with areas of lakes, swamp, muskeg and hummocks (Mackenzie River Basin Committee 1981). The Canadian Cordillera, which includes the Rocky, Mackenzie, Selway, and Richardson mountain ranges, occupies the western part of the Mackenzie Basin. High precipitation and lack of natural water storage (due to the region's steep topography, impermeable permafrost and paucity of lakes) account for the fact that the tributaries draining the Cordillera make the biggest contribution by far of water to the Mackenzie River (Mackenzie River Basin Committee 1981). The rocks of the Cordillera are strongly folded and thrust faulted, nearly all marine (mainly Paleozoic and Mesozoic) with some volcanic intrusions. Between the Cordillera and the Shield lies the Interior Plain, which is extremely flat and composed virtually entirely of sedimentary rocks (mostly marine Cretaceous). Much of the Cordillera has been interpreted as shelf deposits that were originally continuous with those of the Interior Plain, becoming folded and faulted during later orogenic events (McCrossan and Glaister 1966).

While the Mackenzie River is only the fourth largest Arctic river in terms of water discharge, it is the largest in terms of sediment discharge ($127 \times 10^6 \text{ t yr}^{-1}$; Carson 1994) (Table 1). Although eastern tributaries draining the Shield are relatively sediment-free, western tributaries draining the Cordillera and Interior Plain (whose watersheds include glacial terrain and extensive areas of easily-erodible sedimentary rocks) deliver large amounts of sediment to the Mackenzie River. These western tributaries are consistent with studies of rivers worldwide (Milliman and Meade 1983; Milliman and Syvitski 1992) that

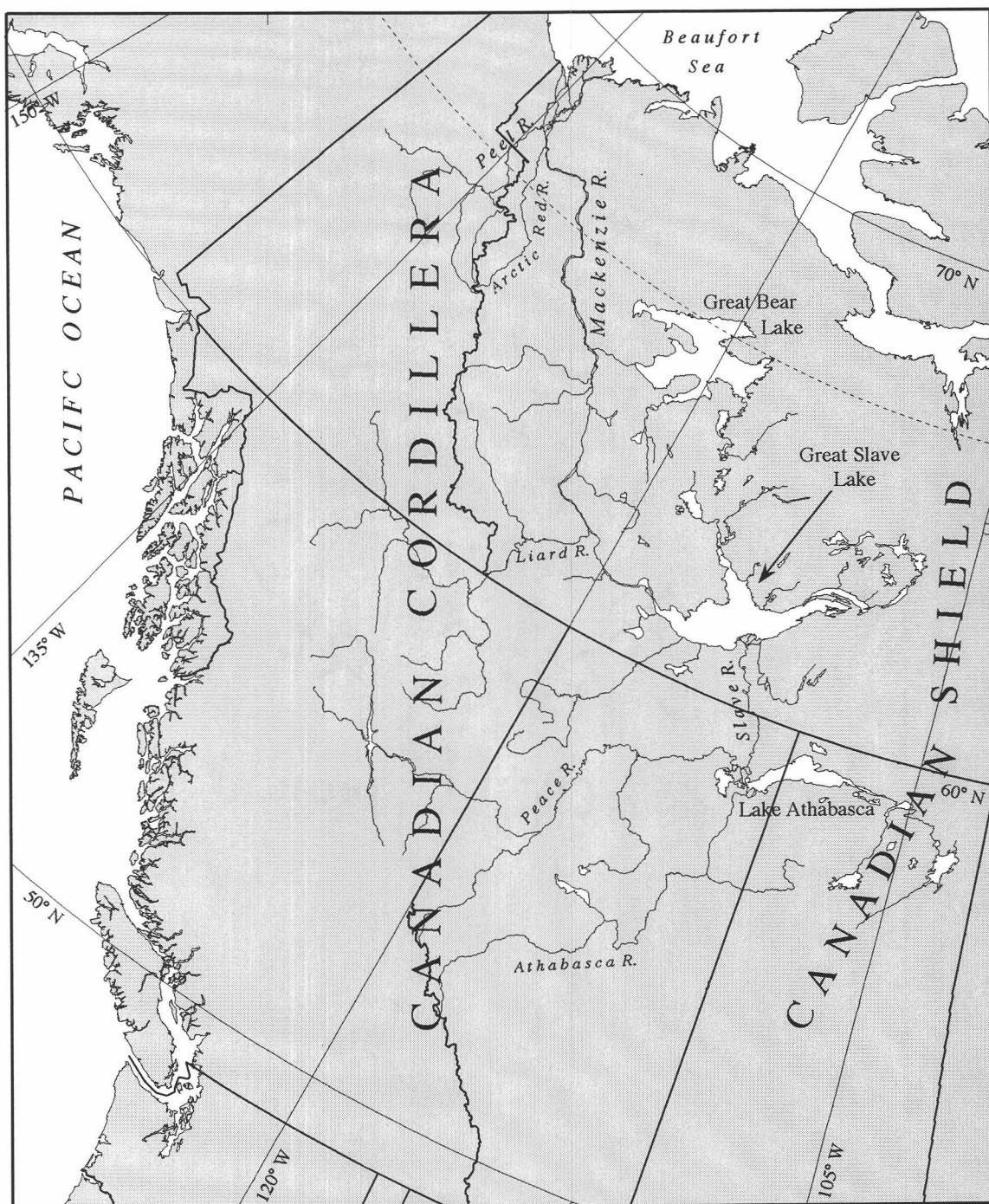


Figure 4: Drainage basin of the Mackenzie River.

observe correlation between high sediment loads and rivers draining mountainous regions, especially active orogenic belts. The Liard River supplies more sediment to the Mackenzie River than any of its other tributaries, and significant amounts of sediment are also contributed by the Peel and Arctic Red rivers (Mackenzie River Basin Committee 1981). The Peace and Athabasca rivers also carry large amounts of sediment but deposit virtually all of it in the extensive Peace-Athabasca and Slave River deltas and Great Slave Lake.

2.1.2 Eurasian Arctic rivers

2.1.2.1 Rivers flowing into the White and Barents seas (Figure 5)

The Severnaya Dvina River drains the northeastern part of the Russian Platform, a vast area of taiga and tundra west of the Ural Mountains consisting mostly of horizontally bedded upper Paleozoic and Mesozoic deposits (Nalivkin 1960). The Severnaya Dvina River flows into the White Sea, a shallow interior sea that opens into the southern Barents Sea. The Mezen and Onega rivers also flow into the White Sea. The Pechora River has its headwaters in the Northern Ural and Polar Ural mountain ranges, from whence it flows through the Quaternary deposits of the Bolshzemelskaya Tundra and enters the Gulf of Pechora in the southeast Barents Sea (Belaglazova et al. 1994).

2.1.2.2 Rivers flowing into the Kara Sea (Figure 5)

The Ob river has the largest drainage basin of all Arctic rivers, encompassing areas of western Siberia and central Asia as far south as 48° N latitude. The basin is bounded on the west by the Ural Mountains and extends eastwards across the West Siberian Lowlands (a vast depression covered almost completely by Quaternary deposits, with outcrops of older rocks in only a few localities); the central part of the West Siberian Lowlands is characterized by swamps and taiga, giving way to tundra in the north and steppes in the south (Nalivkin 1960). The mainstem Ob River begins in the Altai mountains in the region of southern Russia which borders northeastern Kazakhstan, northern China, and northwestern Mongolia. Three large tributaries to the Ob River, the Tobol, Ishim and

Irtyshev rivers, originate in northern Kazakhstan. There are a number of artificial reservoirs behind dams on the upper reaches of the Ob River and its major tributaries; the largest are Novosibirskoe Reservoir (on the mainstem Ob River above Novosibirsk) and Bukhtarminskoe Reservoir (which lies upstream of Ust-Kamenogorsk on the Irtyshev River and is connected with Lake Zaysan, an adjacent natural lake) (Belaglazova et al. 1994). The Ob River flows into the Gulf of Ob, which extends northwards for over 800 km before meeting the Kara Sea. Through its confluence with the Tazovskaya Gulf, the Gulf of Ob also receives the discharge of the Taz and Pur rivers, which drain the West Siberian Lowlands. Releases of radionuclides into the Ob watershed associated with nuclear fuel processing in Chelyabinsk and Tomsk have been documented (Select Committee on Intelligence 1993; Macdonald and Bowers 1996).

The Yenisey River is the largest Arctic river in terms of discharge. Its drainage basin encompasses parts of Siberia and central Asia, extending as far south as 48° N latitude. The drainage basin contains the West Siberian Lowlands in the west, mountainous territory in the vicinity of the Russia-Mongolia border in the south, and the horizontally bedded Paleozoic and Mesozoic deposits of the Mid-Siberian Plateau in the east (Nalivkin 1960; Belaglazova et al. 1994). The Yenisey River originates in the Sayan Mountains north of Mongolia. Its largest tributaries are the Angara, Podkamennaya Tunguska and Nizhnyaya Tunguska rivers. The Angara River flows out of Lake Baikal (the world's deepest, most voluminous lake), whose watershed includes the surrounding mountains and a large area of northern Mongolia. The Podkamennaya Tunguska and Nizhnyaya Tunguska rivers drain the Mid-Siberian Plateau, which is almost completely covered by continuous forest and taiga. A number of moderately large natural lakes occur in the Putoran Mountains, situated in the northwestern region of the Mid-Siberian Plateau. This area is drained by both the Yenisey River and the neighboring Pyasina River, which flows through the North Siberian Lowlands (Cretaceous and Quaternary deposits) and enters the Kara Sea at the western end of the Taymyr Peninsula (Nalivkin 1960). Large reservoirs exist behind dams on the

Angara River at Ust'-Il'msk (Ust'-Il'mskoe Reservoir) and Bratsk (Bratskoe Reservoir), and on the upper Yenisey River at Krasnoyarsk (Krasnoyarskoe Reservoir) and Cheremushki (Sayano-Shushenskoe Reservoir). A smaller reservoir (Khantayskoe Reservoir) exists on the Khantayskaya River, a tributary to the Yenisey draining the Putoran Mountains (Belaglazova et al. 1994). The Yenisey River flows into the Kara Sea via the 225 km-long Yeniseysky Bay. Releases of radionuclides into the Yenisey watershed associated with nuclear fuel processing in Krasnoyarsk have been documented (Select Committee on Intelligence 1993; Macdonald and Bowers 1996).

2.1.2.3 *Rivers flowing into the Laptev Sea (Figure 6)*

The Lena River drains a large area of Siberia and the Russian Far East, covering a range of latitudes between 52°-74° N. The western part of the basin drains the Mid-Siberian Plateau and Precambrian Anabar Shield. The eastern part of the basin includes the mountains of the Verkhoyansk fold-and-thrust belt (upper Paleozoic-Mesozoic shelf complexes) and the Okhotsk-Chukchi volcanic belt (mid-to-late Cretaceous). The southern part of the basin encompasses the mountains of the Stanovoy fold belt and the Precambrian Aldan Shield north of Russia's borders with Mongolia and China (Bogdanov and Tilman 1993; Rundkvist and Mitrofanov 1993). The mainstem Lena River begins in the mountains west of Lake Baikal and is fed by a number of major tributaries, which include: the Vitim, Olyokma, Aldan, Amga, Uchur, Maya and Yudoma rivers (draining the southern and southeastern mountains), and the Vilyuy River (draining the Central Yakutian Lowlands and Mid-Siberian Plateau). There is a large reservoir (Vilyuyskoe Reservoir) behind a dam at Chernishevsky on the upper reaches of the Vilyuy River (Belaglazova et al. 1994). The delta formed by the Lena River where it enters the Laptev Sea is the largest in the Arctic, having over 800 branches and covering an area of 30,000 km² (Telang et al. 1991).

The Khatanga River drains an area south of the Taymyr Peninsula which includes the North Siberian Lowlands, the Mid-Siberian Plateau and the Anabar Shield. The Khatanga

River begins at the confluence of the Kheta and Kotuy Rivers and enters the western Laptev Sea via the 300 km-long Khatangsky Bay. Other large rivers flowing into the Laptev Sea include the Olenyok, Yana, and Anabar rivers.

2.1.2.4 *Rivers flowing into the East Siberian Sea (Figure 6)*

The Kolyma and Indigirka rivers are the two largest rivers flowing into the East Siberian Sea. These rivers drain a geologically complex area bordered by the Verkhoyansk fold-and-thrust belt to the west and south, and the Okhotsk-Chukchi volcanic belt to the east. This region of northeast Asia consists of terranes of different composition and ages that were accreted to the North Asian craton (the Precambrian core of northern Asia) during the Mesozoic and Cenozoic eras (Parfenov 1994; Stone et al. 1994). An artificial reservoir exists on the upper Kolyma River associated with the Kolymskoe hydroelectric station near Sinyegorye (Treshnikov 1985).

The combined watersheds of the Eurasian Arctic rivers accounts for nearly 10% of the total land area draining into the oceans (Milliman and Meade 1983). Despite their large drainage basins and discharges, the major Eurasian Arctic rivers deliver small amounts of sediment to the Arctic Ocean (Table 1). While appearing to have anomalously low sediment loads, Eurasian Arctic rivers are consistent with the relationship between drainage basin elevation and sediment load observed in rivers worldwide (Milliman and Meade 1983; Milliman and Syvitski 1992). Using a classification scheme based on maximum headwater elevation (Milliman and Syvitski 1992), the Eurasian Arctic rivers were shown to correlate well with other upland and lowland rivers throughout the world in terms of sediment yield. Upland rivers were defined as having maximum headwater elevation between 500 and 1000 m (included in this category are the Yenisey, Ob, Lena, Pechora and Indigirka rivers), and lowland rivers were defined as having maximum headwater elevation between 100 and 500 m (included in this category are the Severnaya Dvina and Kolyma rivers); the Mackenzie River was classified as a mountain river, defined as having

maximum headwater elevation between 1000 and 3000 m. The large artificial reservoirs present on some of the major Eurasian Arctic rivers and their tributaries further reduce the sediment loads of these rivers.

2.2 Freshwater budget of the Arctic Ocean

This section begins with a brief review of the freshwater budget of the upper Arctic, for which there remain a number of substantial uncertainties. For the budget discussion, the Arctic is taken to be bounded by Bering and Fram Straits and the northern limit of the Canadian Archipelago, and to include the Barents, Kara, Laptev, East Siberian, Chukchi and Beaufort seas (Figure 1). All freshwater fluxes are calculated relative to a reference salinity of 34.80, the estimated mean salinity of the Arctic Ocean (Aagaard and Carmack 1989).

The largest freshwater source to the Arctic is fluvial discharge. On an annual basis, approximately 10% ($3300 \text{ km}^3 \text{ yr}^{-1}$) of the world's total river runoff flows into the Arctic, whose surface area and volume constitute only about 5 and 1.5%, respectively, of the global oceans. A third of this disproportionately large flux is contributed by a combination of the three largest Siberian rivers, the Yenisey ($603 \text{ km}^3 \text{ yr}^{-1}$), Ob ($530 \text{ km}^3 \text{ yr}^{-1}$) and Lena ($520 \text{ km}^3 \text{ yr}^{-1}$), and the largest North American river, the Mackenzie ($340 \text{ km}^3 \text{ yr}^{-1}$) (Aagaard and Carmack 1989). While interannual variability in the discharge of the major Arctic rivers is typically between 5-20% of the mean annual flow (Carmack 1990), seasonal variability is considerably higher. Low flows occur during the winter when freezing occurs in the rivers and their drainage areas, and high flows occur in spring and summer when large amounts of snow and ice melt in the watersheds. In the Yenisey and Lena rivers, the maximum peak flows in June and July are on average about 40 times higher than the minimum monthly flows in winter (Carmack 1990). In the Mackenzie River, the maximum flow in early June is typically about 6-8 times higher than minimum flows between January and April (Carmack et al. 1989) (Table 1, Figure 3).

The next largest source of freshwater to the Arctic is the relatively fresh seawater entering through Bering Strait. The annual mean inflow through Bering Strait is about 0.8 Sv ($1 \text{ Sv} = 10^6 \text{ m}^3 \text{ s}^{-1}$), characterized by a summer maximum, a winter minimum, and interannual variability at times approaching 50% of the mean (Coachman and Aagaard 1988; Roach et al. 1995). Current meters deployed between September 1990 and September 1994 recorded transports through Bering Strait close to the mean during 1990-1993; but the largest transport in nearly 50 years of observations ($\approx 1.1 \text{ Sv}$) was recorded during the first 9 months of 1994 (Roach et al. 1995). Taking a value of 32.5 for the mean salinity of the Bering inflow, the corresponding mean freshwater flux through Bering Strait is $1670 \text{ km}^3 \text{ yr}^{-1}$ --roughly half of the fluvial contribution (Aagaard and Carmack 1989). An additional freshwater influx of $400\text{-}1400 \text{ km}^3 \text{ yr}^{-1}$ results from the net excess of precipitation over evaporation in the Arctic (Aagaard and Carmack 1989).

The major sinks in the freshwater budget of the Arctic are outflow through the Canadian Archipelago and Fram Strait. Estimates of total seawater outflow through the Canadian Archipelago range widely (0.7 Sv , Steele et al. 1996; 1.0 Sv , Rudels 1986; 1.7 Sv , Fissel et al. 1988; 2.1 Sv , Muench 1971), as do estimates of its salinity (32.3 , Steele et al. 1996; to 34.2 Aagaard and Greisman 1975) and corresponding fresh water export ($900 \text{ km}^3 \text{ yr}^{-1}$, Aagaard and Greisman 1975; to $1200 \text{ km}^3 \text{ yr}^{-1}$ Steele et al. 1996). It has been estimated from observational data that $2790 \text{ km}^3 \text{ yr}^{-1}$ of freshwater is exported through Fram Strait as ice, with an additional $820 \text{ km}^3 \text{ yr}^{-1}$ exported as liquid water in the East Greenland Current (Aagaard and Carmack 1989). A recent ice-ocean model derived smaller mean freshwater exports through Fram Strait of $1600 \text{ km}^3 \text{ yr}^{-1}$ as ice and $700 \text{ km}^3 \text{ yr}^{-1}$ as liquid water (Steele et al. 1996). The discrepancy was attributed largely to a significant downwelling term within the Arctic generated by the model. For this result to be consistent with observations of deep water properties entering and exiting Fram Strait, it was suggested that downwelling-induced freshening required by the model may be compensated in part by mixing with relatively saltier deep waters of the Arctic interior

(Steele et al. 1996). The model results also suggested that variability in the Fram Strait and Canadian Archipelago freshwater export terms is compensatory in that when one is larger the other tends to be smaller (Steele et al. 1996).

Albeit with limited resolution (7 regional areas), the model exercise showed that upper Arctic stratification and export terms are highly dependent upon the regional disposition of the factors contributing to them. Neither the magnitudes nor variability of the Canadian Archipelago and Fram Strait freshwater export terms are sufficiently well characterized to determine how realistic the model scenarios are; but it appears that knowledge of the fate of freshwater associated with fluvial discharge and Bering inflow within the Arctic is essential for predicting Arctic Ocean exports.

2.3 Physical and chemical tracers of Arctic circulation

Long-term surface circulation derived from modeling of ice buoy data shows two main features--the broad, anticyclonic Beaufort Gyre centered over the Canadian Basin and a general transpolar drift toward Fram Strait of waters originating from the region of the Siberian seas (Thorndike and Colony 1982; Colony and Thorndike 1985). Average ice thickness increases across the Arctic from 1 m in the Siberian coastal seas up to 7 m just north of the Canadian Archipelago (Gloerson et al. 1992). On average, ice drift time to Fram Strait increases from 1 to 2 years for ice of Barents origin, to three years for Laptev ice, to 6 years in the eastern Beaufort Sea (Rigor 1992).

Exactly how and where Siberian river waters enter the Arctic interior under the ice is unclear. Several chemical tracers, including oxygen isotopes, He-tritium and alkalinity have been used to investigate the distribution and fate of freshwater in the Arctic surface layer; while measured values vary somewhat geographically, it does not appear to be feasible to distinguish between contributions from different fluvial sources to the Arctic on the basis of their oxygen isotope, tritium or alkalinity signatures. Based on measurements of all of these tracers in the central Arctic, it has been speculated that Ob and Yenisey waters flow along the Nansen-Gakkel Ridge and/or transit along-shelf toward the Laptev

Sea, where they merge with Lena influenced waters and are then topographically steered along the Lomonosov Ridge into the interior (Jones et al. 1991; Anderson et al. 1994; Anderson et al. 1994; Schlosser et al. 1995). Unusually fresh, warm waters apparently emanating from the Laptev Sea were observed along the Amundsen flank of the Lomonosov Ridge in 1995 (when ice in the region had retreated further north than had been observed in the previous 50 years), providing further evidence of the transport of Eurasian river waters in this region (R. Muench, personal communication). None of the data coverage is synoptic or extensive enough to determine whether a significant fraction of river-influenced waters continues further along the Laptev and East Siberian shelves and enters elsewhere into the broad transpolar drift indicated by ice studies. Presuming the Lomonosov Ridge pathway, interpretation of the tritium data (Schlosser et al. 1994) and overall freshwater budgets suggest river waters (Hanzlick and Aagaard 1980) reside in the Kara Sea on the order of 2 to 3 years, and that an undetermined fraction of such waters require 5-8 years to transit the interior and exit at Fram Strait.

Apart from a few ice-camp profiles in the Canadian Basin, the published surface tracer work has been conducted largely in the Eurasian sector of the Arctic (Schlosser et al. (1995), and references therein). In that sector, an oxygen isotope/salinity mass balance has been applied to quantitatively map river water, sea-ice melt and underlying Atlantic components. The situation becomes more complicated for the Canadian sector of the Arctic where waters of Pacific origin, which also bear a river water signal, are present in the upper 200 m. An attempt has been made to derive information about the composition of halocline waters from oxygen isotope data, using silicate as an index of Bering Sea input; however this required assumptions about the pathway of Bering Sea water that have yet to be directly observed (Bauch et al. 1995). The longer residence time of ice in the region renders calculations more sensitive to the assumption that the $\delta^{18}\text{O}$ signature of sea-ice melt can be characterized by the surface isotopic composition at the site of measurement.

Additional tracer information is desirable to fully exploit circulation information in the oxygen isotopic compositions encountered in the Canadian Basin.

It has long been appreciated that the temperature and salinity characteristics of Arctic halocline waters do not reflect simple mixing of surface with underlying waters. A variety of processes have been implicated in the establishment and maintenance of chemically-defined structure within the Arctic halocline. These include convection/brine extraction in regions north of Svalbard and toward the Lomonosov Ridge (Rudels et al. 1996), atmospheric cooling and contact of incoming Atlantic waters with the ice edge west of Spitsbergen and in the Barents Sea (Boyd and D'Asaro 1994; Steele and Morison 1995), lateral brine injection at ice edges and polynyas over the shelves (Aagaard et al. 1981; Cavalieri and Martin 1994), cooling of deeper waters via upwelling in coastal canyons (Aagaard and Roach 1990) and lateral intrusion of modified Bering Strait inputs (Aagaard et al. 1981). While all of these processes have been observed, their relative significance and variability have yet to be assessed.

A layer within the halocline that is marked by a distinct maximum in silicate occurring at a salinity of approximately 33.1 is referred to in much of the literature as the upper halocline (Jones and Anderson 1986). The only source capable of supplying a signal of the observed magnitude is the Bering input (Coachman and Aagaard 1974; Jones and Anderson 1986). It has yet to be resolved whether the upper halocline derives directly from a winter Bering input that is moderately salinized by brine injection and/or involves diagenetic remobilization of Si temporarily deposited in association with high productivity in the Chukchi Sea. The limited observations up to 1991 suggested that this upper halocline feature could be found throughout the Canada and Makarov Basins, extending across the Lomonosov ridge to the East Greenland Current. Hydrographic measurements obtained during SCICEX-93 were used to examine the Arctic halocline on a basin-wide scale (Morison et al. 1997). Averaged temperature versus salinity curves, plotted separately for western Arctic and eastern Arctic data, were offset from each other in waters

just above and below the upper halocline; but the two curves were indistinguishable (within analytical uncertainty) in the upper halocline itself (defined by Morison et al. (1997) as waters with salinity between 32.8 and 33.2 and temperature between -1.3°C and the freezing line). Assuming that all waters with these temperature and salinity properties comprised one continuous mass, the upper halocline appeared as a relatively thick layer (75-100 m) throughout much of the Canada Basin, thinning and shoaling towards the eastern Arctic and outcropping at the surface over parts of the Makarov and Amundsen basins in the vicinity of the Lomonosov Ridge.

A lower halocline layer with its core at salinity 34.2-34.4 has been identified on the basis of a minimum in the quasi-conservative NO parameter ($\text{NO} = \{\text{O}_2\} + 9 \times \{\text{NO}_3\}$; (Broecker 1974; Jones and Anderson 1986)). It was initially argued that the NO minimum associated with the lower halocline reflected its region of origin over the Barents and Kara shelves (Jones and Anderson 1986). Subsequent examination of archived data for the shelves showed that values of NO vary considerably in the shelf seas around the Arctic perimeter. It was proposed that the ratio NO/PO (where $\text{PO} = \{\text{O}_2\} + 135 \times \{\text{PO}_4\}$, Broecker 1974), which on the basis of available data appeared to be more geographically specific, might better serve as a determinant of the shelf regions from whence lower halocline waters originate (Wilson and Wallace 1990).

Basin-wide budgets of freshwater, oxygen isotopes and tritium suggest average freshwater residence times in the halocline layer of approximately 10 years (Aagaard and Greisman 1975; Östlund 1982; Östlund and Hut 1984). More detailed studies based on chlorofluorocarbons and oxygen isotopes/tritium/He to obtain ages produce residence times that tend to increase in the vertical in the upper 200 m and vary geographically within the Arctic (Wallace et al. 1987; Schlosser et al. 1990; Wallace et al. 1992; Schlosser et al. 1994). This work suggests surface waters may be renewed much faster (2-6 yr) than

halocline waters (up to 15 yr). Geographical variations can only be properly interpreted in terms of pathways when more is known about the internal workings of upper Arctic circulation.

2.4 Marine geochemical behavior of barium

To improve understanding of the fate of freshwater in the upper Arctic, we have embarked on a program to supplement the tracer suite discussed above with naturally occurring geochemical tracers; barium is the most promising of these tracers so far. The biogeochemical behavior of Ba in the marine environment is summarized below and has been reviewed elsewhere in more detail (Falkner et al. 1993; Falkner et al. 1994). In general, dissolved Ba tends to be depleted in surface oceanic waters and enriched with depth and along advective flow lines, much like a hard-part nutrient such as alkalinity (which reflects CaCO_3 cycling) or Si (Chan et al. 1977; Lea 1990; Falkner et al. 1993). This has been attributed to uptake of Ba at the surface as the mineral barite (BaSO_4), which is formed in association with biological particulate matter and subsequently sinks and can be regenerated at depth or in the sediments (Dehairs et al. 1980; Collier and Edmond 1984; Bishop 1988; Dymond et al. 1992). The exact mechanism by which Ba is removed from surface oceanic waters remains the subject of research (e.g., Fresnel et al. 1979; Dehairs et al. 1987; Bernstein et al. 1992).

Since Ba cycles in a manner similar to that of hard-part constituents, dissolved Ba tends to correlate linearly with dissolved Si and alkalinity in much of the world's oceans (Bacon and Edmond 1972; Chan et al. 1977). The slopes and intercepts of the correlation lines vary somewhat with location, in part because these constituents display diverse surface distributions; Si is a biolimiting element that can be depleted to essentially zero concentrations in surface waters, whereas alkalinity is only slightly altered by biological activities. Barium, being biointermediate, lies between the two in that it is measurably but not fully depleted. In addition, there exist areas of the oceans (the Arctic being one) where Ba, Si and alkalinity regeneration fluxes are likely decoupled, since barite, opal and

carbonate are subject to different dissolution controls. Being more like opal in this regard, elevated barite concentrations are observed in sediments underlying the most highly productive areas of the oceans (Revelle 1944; Revelle et al. 1955; Goldberg and Arrhenius 1958; Turekian and Tausch 1964).

The principal external sources of dissolved Ba to the world's oceans are rivers (Martin and Meybeck 1979) and hydrothermal venting at mid-ocean ridges (Edmond et al. 1979; Von Damm et al. 1985). Both sources tend to be elevated in Ba content over the seawater into which they arrive; this situation holds true for the major Arctic rivers (Guay and Falkner 1997). Although the extent to which hydrothermal activity occurs along the extremely slow-spreading Nansen-Gakkel Ridge and in other areas of the Arctic is not well known, most hydrothermal Ba is generally thought to precipitate inorganically as barite in the vicinity of hot spring sources (Von Damm 1990). Fluvial inputs, in contrast, are enhanced in estuaries where Ba adsorbed onto riverborne clays becomes desorbed in exchange for the more abundant cations of seawater (Hanor and Chan 1977; Edmond et al. 1978; Li and Chan 1979; Carroll et al. 1993). Recent work has suggested that brackish groundwater discharge also represents a significant source of Ba to coastal waters in some regions (Moore 1996). This should be less significant in the Arctic, where groundwater flow is limited by permafrost, but could be expected to play an increasing role in the event of rising global temperatures.

3. SURVEY OF BARIUM IN ESTUARIES OF MAJOR ARCTIC RIVERS

3.1 Experimental design

Analyses for dissolved Ba were performed on 315 water samples obtained from major Arctic river estuaries and adjacent regions of Arctic seas between 1993 and 1996. The purpose of this endeavor was to compare Ba concentrations in the major Arctic rivers, to assess seasonal and temporal variability, and determine how riverine Ba signals are altered in the mixing zones between fluvial and oceanic waters.

3.1.1 Sample collection

Water samples for Ba analyses were generally collected in high-density polyethylene (HDPE) bottles previously leached (≥ 10 hr) at 50° C with 1N HCl. Samples were filtered no later than 4 days after collection through HCl-leached 0.45- μ m Nuclepore polycarbonate filters. Precautions were taken to insure that the water samples did not freeze. Vertical profiles of salinity and temperature were generally recorded at each sampling location using a Seabird conductivity-temperature-depth (CTD) profiler. Exceptions to this procedure and further details are summarized below for each of the suites of samples collected between 1993 and 1996.

3.1.1.1 1993 Russia samples

Between 15 and 29 September 1993, 20 sub-surface water samples were collected in the Ob and Yenisey River estuaries and the Kara Sea aboard the *R/V Dmitriy Mendeleev* (Figure 7). The rivers were completely ice-free during the time of sampling. Water samples were obtained using Niskin bottles equipped with silicone rubber o-rings and nylon-coated internal springs. Aliquots for Ba analyses were collected in HDPE bottles previously leached with reverse-osmosis deionized water (RODW) instead of 1N HCl. The samples were not filtered, with the exception of one sample from the Ob river (furthest-upstream station) which contained a visibly high amount of suspended sediment.

△ 1993 Stations (September) □ 1994 Stations (July-September) ○ 1995 Stations (August-September)

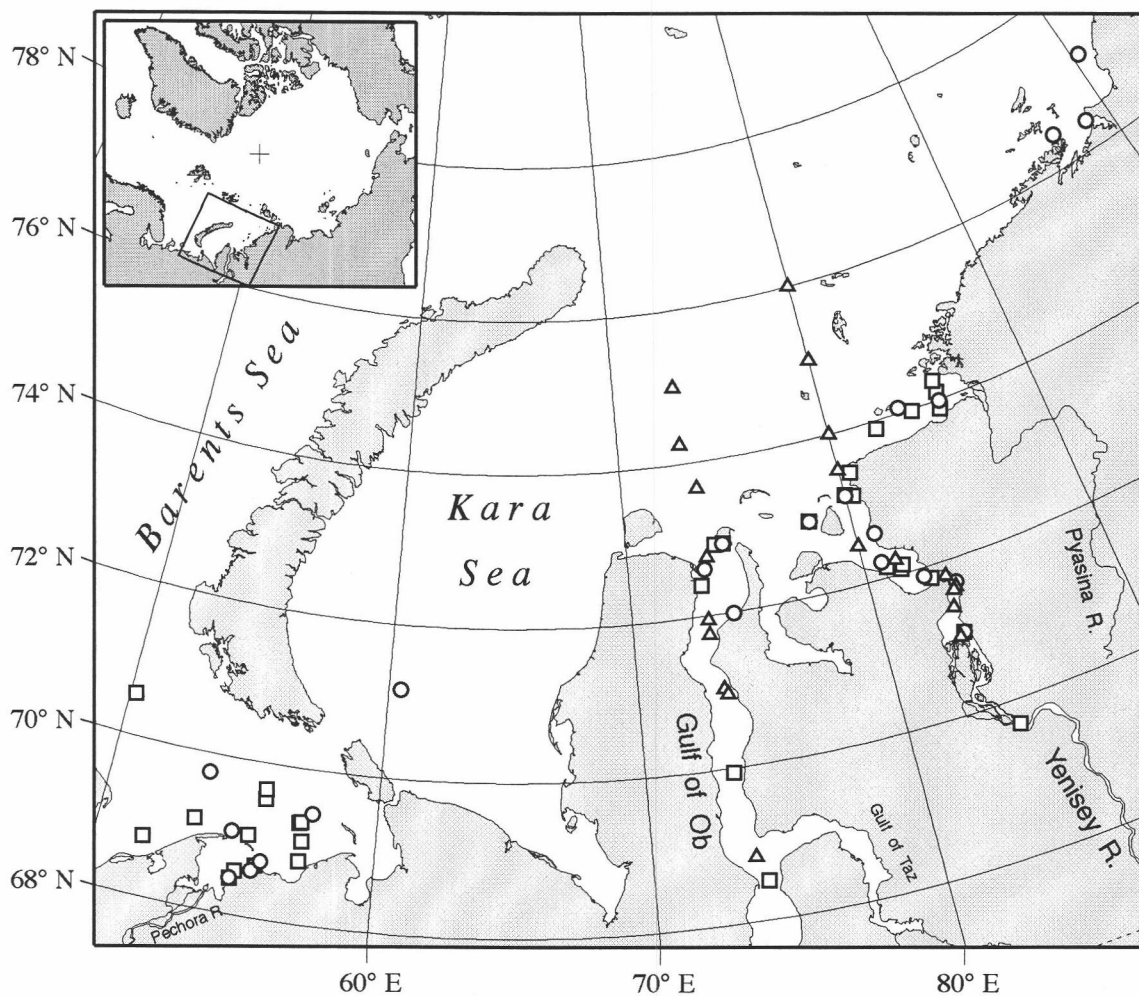


Figure 7: Locations of samples obtained in 1993-1995 from the estuaries of major Eurasian Arctic rivers and adjacent shelf areas (Barents and Kara seas).

It was filtered (0.45 μm) inside a laminar flow hood in our laboratory at OSU approximately 3 years after the date of collection. Portions of the samples collected for Ba analyses were used for salinity analyses.

3.1.1.2 1994 Russia samples

Between 12 July and 24 September 1994, 87 water samples (surface and sub-surface) were collected in the Pechora, Ob, Yenisey and Pyasina River estuaries and the White, Barents and Kara Seas aboard the *R/V Yakov Smirnitsky* and *R/V Valerian Al'banov* (Figure 7). The rivers were completely ice-free during the time of sampling. Water samples were obtained using standard Niskin bottles. The Niskin bottles and CTD profiler were deployed on a steel wire from a hydraulic winch on the port side of the vessel (opposite from engine and sanitation system discharges) situated roughly halfway between the bow and the stern. After filtration, aliquots were taken from each sample for salinity analyses; since the samples were initially collected in HCl-leached bottles, these salinity data are not necessarily accurate due to possible leaching of Cl^- from the bottle walls. While not suitable for high-precision work, these salinity data are useful for semi-quantitative assessment.

3.1.1.3 1995 Russia samples

Between 7 August and 18 September 1995, 188 water samples (surface and sub-surface) were collected in the Pechora, Ob, Yenisey, Pyasina, Khatanga, Lena, Yana, Indigirka and Kolyma River estuaries and the Barents, Kara, Laptev and East Siberian Seas aboard the *R/V Yakov Smirnitsky* (Figures 7 and 8). The rivers were completely ice-free during the time of sampling. Water samples were obtained using Niskin bottles equipped with epoxy-coated springs and silicone rubber o-rings and closure tubing. The Niskin bottles and CTD profiler were deployed on a rubber-jacketed wire from a hand-operated winch mounted on the bow of the vessel. Separate samples for salinity analyses were collected into glass bottles with caps containing conical teflon inserts.

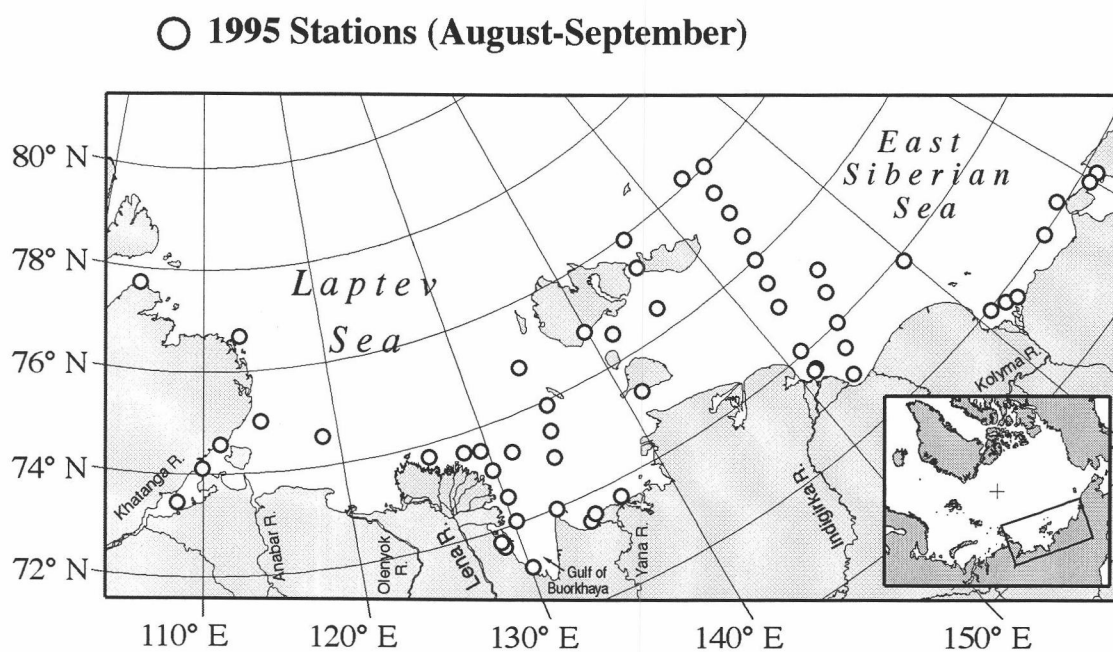


Figure 8: Locations of samples obtained in 1995 from the estuaries of major Eurasian Arctic rivers and adjacent shelf areas (Laptev and East Siberian seas).

3.1.1.4 1994 Canada samples

Between 7 and 14 April 1994, 16 water samples (surface and sub-surface) were collected in the Mackenzie estuary in the vicinity of the Polar Continental Shelf Project (PSCP) facility at Tuktoyaktuk (Figure 9). All of the samples were collected in Kugmallit Bay, into which flows the East Channel of the Mackenzie River (accounting for approximately 1/3 the total discharge of the Mackenzie River). The river and adjacent area of the Beaufort Sea were completely ice-covered during the time of sampling. Water samples were obtained using Niskin bottles equipped with epoxy-coated springs and silicone rubber o-rings and closure tubing. In addition to samples for Ba analyses, separate samples for salinity analyses were collected in HDPE bottles leached with RODW. The Niskin bottles and CTD were deployed on a nylon line lowered by hand through holes drilled in the ice. No reliable CTD data were obtained due to instrument icing.

3.1.1.5 1996 Canada samples

Between 21 and 31 August 1996, 4 water samples were collected in the Mackenzie River and its estuary (Figure 9). The river was completely ice-free during the time of sampling. These samples were collected by hand from an inflatable rubber boat. While the boat was moving slowly upstream, a capped HDPE bottle was submerged forward of the bow. The cap was removed underwater, allowing water to displace the air in the bottle. As soon as the bottle filled with water, it was capped underwater and brought to the surface. No CTD casts were taken in association with these samples. The samples were filtered (0.45 μm) inside a laminar flow hood in our lab at OSU upon their delivery approximately 2 months after collection. Prior to filtration, aliquots were taken from each sample for salinity analyses; the same precaution noted for the bottle salinity data from the 1994 Russia samples also applies to these salinity data.

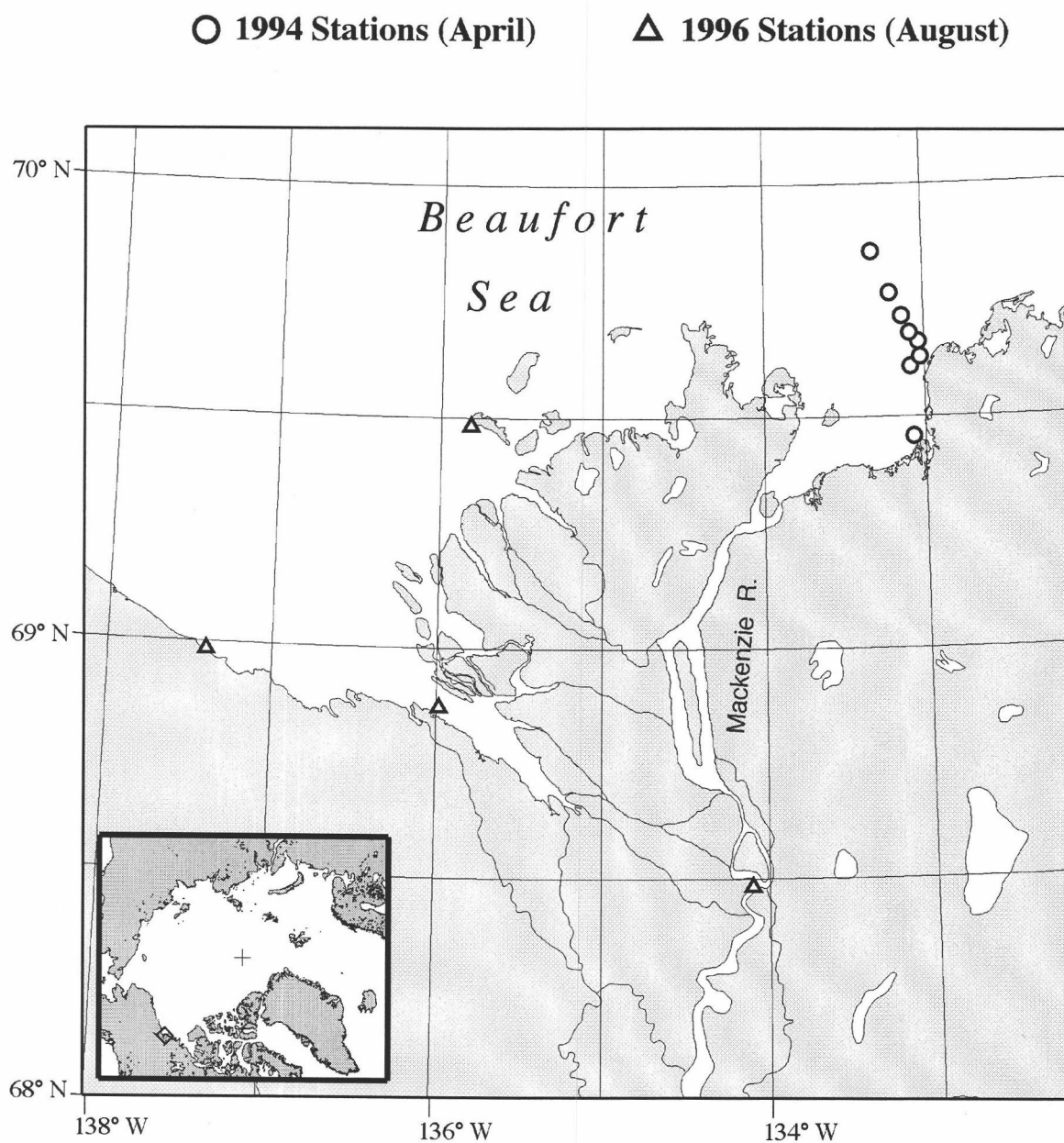


Figure 9: Locations of samples obtained in 1994 and 1996 from the estuaries of the Mackenzie River.

3.1.2 Analytical procedure

Dissolved barium concentrations were determined by isotope-dilution inductively coupled plasma quadrupole mass spectrometry (ID-ICPMS) at OSU using a Fisons PlasmaQuad II equipped with an autosampler. The analytical method employed was similar to those described in more detail elsewhere (Klinkhammer and Chan 1990; Falkner et al. 1993). Sample preparation was carried out entirely in a laminar flow hood. All pipette tips, test tubes and HDPE bottles used for preparing standard and spike solutions were leached overnight with 1N HCl at 50°C and rinsed copiously with RODW. All HCl solutions used for leaching, sample preparation, instrument washout and blanks were diluted with RODW from 6N HCl prepared by triple distillation in a quartz apparatus. Aliquots (250 µl) of samples were spiked with an equal volume of ^{135}Ba -enriched solution (Oak Ridge National Laboratories) and diluted twenty-fold with 0.2N HCl in a polypropylene test tube. Samples were introduced into the instrument via a peristaltic pump ($\approx 1 \text{ ml min}^{-1}$ flow rate) coupled to a Meinhard concentric nebulizer and Scott double by-pass spray chamber. The instrument was operated in peak jump mode, monitoring masses 135 and 138 and acquiring data in three 20-second intervals for each sample. A 4-minute washout with 0.2N HCl was performed after every sample to reduce memory effects. A gravimetric Ba standard (spiked and diluted in an identical manner to the samples) and a 0.2N HCl blank were inserted between every five samples in the autosampler tray for instrumental offset, drift and blank corrections. The accuracy of the method was verified by frequent analyses of an independent gravimetric barium standard. Applying our analytical method to archived GEOSECS samples that were spiked upon collection in the 1970's reproduced GEOSECS values to within 1%. Based on replicate analyses of selected samples and a seawater consistency standard, the analytical uncertainty (2σ) ranges from better than 5% at $10 \text{ nmol Ba L}^{-1}$ to better than 3% at $100 \text{ nmol Ba L}^{-1}$.

Bottle salinities were determined post-cruise on a Guildline Autosol model 8400A laboratory salinometer calibrated with standard sea water. Salinities are reported as unitless values using the practical salinity scale (UNESCO 1983).

3.2 Results

3.2.1 Mixing in Arctic river estuaries and adjacent shelf regions

While temperature and salinity profiles tend to be uniform in Arctic shelf waters during the winter due to convective cooling and ice coverage, brine rejected during ice formation can sink and lead to the formation of colder, denser water masses on the seafloor in shelf regions. Considerable modification of shelf water masses form in the summer by warming due to increased solar radiation and freshening by a combination of melting ice and higher river discharges. Thus water masses over the shelves of Arctic seas have widely differing temperature and salinity characteristics that show strong seasonal variability.

Temperature was plotted against salinity for the CTD data obtained from major river estuaries of the Barents, Kara, Laptev and East Siberian seas (Figure 10); as mentioned previously, no reliable CTD data were obtained from the Mackenzie River estuary in either 1994 or 1996. The T-S plots show warm, fresh river waters mixing with various shelf water masses to form intermediate waters with a wide range of temperatures and salinities. As salinity increases with depth and distance offshore, the various mixing paths converge to endpoints having temperatures and salinities characteristic of the surface mixed layer of the Arctic Ocean (i.e. salinities < 34.5 , temperatures close to the freezing point at a given salinity). The influence of relatively warm, saline waters of Atlantic origin (defined by Carmack, 1990 as water with $S > 34.9$ and $T > 3^{\circ}\text{C}$) can be seen at some of the deeper stations. It is evident that simple mixing between individual riverine end-members and a single oceanic end-member is not characteristic of the mixing zones in Arctic estuaries.

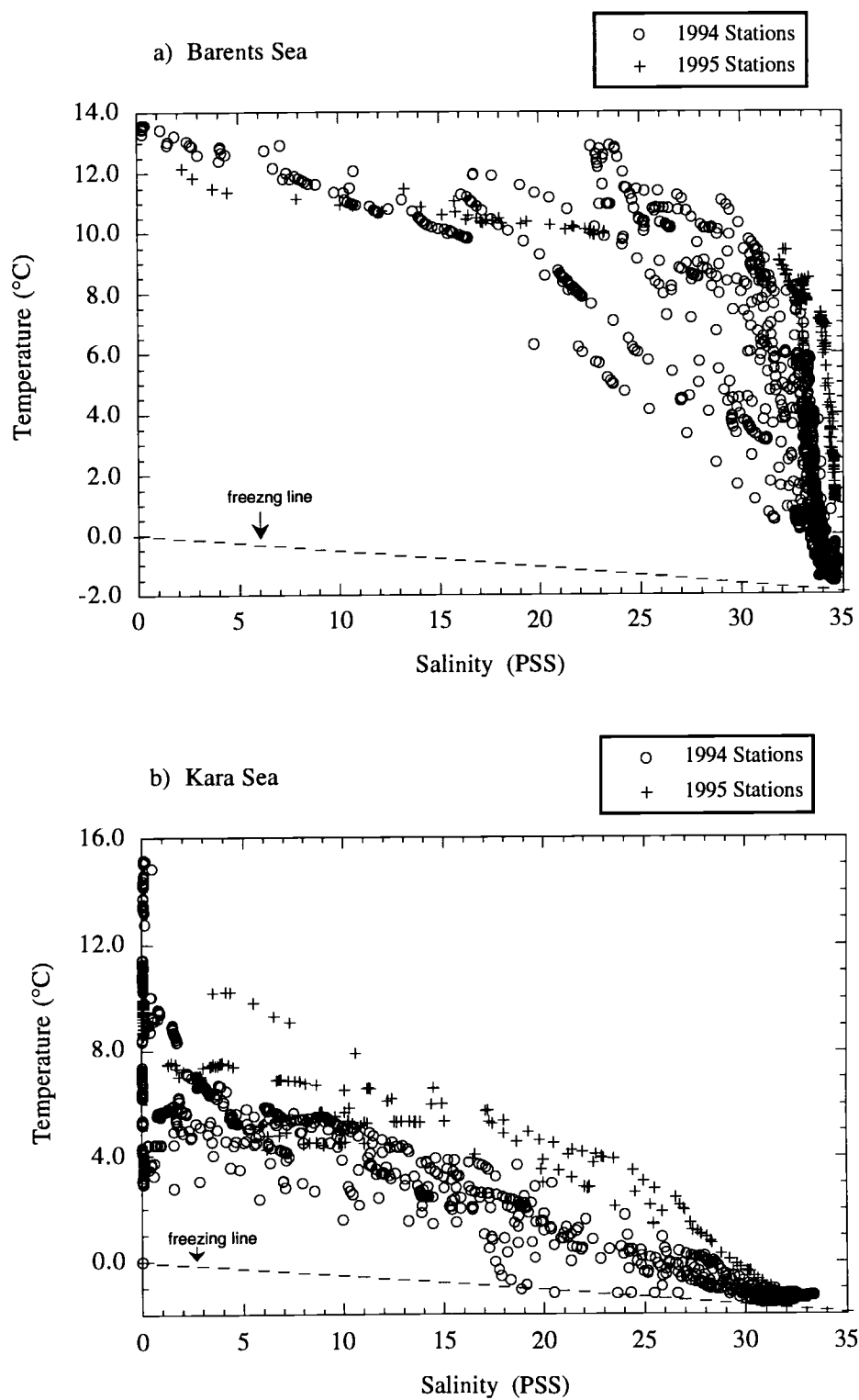


Figure 10: T-S plots of CTD data collected in (a) the Barents Sea in 1994-1995, (b) the Kara Sea in 1994-1995, (cont'd)

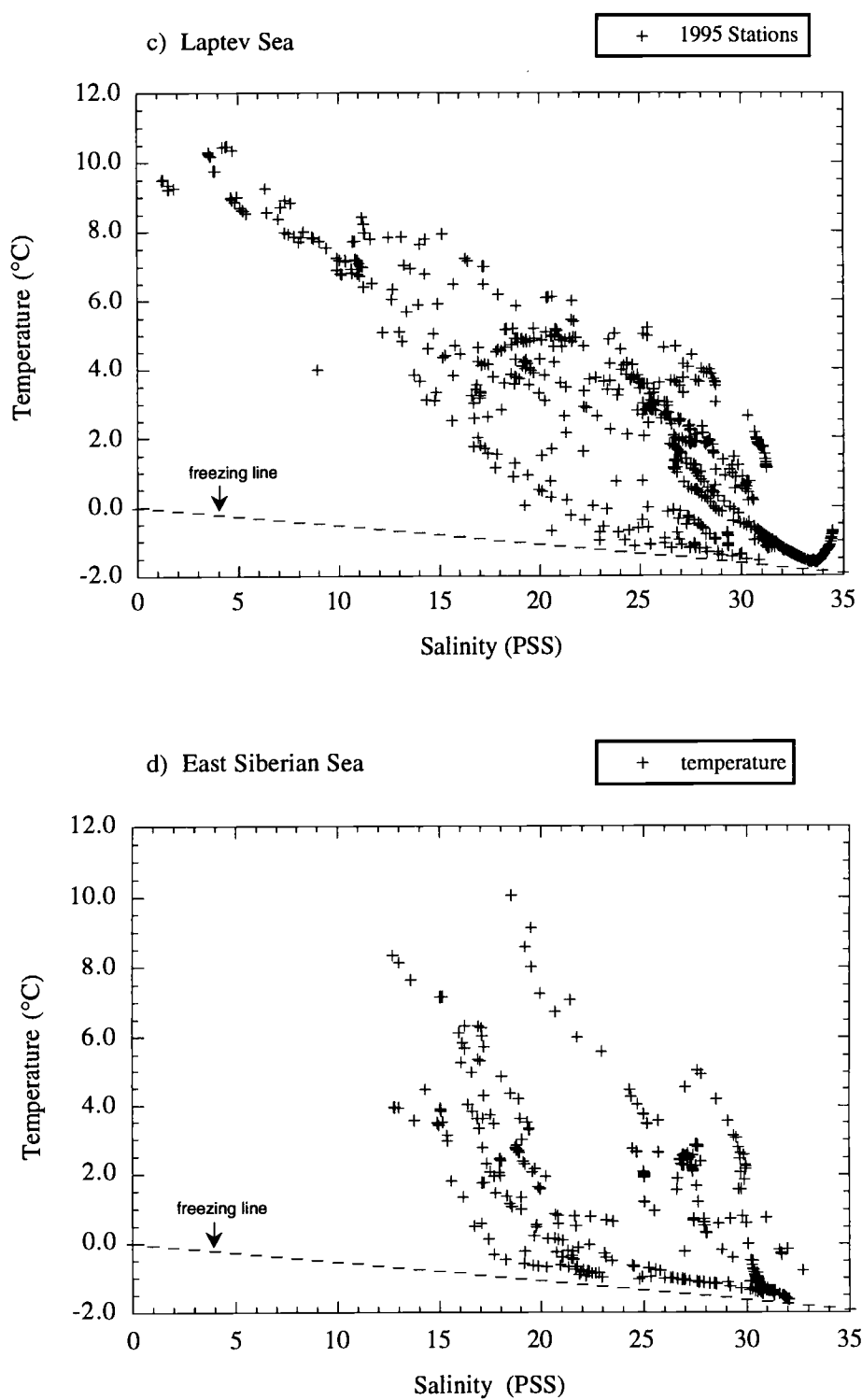


Figure 10 (cont'd): T-S plots of CTD data collected in (c) the Laptev Sea in 1995, and (d) the East Siberian Sea in 1995.

3.2.2 Behavior of Ba in mixing zones

3.2.2.1 Mackenzie River (Beaufort Sea)

In the subsurface samples taken from the Mackenzie estuary in 1994, dissolved Ba concentration ([Ba]) increased from 418 to 574 nmol L⁻¹ (a 37% increase) as salinity increased from near-zero to 1 (Figure 11). In low-latitude rivers, similar sharp increases in

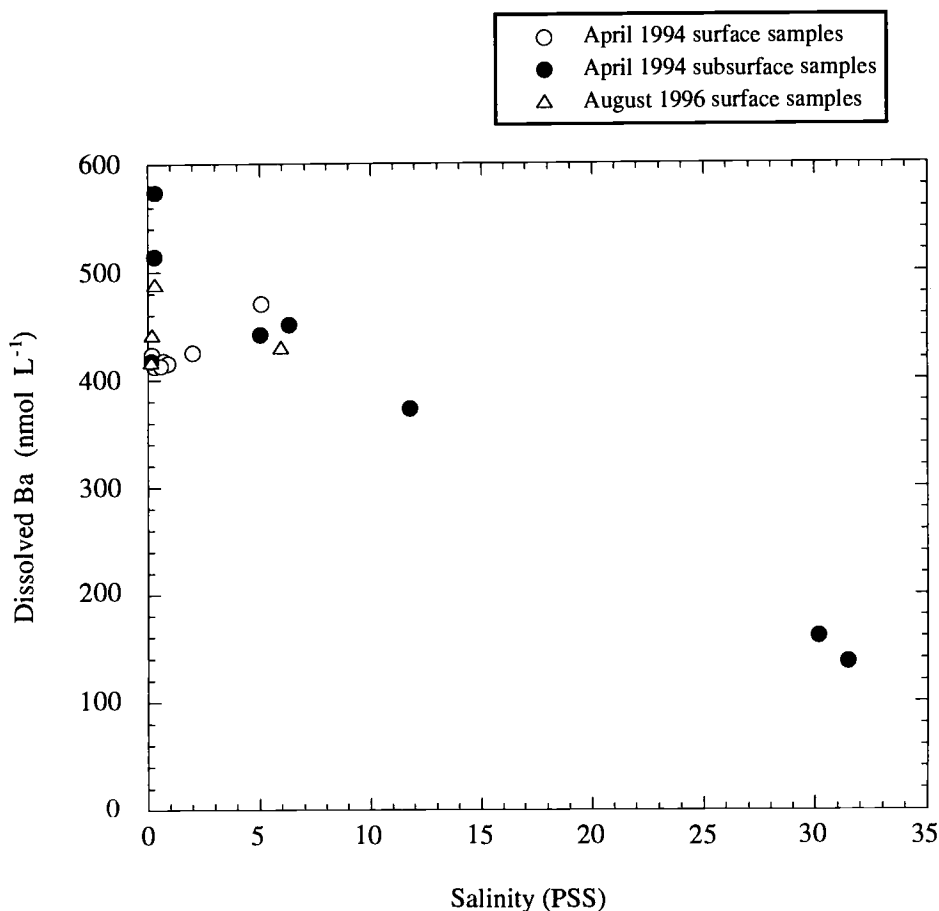


Figure 11: Dissolved Ba in the estuary of the Mackenzie River in 1994 and 1996.

[Ba] have been observed at low to intermediate salinities, and were attributed to desorption of Ba from suspended riverine clay particles (Hanor and Chan 1977; Edmond et al. 1978; Li and Chan 1979; Carroll et al. 1993). In the surface samples, values of [Ba] are clustered between 410 and 425 nmol L⁻¹ at salinity < 1 and gradually increased as salinity

increased to 5. Biological drawdown or dilution with ice meltwater may have given rise to the relatively low values of [Ba] in these surface samples compared with the subsurface samples. An alternate explanation for these data is that deeper waters of the estuary were enhanced by the influx of Ba-rich pore waters (Key et al. 1985) or groundwaters (Moore 1996) during the winter period of low fluvial discharge. A roughly linear decrease in [Ba] was observed as salinity increased above 5, suggesting conservative mixing between riverine and oceanic waters. For the samples taken from the Mackenzie estuary in 1996 (all from the surface), [Ba] increased from 417 to 489 nmol L⁻¹ as salinity increased between 0 and 1, then decreased to 430 nmol L⁻¹ as salinity increased to 6.

3.2.2.2 *Pechora River (Barents Sea)*

In the Pechora estuary and the adjacent region of the southeastern Barents Sea, in both 1994 and 1995, a slight increasing trend was generally observed in [Ba] as salinity increased from near-zero to 15. In both years, samples relatively enriched in Ba were seen in this salinity range ([Ba] = 100 nmol L⁻¹, S = 1.7 in 1994; [Ba] = 126 nmol L⁻¹, S = 8.5 in 1995) (Figure 12). Since these values exceed Ba concentrations in surrounding waters and were encountered at low to intermediate salinity, the most plausible explanation of the elevated [Ba] in these samples is desorption from riverine clay particles. The limited number of samples taken at low salinities and the lack of a riverine end-member make it difficult to quantify the desorption flux of Ba.

At salinity greater than 15, most of the points lie scattered within a limited range of [Ba] values (between 40 and 60 nmol L⁻¹ in 1994 and between 50 and 70 nmol L⁻¹ in 1995), showing no apparent increasing or decreasing trend with increasing salinity. A few samples with lower [Ba] (as low as 12 nmol L⁻¹) were observed. Whether these low [Ba] values were the result of biological uptake or dilution by sea ice meltwater is unclear based on available data.

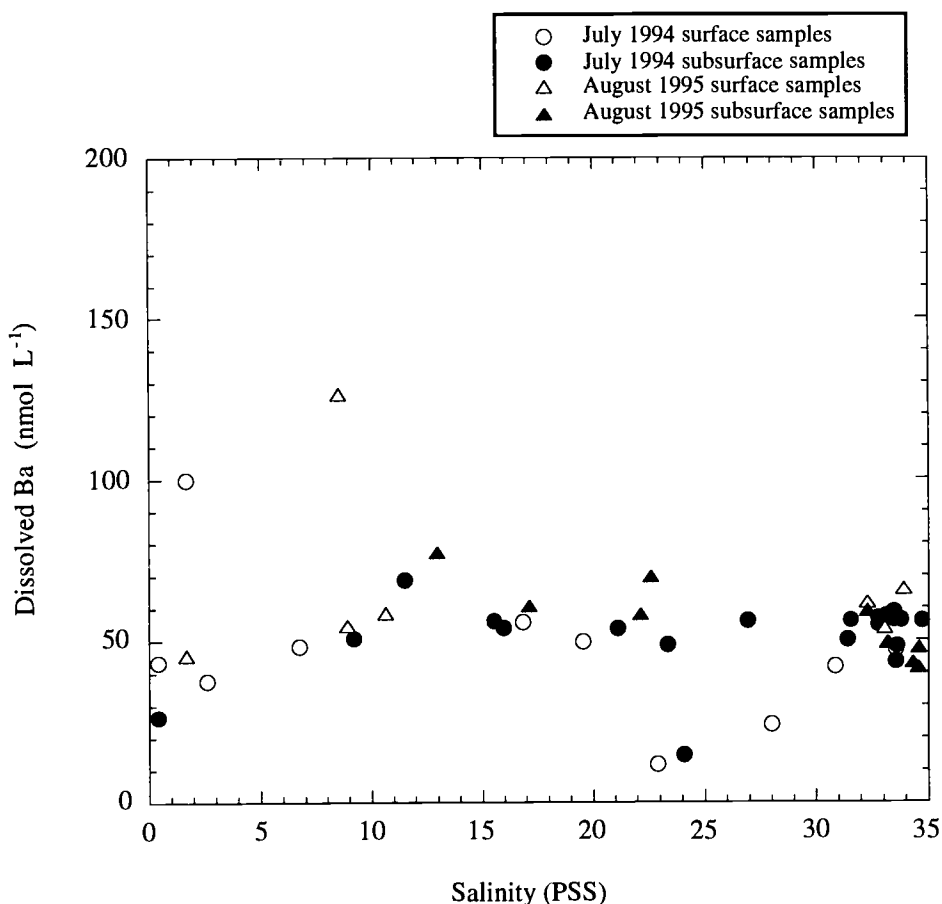


Figure 12: Dissolved Ba in the estuary of the Pechora River in 1994 and 1995.

3.2.2.3 *Ob, Yenisey and Pyasina rivers (Kara Sea)*

In the Ob River in 1993 and in the Yenisey River in both 1993 and 1995, [Ba] increased to maximum values of 91, 175, and 115 nmol L⁻¹ respectively (50-130% above their riverine values) as salinity increased from near-zero to 5 (Figures 13a, 14a, and 14c). Such increases suggest desorption of Ba from suspended riverine clay particles as seawater cations are encountered in the estuary. Past the maxima at low salinity, [Ba] generally decreased as salinity increased to oceanic values. Many of the points at intermediate salinity lie below conservative mixing lines between the Ba maxima and the high-salinity samples. Simultaneous observations of low nitrate in these rivers (Dai and Martin 1995) suggest biological uptake of Ba resulted in these relatively Ba-depleted samples. Dilution

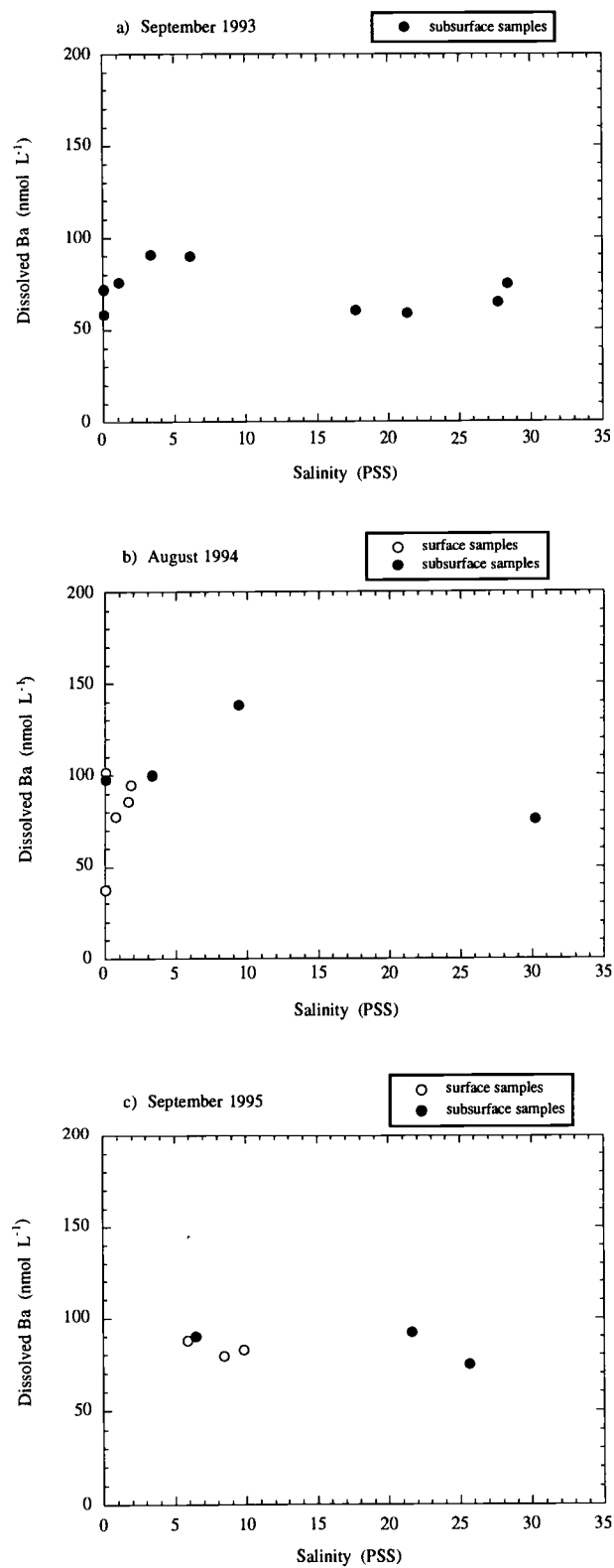


Figure 13: Dissolved Ba in the estuary of the Ob River in (a) 1993, (b) 1994 and (c) 1995.

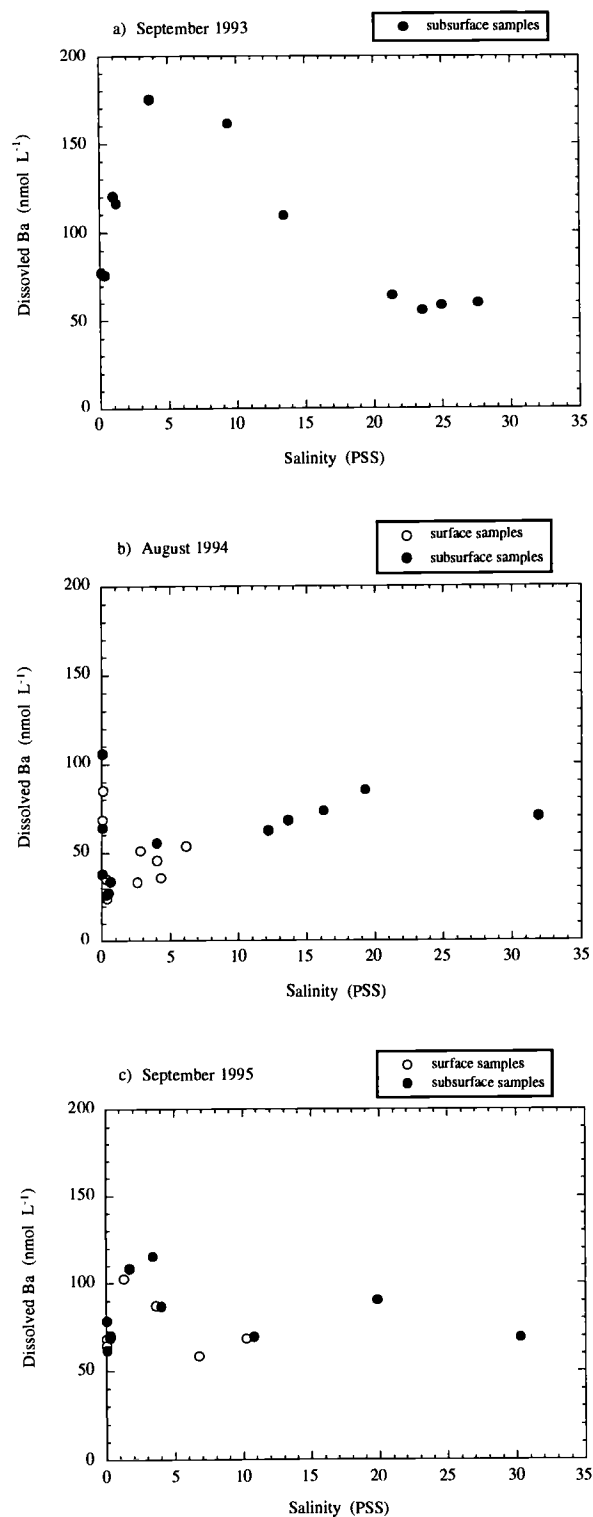


Figure 14: Dissolved Ba in the estuary of the Yenisey River in (a) 1993, (b) 1994, and (c) 1995.

by sea ice meltwater or mixing with modified shelf waters with low [Ba] may have also influenced these samples.

In 1994, [Ba] sharply decreased in both the Ob and Yenisey rivers as salinity increased from near-zero to 1 (Figures 13b and 14b). Over this salinity range, [Ba] in the Ob River dropped from 102 nmol L⁻¹ at the furthest-upstream station (above the Ob-Taz confluence) to 37 nmol L⁻¹ at a station approximately 100 miles downstream (a 63% decrease), and [Ba] in the Yenisey River dropped from 106 nmol L⁻¹ at the furthest-upstream station to 28 nmol L⁻¹ at a station near the mouth of the river (a 74% decrease). As salinity increased above 1, [Ba] increased steadily in both rivers, reaching maxima of 138 nmol L⁻¹ at salinity 9.4 (Ob River) and 86 nmol L⁻¹ at salinity 19.2 (Yenisey River). In both rivers, [Ba] started to decrease again as salinity increased above 20. As with the 1993 data, the reduced values of [Ba] observed at low to intermediate salinities likely resulted from biological uptake associated with seasonal plankton activity in the surface waters of these estuaries at this time of year; dilution by ice meltwater or modified shelf waters with low [Ba] may also contribute.

A limited number of samples were collected in the Ob estuary in 1995 and near the mouth of the Pyasina River in 1994 and 1995 (Figures 13c and 15). No data were obtained for salinity ≤ 5 , the range in which sharp increases or decreases in [Ba] were observed in the 1993-1994 Ob data and 1993-1995 Yenisey data. Values of [Ba] ranged from 75 to 92 nmol L⁻¹ in the 1995 Ob samples, from 51 to 70 nmol L⁻¹ in the 1994 Pyasina samples, and from 64 to 118 nmol L⁻¹ in the 1995 Pyasina samples.

3.2.2.4 *Lena, Khatanga and Yana rivers (Laptev Sea)*

In the Lena estuary in 1995, [Ba] generally increased as salinity increased from near-zero to 10 (Figure 16). Two samples at low salinity had highly elevated [Ba]--the surface sample at station 68 ([Ba] = 130 nmol L⁻¹, S = 3.7) and the surface sample at station 69 ([Ba] = 162 nmol L⁻¹, S = 3.6)--suggest desorption of Ba from riverine clay particles. Values of [Ba] generally decreased as salinity increased above 10. Exceptionally low [Ba]

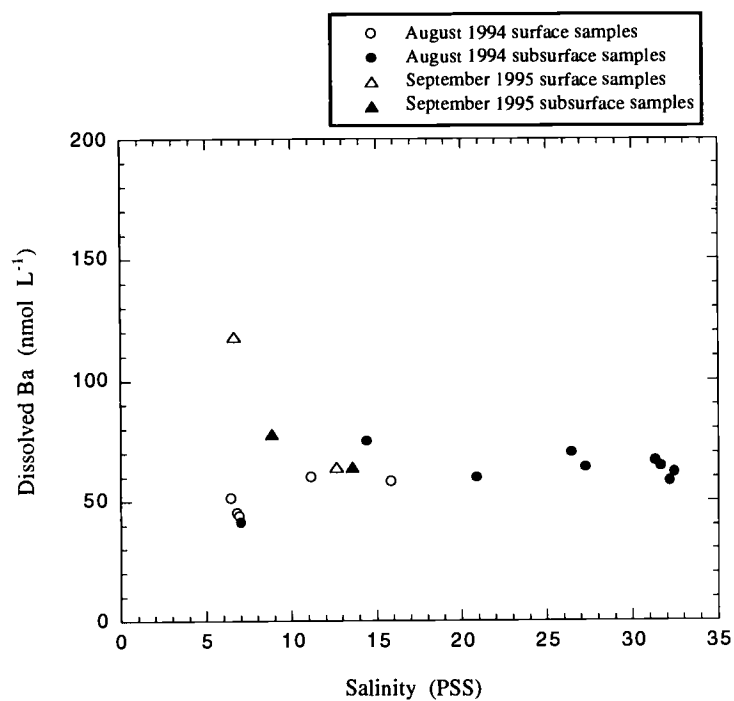


Figure 15: Dissolved Ba in the estuary of the Pyasina River in 1994 and 1995.

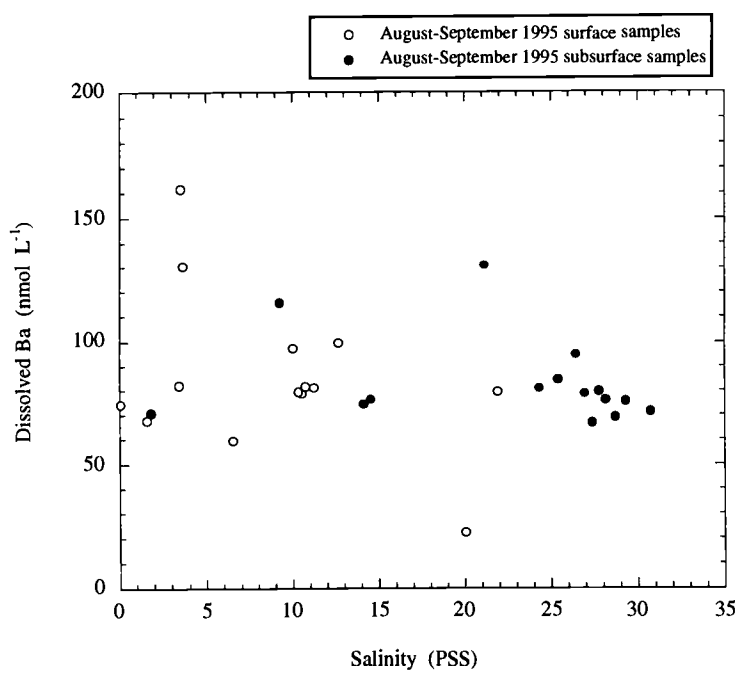


Figure 16: Dissolved Ba in the estuary of the Lena River 1995.

was observed in the surface sample from station 71 ($[Ba] = 22 \text{ nmol L}^{-1}$, $S = 20.0$). This sample, along with the surface sample at station 75 at the mouth of the Khatanga River, suggest the occurrence of a large plankton bloom in the western Laptev Sea which severely depleted Ba from the surface water. Circulation patterns in this region indicate general eastward advection of surface waters in the western Laptev Sea (Pavlov et al. 1996), which is consistent with the somewhat low $[Ba]$ observed in the surface samples from stations 60-67. A relatively high $[Ba]$ value was observed in the sample taken from 9 m depth at station 70 in the Buorkhaya Gulf. Based on anomalous $\delta^{18}\text{O}$ values observed in the Buorkhaya Gulf in 1989, it was hypothesized that Lena River water can become entrapped and recirculate in this area (Létolle et al. 1993).

The samples collected in 1995 from the Khatanga estuary had values of salinity ranging from 16 to 33 (Figure 17). Over this salinity range, $[Ba]$ remained fairly constant, falling between 41 and 50 nmol L^{-1} in all of the samples except the surface sample at station 75 ($[Ba] = 13 \text{ nmol L}^{-1}$, $S = 26.7$). In the samples obtained in 1995 near the mouth of the Yana River, $[Ba]$ ranged between 83-104 nmol L^{-1} , showing a slight decreasing trend as salinity increased between 2 and 16 (Figure 17). No samples were obtained outside this salinity range in this region.

3.2.2.5 *Indigirka and Kolyma rivers (East Siberian Sea)*

In the samples obtained in 1995 from the Indigirka estuary, $[Ba]$ increased from 113 nmol L^{-1} at salinity 2.8 (surface sample at station 43-X) to 172 nmol L^{-1} at salinity 8.5 (surface sample at station 43) (Figure 18). This increase in $[Ba]$ in the estuary suggests desorption of Ba from riverine particles; but the small number of samples taken at low salinities and the lack of any riverine end-member make it difficult to quantify the extent to which desorption affected $[Ba]$ in this area. At salinities above 10, $[Ba]$ generally decreased with increasing salinity although the data show a good deal of scatter. Relatively low $[Ba]$ values were observed in the surface samples at the two northernmost stations in an offshore transect starting near the mouth of the Indigirka river--stations 52 ($[Ba] = 49$

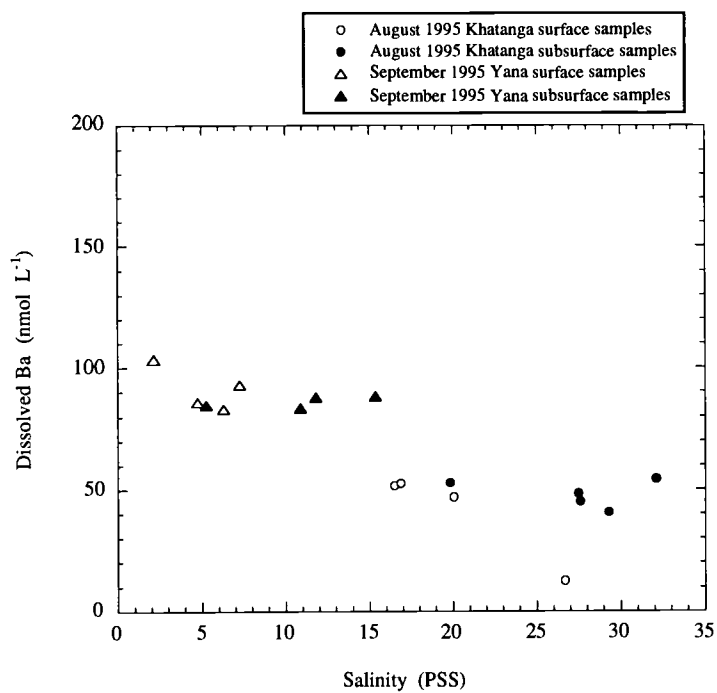


Figure 17: Dissolved Ba in the estuaries of the Khatanga and Yana rivers in 1995.

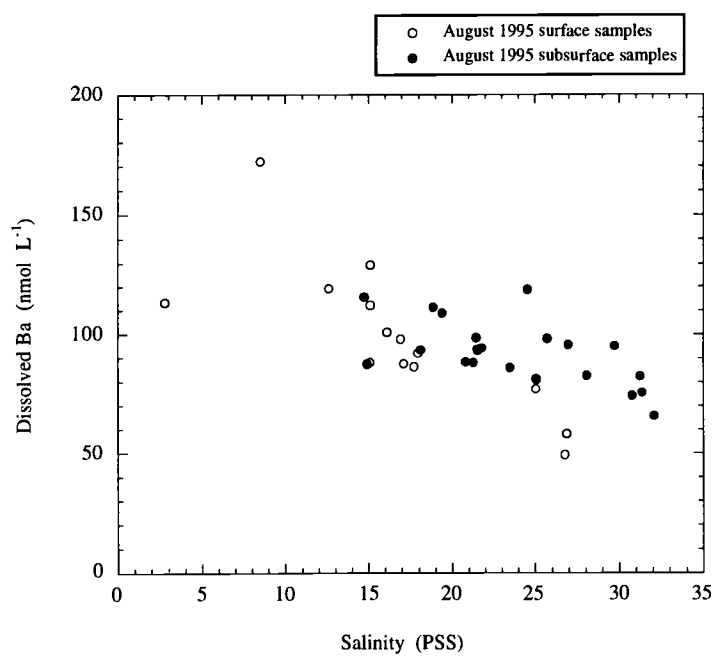


Figure 18: Dissolved Ba in the estuary of the Indigirka River in 1995.

nmol L^{-1} , $S = 26.8$) and 53 ($[\text{Ba}] = 58 \text{ nmol L}^{-1}$, $S = 26.9$). Biological drawdown, dilution by ice meltwater, or mixing with relatively Ba-depleted waters advected from the north and west are all plausible explanations for the low $[\text{Ba}]$ values in these samples. Samples obtained in 1995 near the mouth of the Kolyma River had values of salinity ranging from 11 to 29 (Figure 19). Over this salinity range, $[\text{Ba}]$ remained fairly constant, ranging between 79 and 85 nmol L^{-1} .

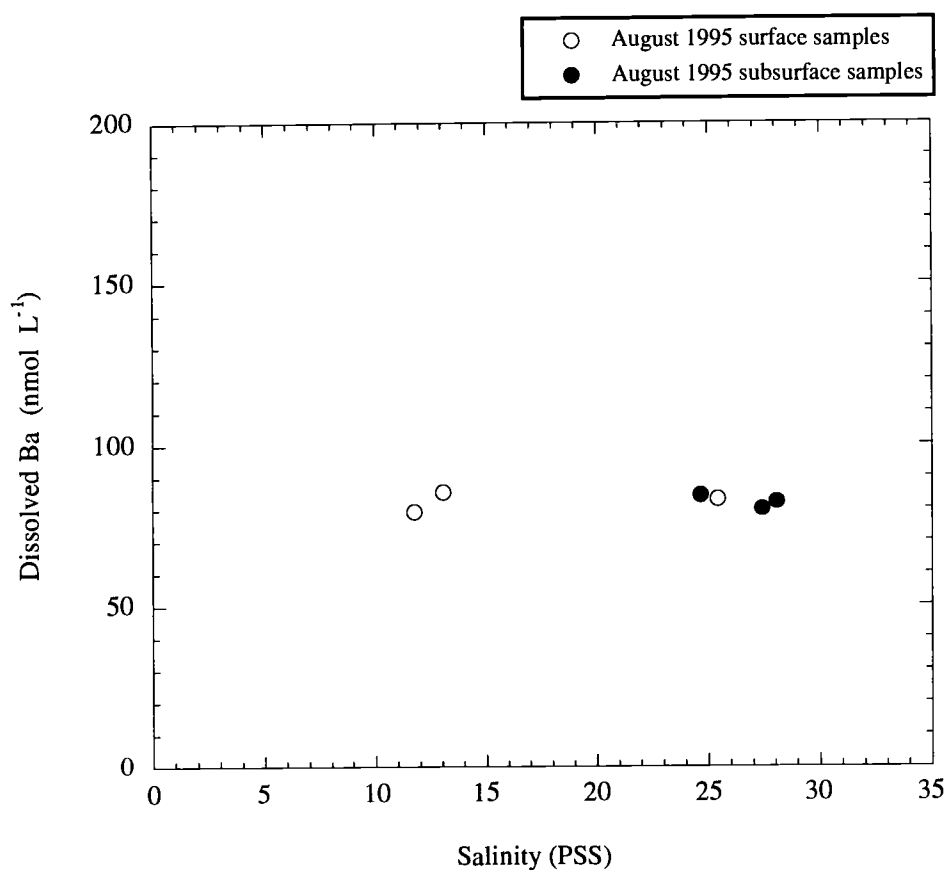


Figure 19: Dissolved Ba in the estuary of the Kolyma River in 1995.

3.3 Discussion

3.3.1 Elevated Ba in Mackenzie River relative to Eurasian rivers

Much higher [Ba] values were observed in the samples collected in the Mackenzie River estuary than in the samples collected in Eurasian river estuaries and seas (Figure 20).

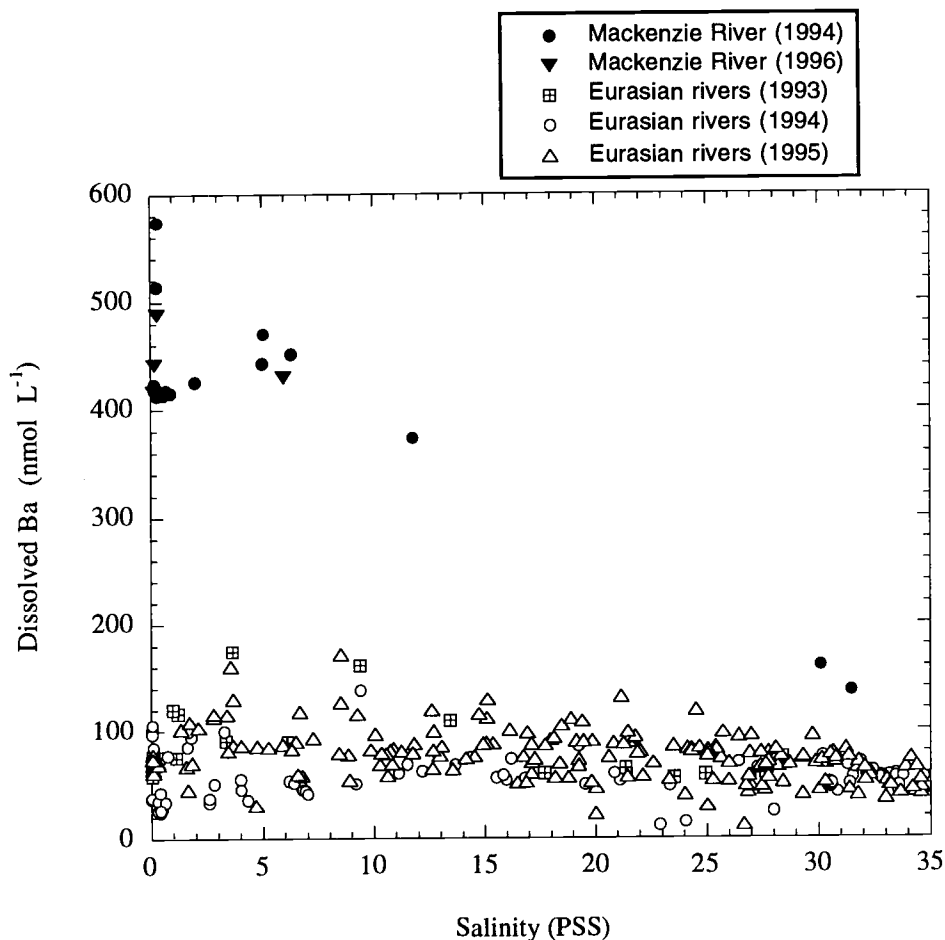


Figure 20: Composite plot of dissolved Ba versus salinity for 311 water samples collected between 1993 and 1996 from the estuaries of the ten largest rivers discharging directly into the Arctic Ocean.

In riverine waters (salinity < 1), [Ba] values between 413-574 nmol L⁻¹ were observed in the Mackenzie samples, and values between 24-120 nmol L⁻¹ were observed in the Eurasian samples. The high [Ba] observed in the Mackenzie River are consistent with

measurements of high [Ba] values in low-latitude rivers bearing large suspended sediment loads, such as the Mississippi and Ganges-Brahmaputra rivers (Hanor and Chan 1977; Edmond et al. 1978; Carroll et al. 1993).

Since the inorganic composition of surface waters in the Mackenzie River system is primarily controlled by the bedrock encountered by these waters during their residence in the drainage basin (Reeder et al. 1972), the high Ba load of the Mackenzie River implies the existence of Ba-rich rocks in its watershed. The marine sedimentary rocks which occupy much of the drainage area of the Mackenzie River likely contain considerable amounts of biogenic Ba (e.g., Collier and Edmond 1984; Bishop 1988; Dymond et al. 1992). Economic deposits of barite have been documented in regions of British Columbia and the Yukon Territory drained by the Mackenzie River (Dawson 1975; Dawson 1977; Morrow et al. 1978). In addition to the chemical composition of rocks in the drainage basin, their susceptibility to weathering must also be considered. For example, slow-moving rivers draining Cretaceous shales in north-central Alberta have very high abundances of B, Li, Zn, Cu, U, and Fe compared with the faster-moving, larger rivers in the Mackenzie watershed; this is thought to reflect the relative ease of removal during weathering of trace and minor elements adsorbed on clay components of the shales (Reeder et al. 1972). Similar behavior would be expected for Ba, which is known to participate in adsorption-desorption interactions with clay particles (Hanor and Chan 1977; Edmond et al. 1978; Li and Chan 1979; Carroll et al. 1993).

As higher salinities are approached, the riverine Ba signals are attenuated by dilution with oceanic waters having relatively low [Ba]. At salinities above 30, [Ba] ranged between 137-161 nmol L⁻¹ in the Mackenzie samples, while [Ba] ranged between 37-83 nmol L⁻¹ in the Eurasian samples. These data show that while the riverine [Ba] signals become reduced at higher salinities, shelf waters influenced by the Mackenzie River still are clearly elevated in [Ba] relative to shelf waters influenced by Eurasian rivers. Data

presented in Chapter 4 demonstrate that the difference between [Ba] levels in the Mackenzie and Eurasian rivers is reflected in surface distributions of [Ba] in the interior basins of the Arctic Ocean.

3.3.2 Interannual and seasonal variability in riverine Ba signals

Multi-year data were obtained only for the Ob and Yenisey Rivers (1993-1995), the Pechora and Pyasina Rivers (1994-1995), and the Mackenzie River (1994 and 1996). Due to the limited number of samples at low salinities in some years, these data are not sufficient for defining the temporal variability of [Ba] in these rivers. It is apparent, however, that while some degree of interannual variability exists for [Ba] in the riverine end-members, the year-to-year differences for individual rivers are generally smaller than the difference between the Mackenzie River and Eurasian rivers (Figures 11-15). Additional data, especially from samples taken at fresh to low salinities in the estuaries, will be necessary to quantitatively assess the interannual variability in [Ba] signals of Arctic rivers.

Our only information about the seasonal variability in [Ba] signals of Arctic rivers comes from comparing the samples collected from the Mackenzie estuary in 1994 and 1996 (Figure 11); while the 1994 samples were collected during low-discharge, completely ice-covered conditions in early spring, the 1996 samples were collected during high-discharge, completely ice-free conditions in the summer. Despite these widely different hydrologic conditions, [Ba] values observed at low salinities (< 1) in the 1996 samples (417-489 nmol L⁻¹) were similar to [Ba] values observed in the 1994 samples having similar salinity (410-574 nmol L⁻¹). These data suggest that high [Ba] values persist throughout the year in the Mackenzie River, despite variability in hydrologic conditions. These data further suggest that the difference observed between [Ba] values in the Mackenzie River and [Ba] values observed in Eurasian rivers (which were all sampled during high-discharge, completely ice-free conditions in the summer) was not merely due to variations in riverine [Ba] signals

associated with seasonally varying hydrologic conditions. Additional data from Eurasian rivers during periods of complete ice coverage and data collected from individual rivers under different seasonal conditions within a single year are required to fully evaluate seasonal variability in [Ba] signals of Arctic rivers.

4. BARIUM DISTRIBUTIONS IN THE SURFACE MIXED LAYER AND HALOCLINE OF THE ARCTIC OCEAN

4.1 Field program

The purpose of this program was to examine basin-wide distributions of [Ba] in the Arctic Ocean in light of known sources and sinks. Of particular interest was determining whether riverine [Ba] signals persisted beyond the shelves and into the interior basins of the Arctic Ocean, and whether oceanic waters influenced by North American and Eurasian sources of river water could be distinguished by their Ba content.

Water samples for Ba analyses were collected during six oceanographic cruises to the Arctic in 1993 and during the Arctic Ocean Section in 1994 (Table 2, Figure 21). On all of the cruises except SCICEX-93 (which took place on board the nuclear submarine *USS Pargo*), water samples were obtained from depths throughout the water column using standard Niskin bottles deployed on a rosette equipped with a CTD profiler. Samples from SCICEX-93 were obtained by casting standard Niskin bottles on a hydrowire deployed from a gantry mounted on the hull of the surfaced submarine. Unfiltered samples for Ba analyses were collected into high-density polyethylene (HDPE) bottles previously leached overnight with 1N HCl at 50°C, rinsed in reverse osmosis-deionized water (RODW), and dried in a laminar flow bench. Dissolved Ba concentrations were determined by ID-ICPMS as described in Chapter 3.

4.2 Results

4.2.1 Surface mixed layer in 1993

For each of the 344 stations occupied between June and October 1993, profiles of both continuous-sensor and bottle-derived temperature, salinity and depth records were examined to determine the depth of the surface mixed layer. At 246 stations, a relatively fresh, homogenous surface layer was observed, separated from underlying waters by a

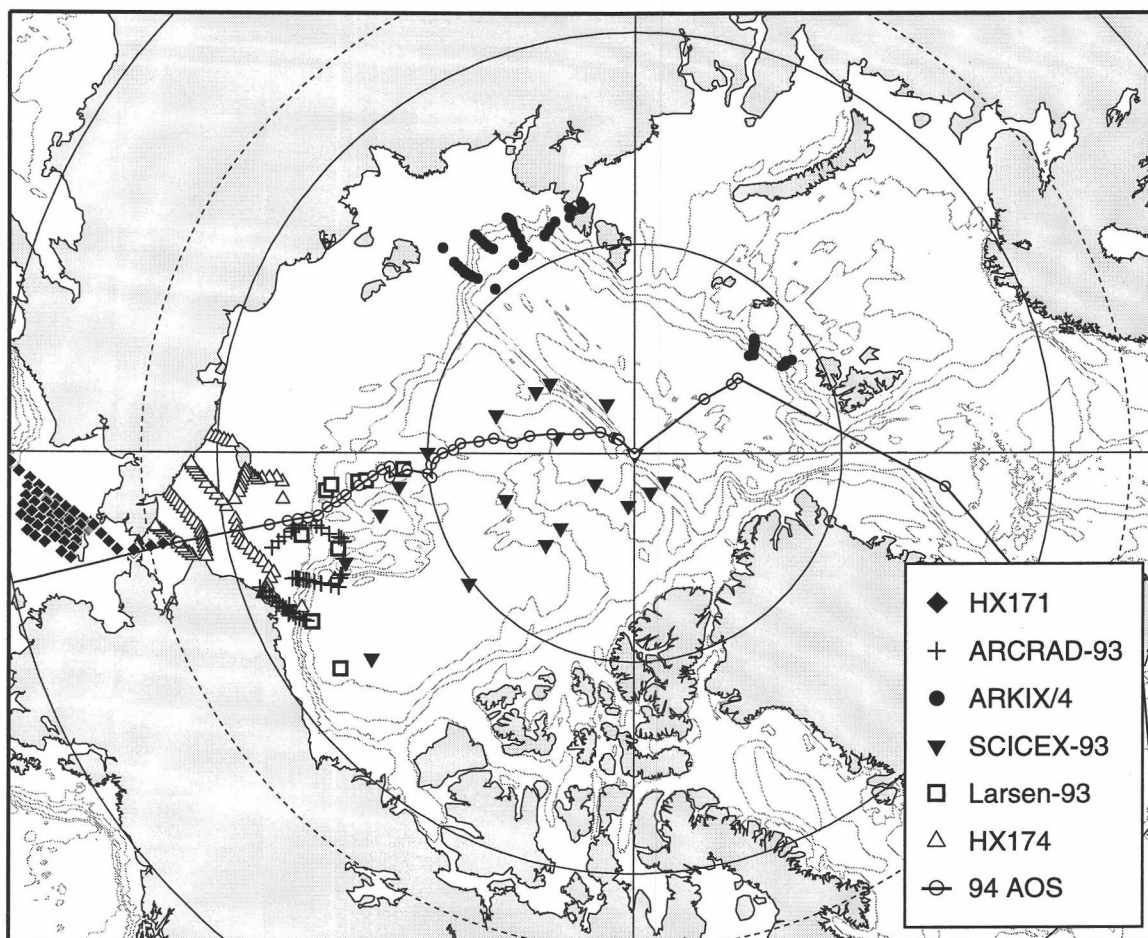


Figure 21: Stations occupied during six oceanographic cruises to the Arctic in 1993 and during the 1994 Arctic Ocean Section.

Table 2: Oceanographic cruises to the Arctic in 1993 and 1994. At all of the stations occupied, a CTD profiler was deployed to obtain continuous profiles of salinity and temperature. Samples for Ba analyses were not collected at every station.

Cruise	Vessel	Dates	Sampling Areas	Total number of stations occupied	Stations with Ba samples
HX171	R/V Alpha Helix	11 Jun-01 Jul 1993	Bering and Chukchi seas	75	43
ARCRAD-93	USCGC Polar Star	30 Jul--15 Aug 1993	Chukchi and Beaufort seas, Canada Basin	62	46
ARK IX/4	R/V Polarstern	10 Aug--20 Sep 1993	Barents and Laptev seas, Eurasian Basin	64	56
SCICEX-93	USS Pargo	26 Aug--11 Sep 1993	Canada, Makarov and Eurasian basins	20	17
Larsen-93	CCGS Henry Larsen	29 Aug--23 Sep 1993	Chukchi Sea, Canada Basin	9	9
HX174	R/V Alpha Helix	09 Sep--10 Oct 1993	Bering and Chukchi seas, Canada Basin	114	68
AOS 94	USCGC Polar Sea CCGS Louis S. St-Laurent	25 Jul--31 Aug 1994	Chukchi Sea, Canada, Makarov and Eurasian basins	39	39*

* The samples for Ba analyses were collected on the *CCGS Louis S. St-Laurent*

steep salinity gradient; a discontinuity and/or gradient in the temperature profile often coincided with the salinity gradient (Figures 22a and 22c). Assigning a depth to the mixed layer at such stations was straightforward. At 98 stations, a unique, distinct, homogenous surface layer was not observed and more than one depth could have been assigned to the mixed layer; the majority of such stations were located over the shelves of the marginal Arctic seas, and the structure observed in the surface layer reflects seasonal processes occurring in those areas. An example is HX174 Station 73, located between Wrangel Island and the Siberian coast (Figure 22b)--a depth of 28 m was assigned to the surface mixed layer at this station, but a depth of 8 m would have been another possible choice. Depths assigned to the surface mixed layer ranged from 5-46 m, with deeper mixed layers (> 20 m) generally observed in the basins of the Arctic interior and shallower mixed layers (< 20 m) observed over the shelves and slopes. Exceptions include areas in the central Chukchi Sea and over parts of the slope north of the Laptev Sea where deeper surface mixed layers were observed.

At each station, a mean value of salinity for the surface mixed layer was calculated from all CTD measurements taken at depths within the surface mixed layer. The distribution of salinity in the surface mixed layer is shown in Figure 23 (the false-color contour images appearing in this paper were generated from the data using the Barnes objective analysis technique ((Barnes 1973; Koch et al. 1983)). Mean surface mixed layer salinity ranged from 25.1 to 33.6. Highest values (32.5-33.6) were observed north of the Barents Sea and over the slope north of the Laptev Sea (adjacent to the region of high salinity north of the Laptev Sea were areas of low salinity (as low as 28) over the shelf near the Novosibirskie Islands and in Vilkitsky Strait). High values (32.8-33.2) were also observed in the Eurasian Basin and central Makarov Basin. Values between 28.5 and 30.0 were generally observed in the Canada Basin, with higher values (30.0-30.5) over the Chukchi Cap and Arlis Plateau and lower values (26.8-28.5) near the southern edge of the Canada Basin. Mean surface mixed layer salinity in the central Chukchi Sea ranged

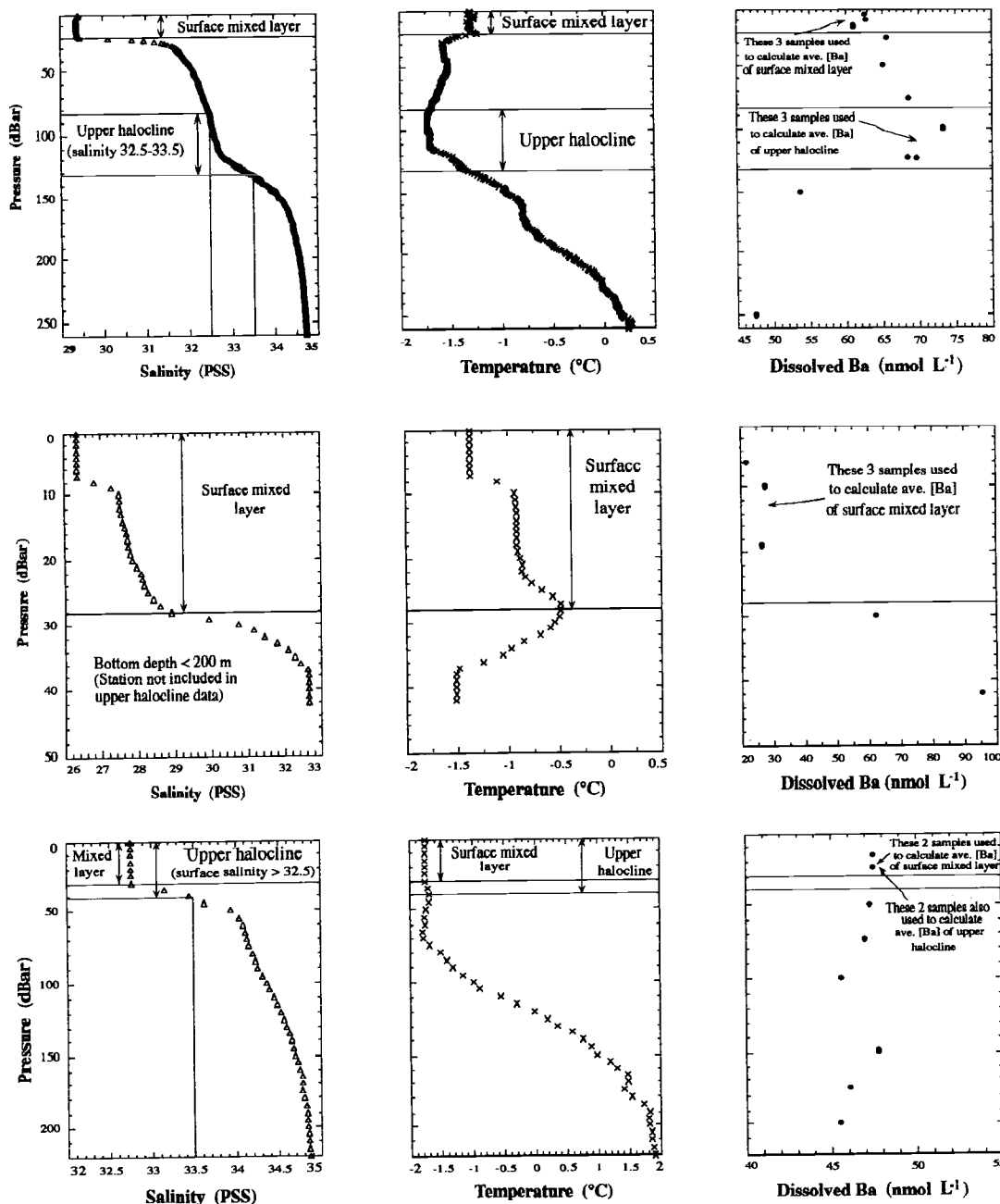


Figure 22: Profiles of salinity, temperature and dissolved Ba at (a) ARCRAD-93 Station 40 north of the Chukchi shelf break in the vicinity of the Chukchi Cap (74.50° N, 166.50° W), occupied on 10 August 1993; (b) HX174 Station 73 between Wrangel Island and the Siberian coast (69.90° N, 177.93°E), occupied on 4 October 1993; and (c) ARK IX/4 Station 51 north of the Laptev shelf break (77.86° N, 125.59° E), occupied on 10 September 1993.

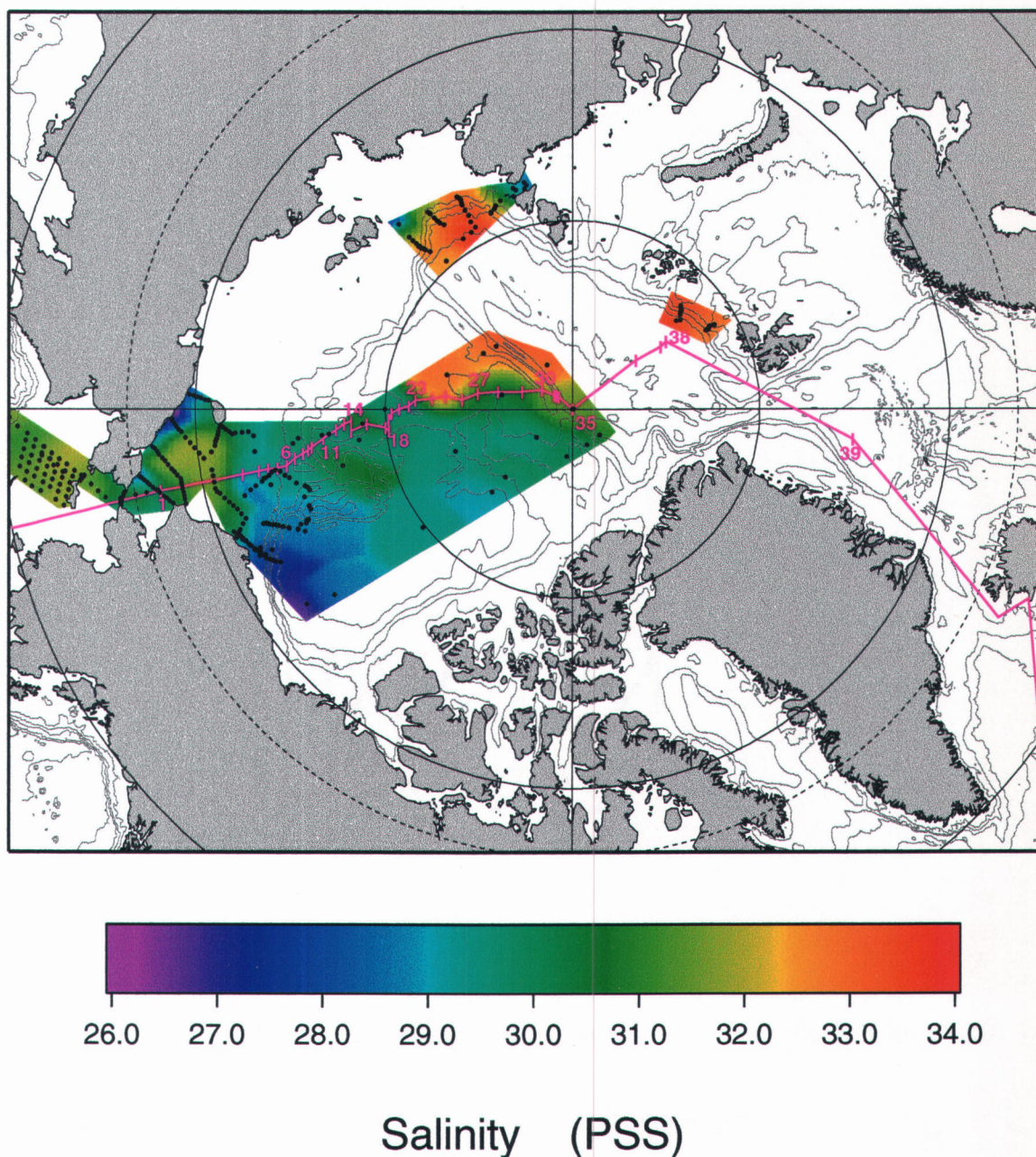


Figure 23: Distribution of salinity in the surface mixed layer in 1993 (the following parameter values were used for the Barnes objective analysis: horizontal and vertical grid spacing (G_x and G_y) = 10 nautical miles, numerical convergence parameter (γ) = 0.2, number of iterations (i) = 2, horizontal data spacing (Δn_x) = 100 nautical miles, vertical data spacing (Δn_y) = 70 nautical miles). Black dots show the locations of all 1993 stations included in the surface mixed layer salinity data. The 1994 AOS cruise track and stations are superimposed in magenta on this figure for reference when comparing 1993 and 1994 results.

between 31.0 and 32.0, with lower values (28.0-30.0) in the northern Chukchi Sea and western Chukchi Sea near Wrangel Island and extremely low values (25.1-27.5) in the western Chukchi Sea along the Russian coast. Values in Bering Strait ranged between 26.9 and 32.6, while values in the Bering Sea ranged between 30.8 and 32.1.

Samples for Ba analysis were collected at 239 of the 344 stations occupied in 1993. There were 183 stations at which more than 1 sample for Ba analysis was collected from within the surface mixed layer. For each of these stations, a mean value of Ba concentration for the surface mixed layer was calculated based from all samples collected at depths within the surface mixed layer (lack of detailed sampling throughout the water column eliminated any advantage to depth-weighted averaging). At 129 of these stations, Ba concentrations were fairly uniform throughout the surface mixed layer; at 54 of these stations, Ba concentrations were not vertically uniform in the surface mixed layer. There were 42 stations at which only 1 sample for Ba analysis was collected from within the surface mixed layer. For each of these stations, the Ba concentration of the single sample was assigned as the mean value of Ba concentration for the surface mixed layer. There were 9 stations at which no samples for Ba analysis were collected from depths within the surface mixed layer; these stations were excluded from the discussion of Ba in the surface mixed layer. Results from an additional 5 stations (2 from SCICEX-93 and 3 from ARK IX/4) were rejected due to ambiguities in depth assignments and other sample identification problems.

The distribution of Ba in the surface mixed layer in 1993 is shown in Figure 24. Mean surface mixed layer Ba concentrations ranged from 19 nmol Ba L⁻¹ to 168 nmol Ba L⁻¹ and were not directly correlated to mixed layer depth. At 89% of the stations, values fell in the range between 35-80 nmol Ba L⁻¹; values below 35 nmol Ba L⁻¹ were limited to areas in the western Chukchi Sea adjacent to the Russian coast and in the vicinity of Wrangel Island, while values above 80 nmol Ba L⁻¹ were limited to the eastern half of Bering Strait and the southern edge of the Canada Basin.

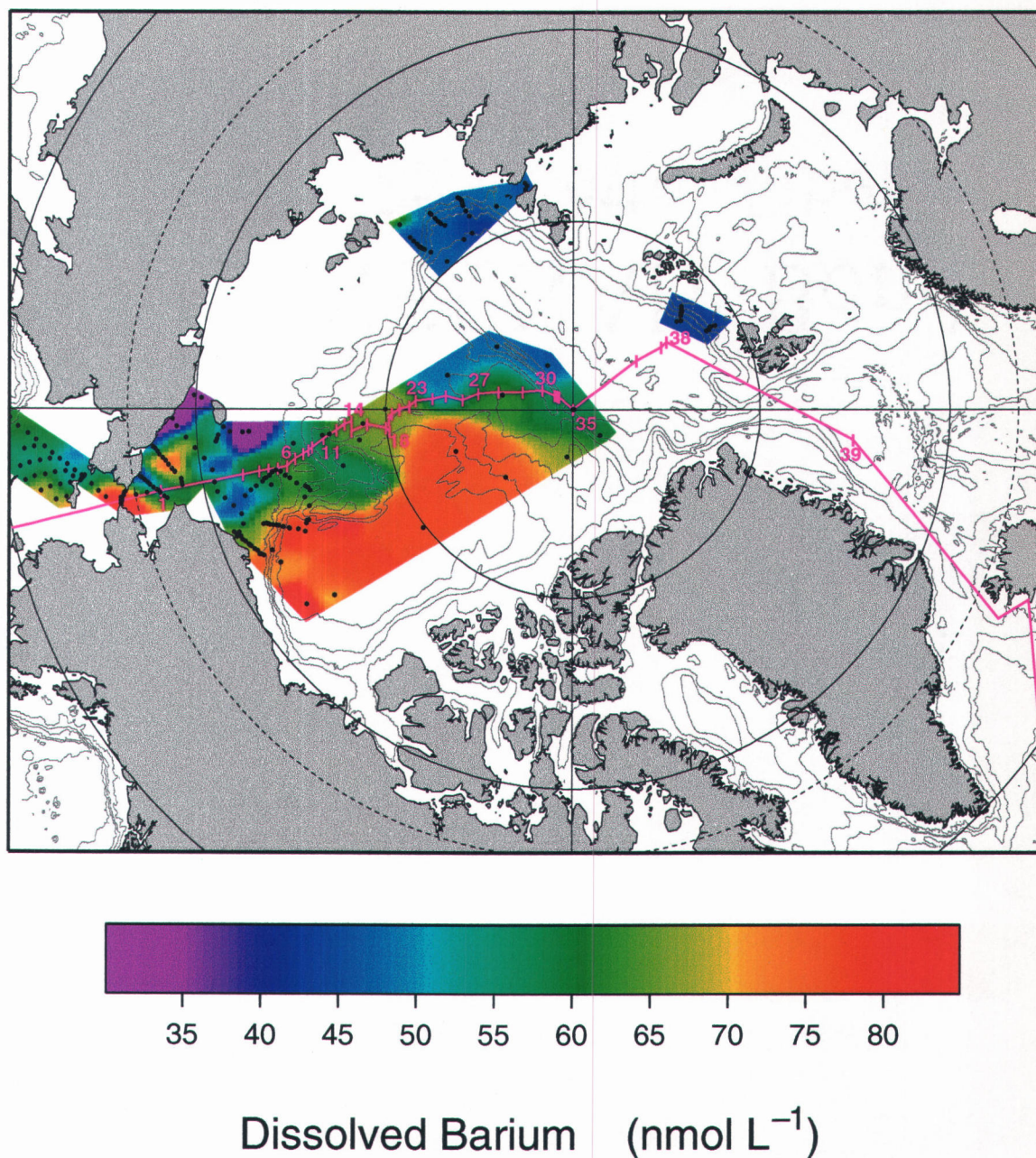


Figure 24: Distribution of Ba in the surface mixed layer in 1993 (G_x and $G_y = 10$ nautical miles, $\gamma = 0.2$, $i = 2$, $\Delta n_x = 100$ nautical miles, $\Delta n_y = 70$ nautical miles). Black dots show the locations of all 1993 stations included in the surface mixed layer Ba data. The 1994 AOS cruise track and stations are superimposed in magenta on this figure for reference when comparing 1993 and 1994 results.

Mean surface mixed layer Ba concentrations between 42 and 45 nmol Ba L⁻¹ were observed north of the Barents Sea, and slightly higher values (45-50 nmol Ba L⁻¹) were observed in the Eurasian Basin, the central Makarov Basin, and the vicinity of the shelf break and slope north of the Laptev Sea (with the exception of one station northwest of the Novosibirskie Islands at which a value of 67 nmol Ba L⁻¹ was observed). High values (> 75 nmol Ba L⁻¹) were observed over most of the Canada Basin, with one notably high value (93 nmol Ba L⁻¹) observed at a station just beyond the slope north of the Beaufort Sea. A branch of water with values between 65-70 nmol Ba L⁻¹ was observed extending over the Arlis Plateau and Mendeleyev Ridge, merging with high-Ba surface waters of the Canada Basin and low-Ba surface waters of the Eurasian Basin in a zone of intermediate values (60-70 nmol Ba L⁻¹) over the northern Makarov Basin and the Lomonosov Ridge in the vicinity of the North Pole.

Over much of the Chukchi Sea and the adjacent Chukchi Cap to the north, mean surface mixed layer Ba concentrations between 55 and 65 nmol Ba L⁻¹ were observed, with areas of elevated values (70-75 nmol Ba L⁻¹) in the central Chukchi Sea, areas of depleted values (40-50 nmol Ba L⁻¹) in the northern Chukchi Sea, and areas of extremely depleted values (< 30 nmol Ba L⁻¹) in the western Chukchi Sea adjacent to the Russian coast and in the vicinity of Wrangel Island. In Bering Strait, values ranged from 50 to 168 nmol Ba L⁻¹, with lower values on the western side and higher values on the eastern side of the strait. Values between 50 and 60 nmol Ba L⁻¹ were generally observed in the Bering Sea, with some elevated values (65-75 nmol Ba L⁻¹) south of St. Lawrence Island.

4.2.2 Upper halocline in 1993

To examine the lateral distribution of Ba in the upper halocline layer, we considered only stations past the shelf break (i.e., stations with bottom depths greater than 200 meters). At each of the 85 such stations occupied during 1993, the upper halocline was taken to be the layer of water having salinity between 32.5 and 33.5. The depth range corresponding to this salinity range was determined from CTD data at each station. At 50

stations, the layer of water with salinity between 32.5 and 33.5 was located entirely below the surface (e.g. Figure 22a). At 30 stations occupied during the ARK IX/4 cruise (all of which were located in the Eurasian sector of the Arctic), salinity at the surface fell between 32.5 and 33.5 (e.g. Figure 22c). At these stations, the upper halocline layer was interpreted to extend from the surface to the depth where salinity of 33.5 was encountered, and the depth range of the upper halocline coincides with that of the surface mixed layer. Five stations north of the Barents and Laptev seas, at which salinity over the entire water column was greater than 33.5, were excluded from the discussion of the upper halocline. The thickness of the upper halocline layer assigned in this manner ranged from 0 to 144 meters, covering depths in the water column between 0 and 226 meters. The layer was thickest in the Canadian Basin, particularly in the southern Canada Basin, and became gradually thinner towards the Eurasian Basin.

There were 47 stations at which more than 1 sample for Ba analysis was collected from within the upper halocline. For each of these stations, a mean value of Ba concentration for the upper halocline was calculated based on all samples collected from depths within the upper halocline (as was the case for the surface mixed layer, lack of detailed coverage over this depth range eliminated any advantage to depth-weighted averaging). There were 22 stations at which only 1 sample for Ba analysis was collected from within the upper halocline. For each of these stations, the Ba concentration of the single sample was assigned as the mean value of Ba concentration for the upper halocline. There were 11 stations at which no samples for Ba analysis were collected from depths within the upper halocline; these stations were excluded from the discussion of Ba in the upper halocline.

The distribution of Ba in the upper halocline in 1993 is shown in Figure 25. Lowest mean upper halocline Ba concentrations (42-45 nmol Ba L⁻¹) were observed north of the Barents Sea, and slightly higher values (45-51 nmol Ba L⁻¹) were observed in the vicinity of the shelf break and slope north of the Laptev Sea, in the Eurasian Basin and

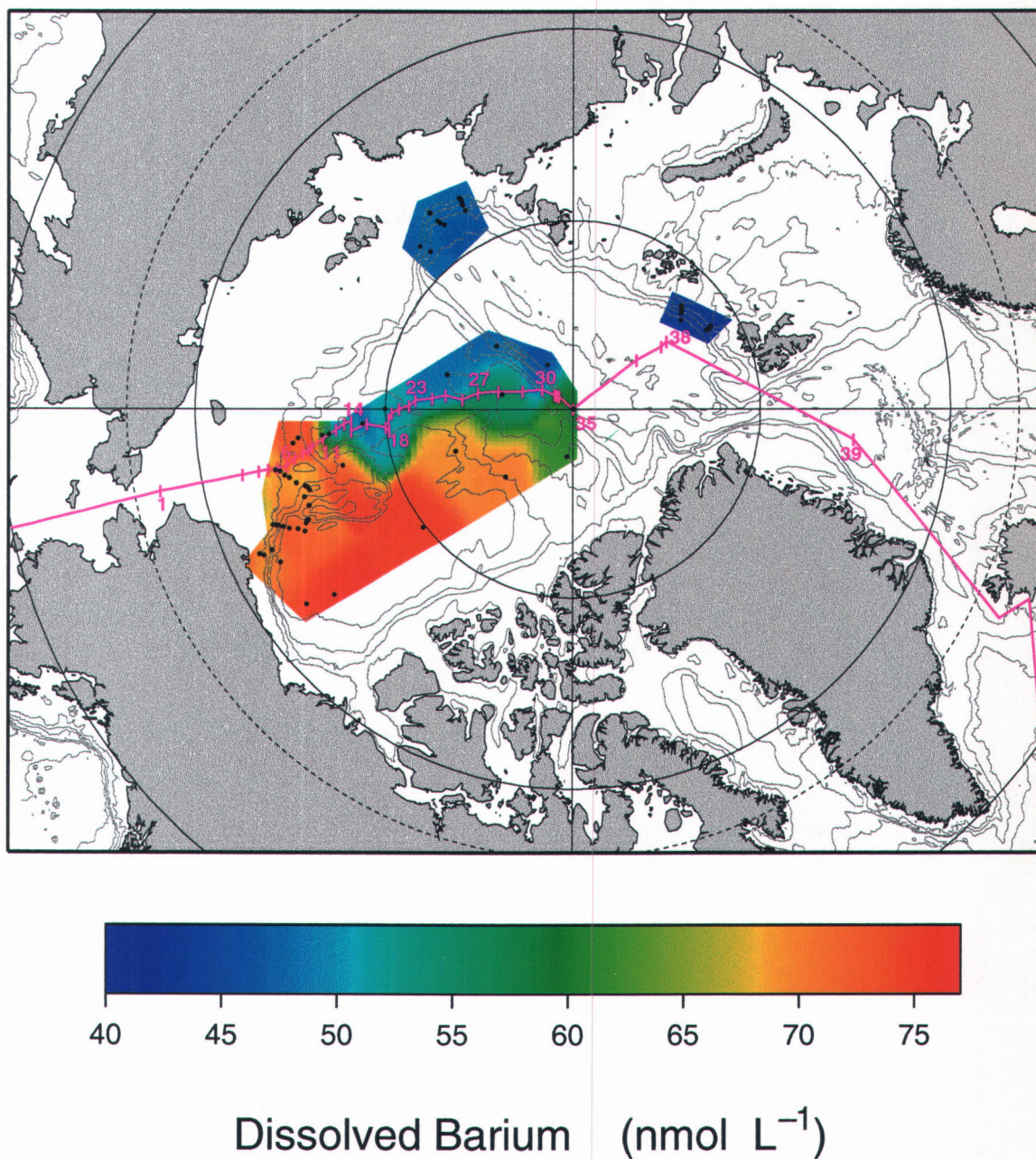


Figure 25: Distribution of Ba in the upper halocline (i.e. the layer of water with salinity between 32.5-33.5) in 1993 (G_x and $G_y = 10$ nautical miles, $\gamma = 0.2$, $i = 2$, $\Delta n_x = 70$ nautical miles, $\Delta n_y = 100$ nautical miles). Black dots show the locations of all 1993 stations included in the upper halocline Ba data. The 1994 AOS cruise track and stations are superimposed in magenta on this figure for reference when comparing 1993 and 1994 results.

central Makarov Basin, and over the Mendeleev Ridge and Arlis Plateau. Mean upper halocline Ba concentrations were highest (70-77 nmol Ba L⁻¹) in the central and southern Canada Basin and over the Chukchi Cap, and slightly lower (65-70 nmol Ba L⁻¹) in the northern Canada Basin and over the north of the Chukchi Sea. A front was observed separating the low-Ba waters characteristic of the eastern Arctic from the high-Ba waters characteristic of the western Arctic, running roughly between the Canada and Makarov basins and extending into a zone of intermediate values (55-65 nmol Ba L⁻¹) over the northern Makarov Basin and Lomonosov Ridge in the vicinity of the North Pole.

4.2.3 1994 Arctic Ocean Section

The distribution of salinity in the upper 400 m along the cruise track of the *CCGS Louis S. St-Laurent* during the 1994 Arctic Ocean Section is shown in Figure 26. Salinity was fairly uniform throughout the water column at station 1 over the southern Chukchi shelf, ranging between 32.6 and 32.7. Across the Arctic interior, a layer of relatively fresh surface water was observed above underlying waters of greater salinity. Surface salinity was lowest north of the Chukchi Sea and over the Arlis Plateau, generally increasing as the transect proceeded across the Makarov Basin and into the Eurasian Basin. Local minima in surface salinity were observed centered on stations 5, 15, 19, 26, 28, 35 and 38.

The distribution of Ba in the upper 400 m along the cruise track of the *CCGS Louis S. St-Laurent* during the 1994 Arctic Ocean Section is shown in Figure 27. Much higher Ba concentrations (> 70 nmol Ba L⁻¹) were observed in the surface waters over the Chukchi shelf (stations 1-6) than were observed in the same area in 1993 (Figure 24). Previous investigators (Falkner et al. 1994) encountered surface Ba concentrations between 12-63 nmol Ba L⁻¹ in the surface waters of the central and eastern Chukchi Sea in September 1992. Between the Chukchi shelf break and the Arlis Plateau (Stations 7-12), surface values dropped to 60-65 nmol Ba L⁻¹, while a prominent subsurface maximum (characterized by values between 65 and 75 nmol Ba L⁻¹) was observed centered at depths between 75 and 100 m. The extent of the subsurface maximum along the AOS94 transect

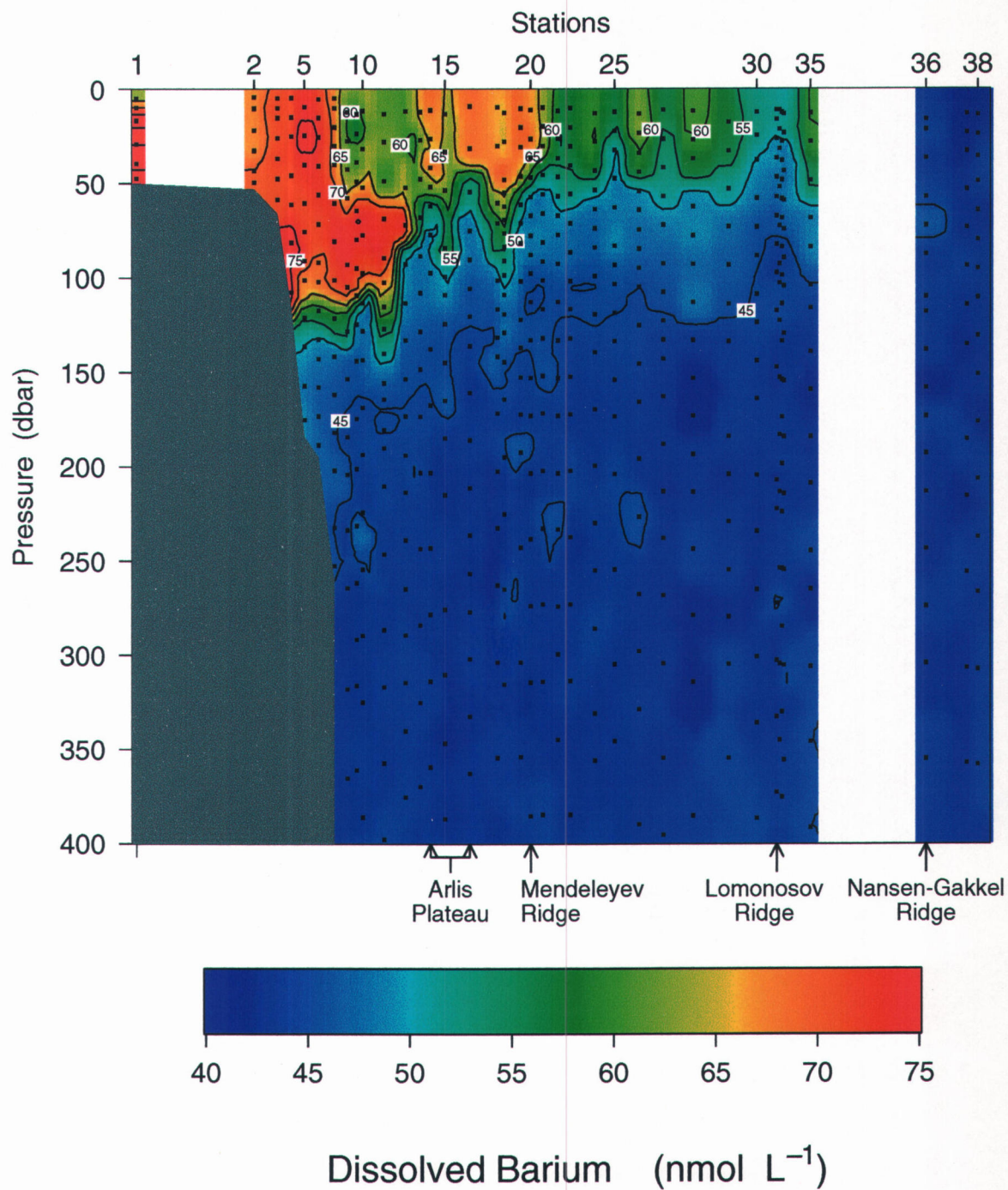


Figure 27: Distribution of Ba along the 1994 Arctic Ocean Section ($G_x = 25$ nautical miles, $G_y = 5$ m, $\gamma = 0.2$, $i = 2$, $\Delta n_x = 25$ nautical miles, $\Delta n_y = 10$ m). Black dots show the locations of samples included in the Ba data.

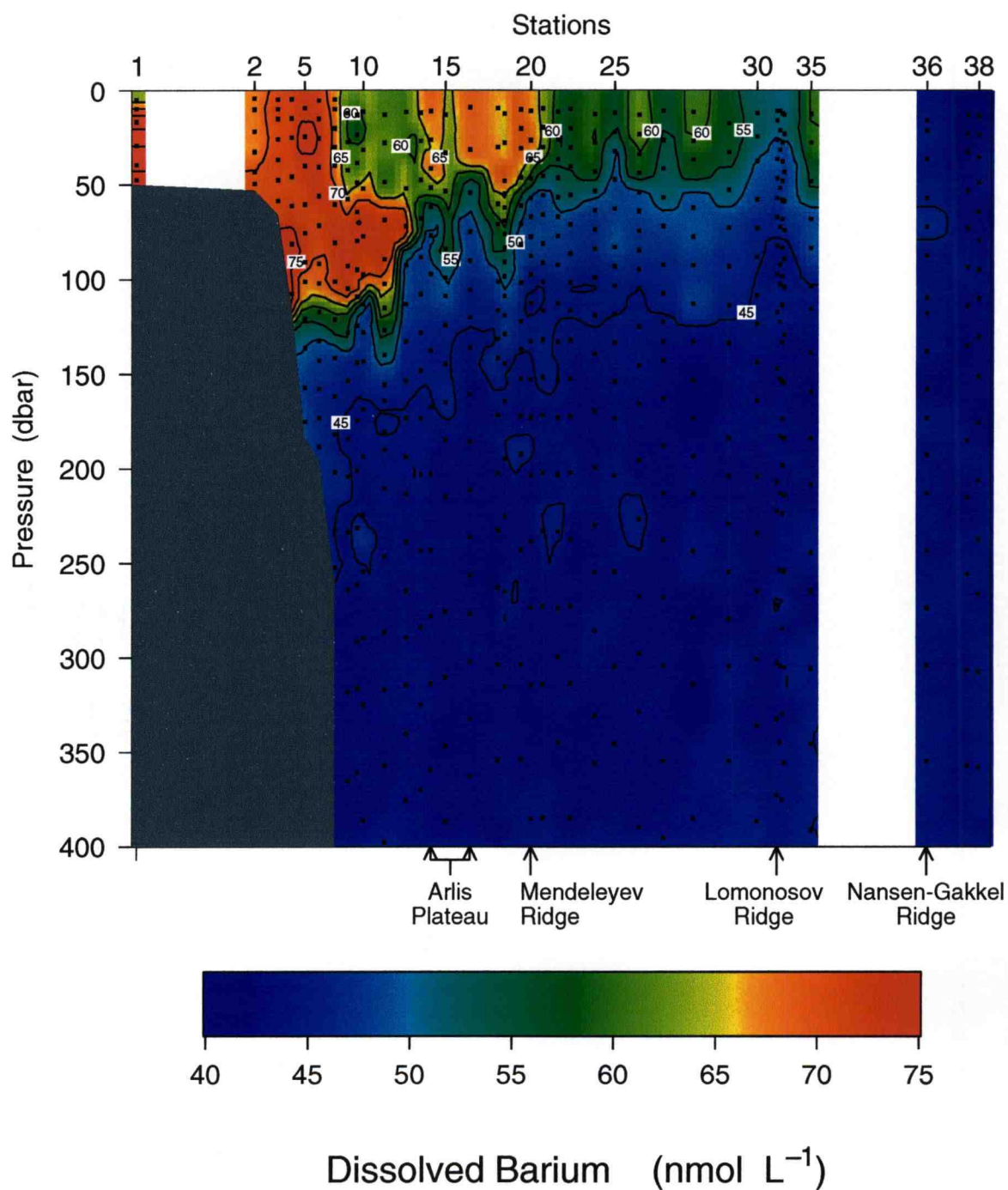


Figure 27: Distribution of Ba along the 1994 Arctic Ocean Section ($G_x = 25$ nautical miles, $G_y = 5$ m, $\gamma = 0.2$, $i = 2$, $\Delta n_x = 25$ nautical miles, $\Delta n_y = 10$ m). Black dots show the locations of samples included in the Ba data.

coincides with the boundary between high-Ba and low-Ba waters in the upper halocline layer observed in this region in 1993 (Figure 25).

A Ba-enriched ($65\text{--}70\text{ nmol Ba L}^{-1}$) feature extending from the surface to depths as great as 55 m was observed over the Arlis Plateau and the Mendeleyev Ridge (Stations 13-21). This feature was located in the same area as the branch of water with similar Ba concentrations observed over the Mendeleyev Ridge in 1993 (Figure 24). As the transect crossed the Makarov Basin to the Lomonosov Ridge (Stations 22-29), intermediate values ($55\text{--}60\text{ nmol Ba L}^{-1}$) were observed down to depths of about 50 m, with local maxima ($60\text{--}65\text{ nmol Ba L}^{-1}$) observed at stations 26 and 28. Values in the upper water column drop to $45\text{--}55\text{ nmol Ba L}^{-1}$ over the Lomonosov Ridge (stations 30-34), rising back up to values above 60 nmol Ba L^{-1} in the surface waters just across the ridge in the Amundsen Basin (station 35). The Ba-enriched features at stations 13-21, 26, 28 and 35 all coincided with local minima in salinity. Relatively low Ba concentrations ($< 45\text{ nmol Ba L}^{-1}$) were observed throughout the water column in the Nansen Basin (Stations 36-38) and below depths of 100-200 m over the entire transect. Results for stations 22-38 are consistent with observations made in the same areas of the Makarov and Eurasian basins in 1993 (Figures 24 and 25).

Measurements of NO (E. P. Jones, personal communication) provided a basis for examining the lower halocline along the AOS94 transect. The lower halocline was taken to be the layer of water having salinity between 34.0 and 34.5 and containing a NO minimum. Highest Ba concentrations ($50\text{--}77\text{ nmol Ba L}^{-1}$) and lowest NO ($223\text{--}380\text{ }\mu\text{mol L}^{-1}$) in the lower halocline were observed over the Chukchi shelf break, with Ba concentrations decreasing steadily and NO increasing steadily as the transect proceeded towards the Eurasian sector of the Arctic (Figure 28). Lowest Ba concentrations ($< 46\text{ nmol Ba L}^{-1}$) and highest NO ($> 400\text{ }\mu\text{mol L}^{-1}$) in the lower halocline were observed in the Eurasian Basin.

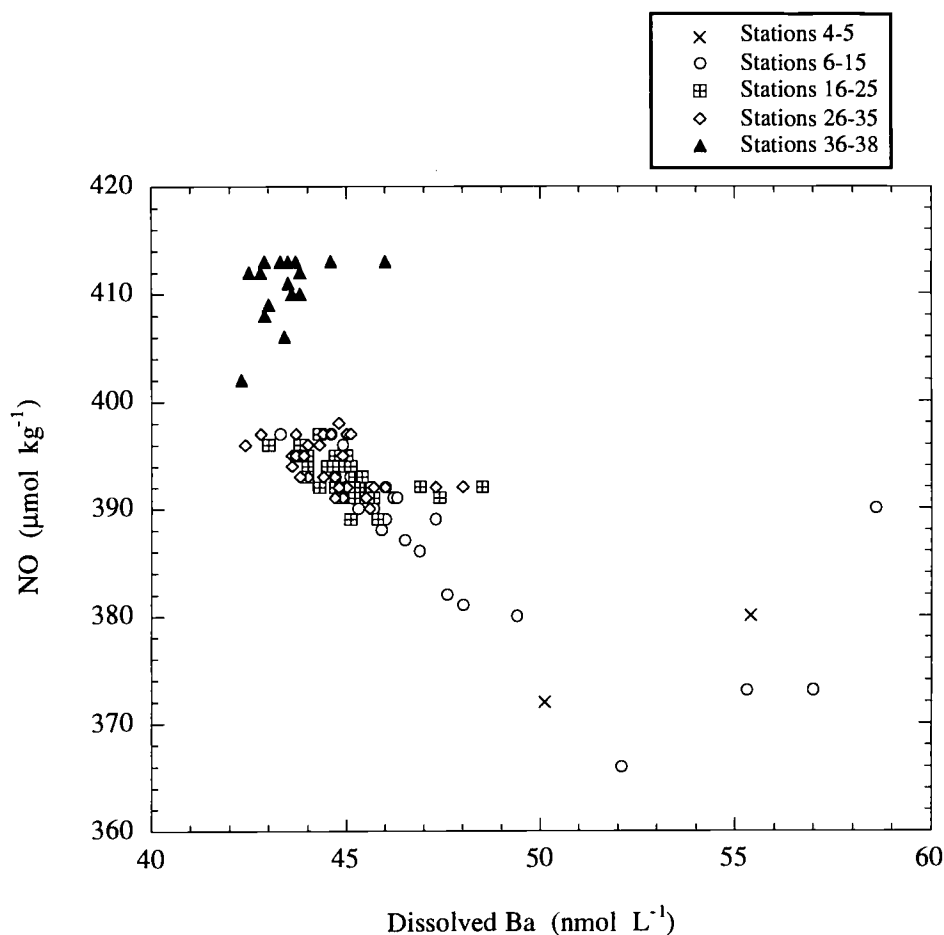


Figure 28: NO versus dissolved Ba for 117 samples taken within the lower halocline (taken to be the layer of water with salinity 34.0-34.5) during the 1994 Arctic Ocean Section. One sample from station 4 ($\text{NO} = 223 \mu\text{mol L}^{-1}$, $[\text{Ba}] = 77 \text{ nmol L}^{-1}$) does not appear within the boundaries of this plot.

4.3 Discussion

While the combined data set for the 6 cruises in 1993 has the advantage of covering a large geographic area (thereby allowing examination of tracer fields in the Arctic on a basin-wide scale), a drawback is that the data are distributed very irregularly within the sampling area. The data from the 1994 Arctic Ocean Section are much more uniformly spaced. The resolution and smoothing scales used for gridding and contouring both sets of data represent a compromise between not obscuring legitimate small-scale features in areas of dense sample coverage and not creating unwarranted detail in areas of sparse sample

coverage. The data were examined thoroughly to verify that the salinity and Ba distributions generated by means of the Barnes objective analysis technique (i.e., Figures 23-27) were consistent with the actual values observed at individual stations; but as holds true for any method of gridding and contouring data, the values in spaces between sampling locations are interpolated estimates and can not be treated as exact.

Because the data were collected over a period of months during the summer and fall (June-October for the 1993 cruises, July-August for AOS94), caution must be exercised when interpreting Figures 23-27 as quasi-synoptic snapshots of basin-wide tracer fields. Although this may not be very realistic for the dynamic areas over the shelves of the marginal seas, it is reasonable for areas in the Arctic interior where waters have longer residence times, are completely ice-covered most or all of the year, and do not experience the large seasonal fluctuations in biological activity and fluvial input characteristic of Arctic nearshore environments.

4.3.1 Surface mixed layer

In both 1993 and 1994, Ba concentrations between 40 and 50 nmol Ba L⁻¹ and high salinity characterized surface waters of the Eurasian Basin, reflecting their North Atlantic origin (Chan et al. 1977). The 1993 distributions of salinity and Ba show surface waters of Eurasian character extending across the Lomonosov Ridge and into the Makarov Basin (Figures 23 and 24). These results are consonant with recent studies (Carmack et al. 1995; McLaughlin et al. 1996; Morison et al. 1997) observing subsurface waters of Eurasian character penetrating the Makarov Basin, in contrast with historical data which show the boundary between Atlantic and Pacific subsurface water mass assemblies lying along the Lomonosov Ridge (Kinney et al. 1970; Gorshkov 1983; Moore et al. 1983; Jones and Anderson 1986; Anderson et al. 1994).

Relative to surface waters in the North Atlantic, surface waters in the North Pacific are fresher (due to greater runoff and net precipitation over evaporation in the North Pacific) and enriched in Ba (reflecting both increased runoff and the accumulation of

regenerated biogenic material in oceanic waters as they transit from Atlantic to Pacific). North Pacific waters entering the Arctic through Bering Strait become further freshened and enriched in Ba by fluvial discharge (Ba enhancement also results from upwelling in the Gulf of Anadyr) (Falkner et al. 1994). The extremely high Ba concentrations observed in the eastern side of Bering Strait in 1993 are associated with the Alaskan Coastal Current, which receives large amounts of fluvial discharge (primarily from the Yukon River) as it flows northward into the Arctic along the coast of Alaska (Coachman and Shigaev 1992).

Falkner et al. (1994) showed that biological activity is capable of severely depleting Ba in the surface waters of the Chukchi Sea (Ba concentrations as low as $12 \text{ nmol Ba L}^{-1}$ were observed in September 1992), resulting in the transport of Ba to deeper waters. In 1993, the high Ba concentrations observed in surface waters in Bering Strait and the southern Chukchi Sea did not extend continuously along the advective flow path northward over the shelf; this further demonstrates that Ba can be stripped from surface waters of the Chukchi Sea by the intense biological activity known to occur in the area during the summer (Coachman and Shigaev (1992), and references therein). The area of extreme surface Ba depletion in the vicinity of Wrangel Island and the Siberian coast was associated with very low surface salinity and elevated Ba concentrations in deeper waters (Figure 22b), suggesting the occurrence of a large plankton bloom in conjunction with seasonal increases in solar radiation and melting ice. Both the 1992 and 1993 Ba data suggest that removal of Ba from surface waters in association with the extremely high productivity over the Chukchi shelf outpaces advective delivery when the ice has retreated in the summer. The extent of removal is not as pronounced as it is for silicate, which approaches analytically undetectable levels over the Chukchi shelf.

Special attention must be given to the area north of the Alaskan coast in the vicinity of Barrow Canyon. Stations were occupied in this region on two different cruises in 1993: 12 stations were occupied between 13-14 August during the ARCRAD-93 cruise and 7 stations were occupied between 24-26 September during the HX174 cruise. At all stations

from both cruises located north of the Chukchi shelf break and the mouth of Barrow Canyon, the surface mixed layer was characterized by high Ba concentrations (mean values above $75 \text{ nmol Ba L}^{-1}$). But over Barrow Canyon itself, Ba concentrations in the surface mixed layer were quite different during the two cruises: mean values between 55 and 66 nmol Ba L^{-1} were observed at the ARCRAD-93 stations, and mean values between 71 and 87 nmol Ba L^{-1} were observed at the HX174 stations (note that the data collected at different times from the same area during these two cruises are averaged during the Barnes objective analysis, resulting in the appearance of intermediate values around $65 \text{ nmol Ba L}^{-1}$ over Barrow Canyon in Figure 24). While the values observed at the ARCRAD-93 stations are similar to those seen in other areas over the northern and central Chukchi shelf, the values observed at the HX174 stations are comparable to those seen in Bering Strait and the southern Chukchi Sea; this suggests that during the time in which the HX174 stations were occupied, the Alaska Coastal Current was transporting Ba-enriched surface waters directly into the Arctic interior in the vicinity of Barrow Canyon. Thus the observation of Ba-depleted surface waters over most of the Chukchi shelf in 1992 and 1993 does not rule out direct delivery of Ba associated with Bering inflow to the surface waters of the Arctic interior during certain times of the year.

Data collected along the AOS94 transect in summer 1994 further illustrate this point. In contrast to summer/fall conditions in 1992 and 1993, Ba-enriched surface waters were observed at all stations occupied over the Chukchi shelf and slope. This may be a direct result of the 50 year high in transport through Bering Strait (1.1 Sv) observed in the first 9 months of 1994 (Roach et al. 1995). The seasonal differences between sampling periods in the different years must also be taken into account. While most of the 1992 and 1993 stations in the Chukchi Sea were occupied between August and October, stations in the Chukchi Sea along the AOS94 transect were occupied in late July. In general, it must be remembered that the shelves of the Arctic's marginal seas are very complex, dynamic

regions subject to significant temporal variability, and that observations made during one particular interval of time do not necessarily represent conditions prevailing throughout the entire year.

We hypothesize that although waters entering the Arctic through Bering Strait (which includes the discharge from the Yukon River) may significantly contribute to the Ba inventory of surface waters in the Canada Basin during certain times of the year, much of the Ba contained in the Bering inflow is not delivered directly to the surface waters of the Arctic interior. In addition to the biologically mediated transfer of Ba from surface to deeper waters in the Chukchi and Bering seas described above, waters of Pacific origin flowing northward through Bering Strait in winter are generally more saline than surface waters covering the Canadian Basin and thus tend to enter the Arctic interior below the surface mixed layer (Coachman and Shigaev 1992; Weingartner et al. 1997). We therefore hypothesize that the Mackenzie River is the dominant source of the high Ba levels observed in the surface waters of the Canada Basin. The Mackenzie River is the fourth largest Arctic river in terms of discharge and the largest entering from North America (the average annual discharge of the Yukon River is only about 60% that of the Mackenzie River). The Mackenzie River is highly enriched in Ba; during a survey of Arctic rivers carried out between 1993 and 1996, Ba concentrations observed in the Mackenzie River were 5-20 times greater than those observed in any of the major Eurasian Arctic rivers (Guay and Falkner 1997). The notably high surface Ba concentrations and low surface salinity observed at the station north of the Beaufort slope in 1993 likely reflect the influence of the Mackenzie River.

A simplified mass balance provides a first-order test of this hypothesis. The surface area of the Canada Basin (not including the area over the Chukchi Cap and Arlis Plateau, where surface Ba concentrations were significantly lower than values over the rest of the Canada Basin) was estimated to be $1.36 \times 10^6 \text{ km}^2$. Values of 25 m (± 5 m estimated error) and $75 \text{ nmol Ba L}^{-1}$ ($\pm 5 \text{ nmol Ba L}^{-1}$ estimated error) were used for the

depth and mean Ba concentration of the surface mixed layer in the Canada Basin, resulting in an estimate of 2.6×10^9 moles ($\pm 0.7 \times 10^9$ moles, or 27% estimated error) for the Ba inventory of the surface mixed layer in the Canada Basin. A value of $515 \text{ nmol Ba L}^{-1}$ is taken for the effective end-member Ba concentration (i.e., accounting for estuarine desorption of Ba from riverborne clay particles (Boyle et al. 1974)) of the Mackenzie River (Guay and Falkner 1997). Multiplying this value by the average annual discharge of the Mackenzie River ($340 \text{ km}^3 \text{ yr}^{-1}$) results in an estimate of 1.75×10^8 moles Ba yr^{-1} for its annual delivery of Ba to the Arctic Ocean. Thus over a period of 10 years (the estimated residence time of surface waters in the Beaufort Gyre), the Mackenzie River can supply approximately 53-92% (with a best estimate of 68%) of the total Ba inventory of the surface mixed layer in the Canada Basin. The remainder of the Ba inventory can be supplied by a combination of North Pacific waters, discharge from other rivers (the Yukon River in particular), and vertical mixing. While fairly crude, the above calculation demonstrates that it is reasonable to consider the Mackenzie River as the dominant source of the elevated Ba levels observed in surface waters of the Canada Basin.

Various combinations of source waters could have produced the surface features observed in 1993 and 1994 over the Arlis Plateau and Mendeleyev Ridge and at AOS94 stations 26, 28 and 35. The local salinity minima and Ba maxima associated with these features suggest the influence of discharge from the Mackenzie and/or Eurasian Arctic rivers (although Eurasian Arctic rivers are low in Ba compared to the Mackenzie River, they are highly elevated in Ba relative to oceanic surface waters entering the Arctic from the North Atlantic and North Pacific (Guay and Falkner 1997)). The features also coincided with local maxima in vertically integrated dissolved C/N ratios (14.6-25.1) and normalized alkalinity ($2.43\text{-}2.50 \text{ meq L}^{-1}$) during the AOS94 transect; in addition, the most extreme maximum in vertically integrated DOC (121.58 g m^{-2}) observed during the AOS94 transect was observed at station 28 (C/N and DOC data from Wheeler et al. (1996); alkalinity data from E. P. Jones, personal communication). These chemical signatures provide further

evidence that the salinity minima resulted primarily from fluvial discharge. The features may indicate areas where shelf waters containing discharge from Eurasian rivers flow into the Arctic interior. Alternatively, the features may have occurred in areas where the Beaufort Gyre merges with the transpolar drift flowing toward Fram Strait, thus reflecting contributions from both the Mackenzie and Eurasian Arctic rivers.

Ignoring ice-melt, we examined linear combinations of end-members representing Atlantic inflow, Pacific inflow and fluvial discharge capable of reproducing the salinity and Ba concentrations of the features (Table 3). Waters with the physical and chemical properties of the features could result from a mixture containing 86-92% of the Atlantic end-member and 8-14% of a fluvial end-member with Ba concentration between 179 and 319 nmol Ba L⁻¹; or from a mixture containing 91-98% of the Pacific end-member and 2-9% of a fluvial end-member with Ba concentration between 60 and 1025 nmol Ba L⁻¹. For most of these combinations, the required fluvial end-members had Ba concentrations between 100 and 515 nmol Ba L⁻¹ and can therefore represent mixtures of discharge from both the Mackenzie and Eurasian Arctic rivers. While this exercise demonstrated that combinations of Pacific and Atlantic inflow and fluvial discharge could have given rise to the surface features observed in 1993 and 1994, the limitations of a mixing model based solely on salinity and Ba are readily apparent. Additional oceanographic tracers must be incorporated to simultaneously account for Atlantic and Pacific inflow, ice-melt, and discharge from the Mackenzie and Eurasian Arctic rivers and to explicitly determine their relative contributions to Arctic circulation. In particular, adding Ba to mass balances based on salinity, $\delta^{18}\text{O}$, and silicate (which have been used by Schlosser et al. (1994) and Bauch et al. (1995) to distinguish between Atlantic, Pacific, ice-melt and fluvial components of Arctic surface and halocline waters) would allow the fluvial component of Arctic circulation to be resolved into separate contributions from the Mackenzie River and Eurasian Arctic rivers.

Table 3a: Salinity and Ba concentrations of source waters to the upper Arctic

Source	Salinity	Ba concentration (nmol Ba L ⁻¹)
Atlantic	34.9 ^a	42-45
Pacific	32.5-33.0 ^b	50-60
Mackenzie River	0	515 ^c
Eurasian rivers	0	100-200 ^c
Sea-ice melt	3	≤ 5 ^d

^aSchlosser et al., 1994

^bCoachman and Shigaev, 1992

^cGuay and Falkner, 1997

^dWagner and Falkner, unpublished data

Table 3b: Salinity and Ba concentrations in the surface features observed in 1993 and 1994

	Salinity	Ba concentration (nmol Ba L ⁻¹)
Feature over the Arlis Plateau and Mendeleyev Ridge (1993 and 1994)	30.0-31.0	65-70
Features at AOS94 stations 26, 28 and 35	31.0-32.0	60-65

4.3.2 Upper halocline

In 1993, upper halocline waters with high mean Ba concentrations ($> 65 \text{ nmol Ba L}^{-1}$) were separated from upper halocline waters with low mean Ba concentrations ($< 50 \text{ nmol Ba L}^{-1}$) by a front lying roughly between the Canada and Makarov basins (Figure 25). Along the AOS94 transect, the upper halocline between the Chukchi shelf and the Arlis Plateau is marked by high Ba concentrations ($65\text{-}75 \text{ nmol Ba L}^{-1}$) and a subsurface Ba maximum occurring at depths between 50 and 200 m; beyond the Arlis Plateau, waters with upper halocline temperature and salinity characteristics had Ba concentrations $< 60 \text{ nmol Ba L}^{-1}$ (Figure 27). These observations demonstrate that upper halocline waters characterized by elevated Ba concentrations are confined to the Canadian Basin and are chemically distinct from waters with similar temperature and salinity properties in the Eurasian Basin, suggesting that different mechanisms lead to the formation of halocline waters in the different sectors of the Arctic. The limit of the Ba-enriched upper halocline waters along the AOS94 transect approximately coincided with the location of the boundary between high-Ba and low-Ba upper halocline waters observed in the same area in 1993. The position of the front between the two types of upper halocline waters observed in both 1993 and 1994 provides further evidence that the boundary between subsurface water masses of Atlantic and Pacific character has shifted from its historically defined position along the Lomonosov Ridge to a position more closely aligned with the Mendeleyev and Alpha ridges (Carmack et al. 1995; McLaughlin et al. 1996; Morison et al. 1997).

The Ba maximum and the related nutrient maxima and oxygen minimum (Jones and Anderson 1990; Jones et al. 1991; Falkner et al. 1994) which characterize the upper halocline in the Canada Basin suggest sources in the Chukchi and Beaufort seas, and that the mechanism by which these waters are formed is linked with the influx of water through Bering Strait. As was demonstrated in the previous discussion of the surface mixed layer, salinity and Ba data alone are not sufficient for quantitatively determining contributions to the Arctic halocline from different source waters.

4.3.3 Lower halocline

Data from the Eurasian Arctic suggest that the lower halocline achieves its NO levels in the Barents Sea and adjoining Nansen Basin over several seasons (Rudels et al. 1996). Under the proposed scenario, biological productivity depletes nutrients in surface waters and much of the oxygen produced during photosynthesis becomes lost to the atmosphere. Deep convection occurring in the winter drives the surface NO signature to the depth of the lower halocline. As these waters advect under the ice and toward the Siberian seas, further deep convection is inhibited by capping with fresher waters influenced by the large Eurasian Arctic rivers (Rudels et al. 1996). It has been noted that the NO minimum in the Canadian sector of the Arctic is accompanied by higher temperatures and silicate concentrations than in the Eurasian sector (Salmon and McRoy 1994). Because the NO parameter appeared to remain roughly constant at the few stations occupied in the Canadian Arctic, it was presumed that only small volumes of renewal waters were responsible for the altered temperature and salinity characteristics (Salmon and McRoy 1994; Rudels et al. 1996). In at least one instance, altered lower halocline waters have been found to have a somewhat lower NO signal than unaltered lower halocline water, suggesting that the lower halocline layer can be the recipient of significant additional input as it advects from its supposed region of origin in the Barents toward the Arctic interior (McLaughlin et al. 1996).

The general trends of increasing NO and decreasing Ba concentration observed in the lower halocline along the AOS94 transect (Figure 28) provide further evidence that lower halocline waters are influenced by contributions from additional sources (such as dense shelf waters formed in association with freezing and brine rejection) as they transit from Eurasian to Canadian sectors of the Arctic. Analogous to the situation in the upper halocline, elevated Ba in the lower halocline in the Canada Basin suggests contributions from sources in the Chukchi and Beaufort seas. The low NO in the lower halocline in the

Canada Basin may result from denitrification thought to be occurring in association with biological activity over the highly productive Bering, Chukchi and East Siberian shelf regions (Codispoti et al. 1991).

5. CONCLUSIONS

The Mackenzie River is highly elevated in Ba relative to the major Eurasian Arctic rivers. Despite complex modification in the mixing zones between riverine and oceanic waters, riverine Ba signals extend beyond the shelves of the Arctic seas. Quasi-synoptic Ba distributions in the Arctic in 1993 and 1994 show that the surface mixed layer reflects the pronounced differences which exist between Ba concentrations in various source waters. Below the surface layer, Ba distributions delineate the present lateral extent of the nutrient-enriched upper halocline layer in the Canadian sector of the Arctic, confirm its general source region in the Chukchi and Beaufort seas, and show it to be discontinuous with waters of similar temperature and salinity properties that outcrop in the Eurasian Basin. Data from the 1994 Arctic Ocean Section suggest that lower halocline waters, which are established in the Eurasian sector of the Arctic, continue to be imprinted by shelf processes as they transit to the Canadian sector.

In future work, applying multivariate analysis techniques to combined tracer data sets (salinity, $\delta^{18}\text{O}$, alkalinity, Si, Ba, etc.) will allow more quantitative mapping of components contributing to stratification of the upper Arctic and thus reveal circulation patterns in its sublayers. In particular, Ba shows unique promise for distinguishing between North American and Eurasian riverine components of oceanic in within the Arctic. In addition to addressing questions about circulation in the Arctic Ocean and its links to global oceanic circulation and climate, the ability to track river waters from different sources will yield insight into the transport and fate of pollutants (e.g. organic compounds, heavy metals, radionuclides) released into river and shelf waters of the Arctic.

BIBLIOGRAPHY

- Aagaard, K., and E. C. Carmack. "The role of sea ice and other fresh water in the Arctic circulation." *J. Geophys. Res.* 94, no. C10 (1989): 14,485-14,498.
- Aagaard, K., L. K. Coachman, and E. C. Carmack. "On the halocline of the Arctic Ocean." *Deep-Sea Res.* 28 (1981): 529-545.
- Aagaard, K., and P. Greisman. "Toward new mass and heat budgets for the Arctic Ocean." *J. Geophys. Res.* 80 (1975): 3821-3827.
- Aagaard, K., and A. T. Roach. "Arctic Ocean-Shelf exchange: Measurements in Barrow Canyon." *J. Geophys. Res.* 95, no. C10 (1990): 18163-18175.
- Anderson, L. G., G. Björk, O. Holby, E. P. Jones, G. Kattner, K. P. Koltermann, B. Liljeblad, R. Lindgren, B. Rudels, and J. Swift. "Water masses and circulation in the Eurasian Basin: Results from the Oden 91 Expedition." *J. Geophys. Res.* 99 (1994): 3273-3283.
- Anderson, L. G., K. Olsson, and A. Skoog. "Distribution of dissolved inorganic and organic carbon in the Eurasian Basin of the Arctic Ocean." In *The Polar Oceans and Their Role in Shaping the Global Environment*, edited by O. M. Johannessen, R. D. Muench and J. E. Overland, 255-262. Washington DC, 1994.
- Bacon, M. P., and J. M. Edmond. "Barium at GEOSECS III in the Southwest Pacific." *Earth Planet. Sci. Lett.* 16 (1972): 66-74.
- Barnes, S. L. "Mesoscale Objective Map Analysis Using Weighted Time-Series Observations." Norman, OK: U.S. Department of Commerce, National Oceanic and Atmospheric Administration, National Severe Storms Laboratory, 1973.
- Bauch, D., P. Schlosser, and R. Fairbanks. "Freshwater balance and sources of deep and bottom water in the Arctic Ocean inferred from the distribution of $H_2^{18}O$." *Prog. in Oceanogr.* 35 (1995): 53-80.
- Belaglazova, V. N., V. Y. Mikhailenko, and T. P. Filatova. "Rossiya i sopredelnye gosudarstva." Moscow: Fed. Sluzh. Geodezii i Kartografii Rossii, 1994.
- Bernstein, R. E., R. H. Byrne, P. R. Betzer, and A. M. Greco. "Morphologies and transformations of celestite in seawater: The role of acantharia in strontium and barium geochemistry." *Geochim. Cosmochim. Acta* 56 (1992): 3273-3279.
- Bishop, J. K. B. "The barite-opal-organic carbon association in oceanic particulate matter." *Nature* 332 (1988): 341-343.
- Bogdanov, N. A., and S. M. Tilman. "Tectonics and Geodynamics of Northeastern Asia." Moscow: Inst. of the Lithosphere, Russian Academy of Sciences Circum-Pacific Council for Energy and Mineral Resources, 1993.
- Boyd, T. J., and E. A. D'Asaro. "Cooling of the West Spitsbergen Current: Wintertime observations west of Svalbard." *J. Geophys. Res.* 99, no. C11 (1994): 22596-22618.

Boyle, E., R. Collier, A. T. Dengler, J. M. Edmond, A. C. Ng, and R. F. Stallard. "On the chemical mass-balance in estuaries." *Geochim. Cosmochim. Acta* 38 (1974): 1719-1728.

Broecker, W. S. "'NO", A conservative water-mass tracer." *Earth Planet. Sci. Lett.* 23 (1974): 100-107.

Carmack, E. C. "Large-Scale Physical Oceanography of Polar Oceans." In *Polar Oceanography, Part A: Physical Science*, edited by W. O. Smith, 171-222. San Diego: Academic Press, 1990.

Carmack, E. C., R. W. Macdonald, and J. E. Papadakis. "Water Mass Structure and Boundaries in the Mackenzie Shelf Estuary." *J. Geophys. Res.* 94, no. C12 (1989): 18,043-18,055.

Carmack, E. C., R. W. Macdonald, R. G. Perkin, F. A. McLaughlin, and R. J. Pearson. "Evidence for warming of Atlantic water in the southern Canadian Basin of the Arctic Ocean: Results from the Larsen-93 expedition." *Geophys. Res. Lett.* 22, no. 9 (1995): 1061-1064.

Carroll, J., K. Kenison Falkner, E. T. Brown, and W. S. Moore. "The role of sediments in maintaining high dissolved ^{226}Ra and Ba in the Ganges-Bramaputra mixing zone." *Geochim. Cosmochim. Acta* 57 (1993): 2981-2990.

Carson, M. A. "Mackenzie Delta sediment regime." Unpublished manuscript, Inland Water Directorate, Yellowknife, NWT, 1994.

Cavalieri, D. J., and S. Martin. "The contribution of Alaskan, Siberian, and Candian coastal polynyas to the cold halocline of the Arctic Ocean." *J. Geophys. Res.* 99 (1994): 18343-18362.

Chan, L. H., D. Drummond, J. M. Edmond, and B. Grant. "On the barium data from the Atlantic GEOSECS Expedition." *Deep-Sea Res.* 24 (1977): 613-649.

Coachman, L. K., and K. Aagaard. "Physical oceanography of the Arctic and Subarctic seas." In *Marine Geology and Oceanography of the Arctic Seas*, edited by Y. Herman, 1-72. New York: Springer-Verlag, 1974.

Coachman, L. K., and K. Aagaard. "Transports through Bering Strait: Annual and interannual variability." *J. Geophys. Res.* 93, no. C12 (1988): 15,535-15,539.

Coachman, L. K., and V. V. Shigaev. "Northern Bering-Chukchi Sea ecosystem: The physical basis." In *Results of the Third Joiont US-USSR Bering and Chukchi Seas Expedition (BERPAC), Summer 1988*, edited by P. A. Nagel, 17-27. Washington D.C.: US Fish and Wildlife Service, 1992.

Codispoti, L. A., G. E. Friederich, C. M. Sakamoto, and L. I. Gordon. "Nutrient cycling and primary production in the marine systems of the Arctic and Antarctic." *Journal of Marine Systems* 2 (1991): 359-384.

Collier, R., and J. Edmond. "The trace element geochemistry of marine biogenic particulate matter." *Prog. Oceanog.* 13 (1984): 113-199.

Colony, R., and A. S. Thorndike. "Sea ice motion as a drunkard's walk." *J. Geophys. Res.* 90, no. C1 (1985): 965-974.

Dai, M. H., and J. M. Martin. "First data on trace metal level and behaviour in two major Arctic river-estuarine systems (Ob and Yenisey) and in the adjacent Kara Sea, Russia." *Earth and Planetary Science Letters* 131 (1995): 127-141.

Dawson, K. M. "Regional Metallogeny of the Northern Cordillera." *Report of Activities, Part A: Geological Survey of Canada*, 1977.

Dawson, K. R. "Barite, Fluorite, and Celestite Deposits and Occurrences in Canada." *Report of Activities, Part A*, 257-259: Geological Survey of Canada, 1975.

Dehairs, F., R. Chesselet, and J. Jedwab. "Discrete suspended particles of barite and the barium cycle in the open ocean." *Earth Planet. Sci. Lett.* 49 (1980): 528-550.

Dehairs, F., C. E. Lambert, R. Chesselet, and N. Risler. "The biological production of marine suspended barite and the barium cycle in the Western Mediterranean Sea." *Biogeochem.* 4 (1987): 119-139.

Dymond, J., E. Suess, and M. Lyle. "Barium in deep-sea sediment: A geochemical proxy for paleoproductivity." *Paleoceanogr.* 7, no. 2 (1992): 163-181.

Edmond, J. M., E. D. Boyle, D. Drummond, B. Grant, and T. Mislick. "Desorption of barium in the plume of the Zaire (Congo) River." *Neth. J. Sea Res.* 12 (1978): 324-328.

Edmond, J. M., C. Measures, R. E. McDuff, L. H. Chan, R. Collier, B. Grant, L. I. Gordon, and J. B. Corliss. "Ridge crest hydrothermal activity and the balances of the major and minor elements in the ocean: The Galapagos data." *Earth Planet. Sci. Lett.* 46 (1979): 1-18.

Falkner, K. Kenison, G. Klinkhammer, T.S. Bowers, J. F. Todd, B. Lewis, W. Landing, and J. M. Edmond. "The behavior of Ba in anoxic marine waters." *Geochim. Cosmochim. Acta* 57, no. 3 (1993): 537-554.

Falkner, K. Kenison, R. W. MacDonald, E. C. Carmack, and T. Weingartner. "The potential of barium as a tracer of Arctic water masses." In *The Polar Oceans and Their Role in Shaping the Global Environment: The Nansen Centennial Volume*, AGU Geophys. Monograph Series, edited by O. M. Johannessen, R. D. Muench and J. E. Overland, 63-76. Washington DC: AGU Books, 1994.

Fissel, D. B., D. D. Lemon, H. Melling, and R. A. Lake. *Non-tidal flows in the Northwest Passage*. Vol. 98, *Can. Tech. Rep. Hydrogr. Ocean Sci.* Sidney, BC: Inst. of Ocean Sci., 1988.

Fresnel, J., P. Galle, and P. Gayral. "Resultats de la microanalyse des cristaux vacuolaires chez deux Chromophytes unicellulaires marines: *Exanthemachrysis gayraliae*, Pavlova sp. (Prymnesiophycees, Pavlovacees)." *C. R. Acad. Sc. Paris* 288, no. Serie D (1979): 823-825.

Gloerson, P., W. J. Campbell, D. J. Cavalieri, J. C. Comiso, C. L. Parkinson, and H. J. Zwally. "Arctic and Antarctic sea ice, 1978-1987, Satellite passive-microwave observations and analysis." *NASA SP-511* (1992): 290 pp.

- Goldberg, E. D., and G. O. S. Arrhenius. "Chemistry of Pacific pelagic sediments." *Geochim. Cosmochim. Acta* 13 (1958): 153-212.
- Gordeev, V. V., J. M. Martin, I. S. Sidorov, and M. V. Sidorova. "A reassessment of the Eurasian river input of water, sediment, major elements and nutrients to the Arctic Ocean." *Am. J. Sci.* in press (1995).
- Gorshkov, S. G., ed. *World Ocean Atlas, Arctic Ocean*. Vol. 3. New York: Pergammon, 1983.
- Guay, C. K., and K. Kenison Falkner. "Dissolved barium in Arctic rivers and marginal seas: implications for tracing river waters in the Arctic interior." *Cont. Shelf. Res.* submitted (1997).
- Hanor, J. S., and L-H. Chan. "Non-conservative behavior of barium during mixing of Mississippi River and Gulf of Mexico waters." *Earth Planet. Sci. Lett.* 37 (1977): 242-250.
- Hanzlick, D., and K. Aagaard. "Freshwater and Atlantic water in the Kara Sea." *J. Geophys. Res.* 85 (1980): 4937-4942.
- Jones, E. P., and L. G. Anderson. "On the origin of the chemical properties of the Arctic Ocean halocline." *J. Geophys. Res.* 91 (1986): 10,759-10,767.
- Jones, E. P., and L. G. Anderson. "On the origin of the properties of the Arctic Ocean halocline north of Ellesmere island: results from the Canadian Ice Island." *Continental Shelf Res.* 10, no. 5 (1990): 485-498.
- Jones, E. P., L. G. Anderson, and D. W. R. Wallace. "Tracers of near-surface, halocline and deep waters in the Arctic Ocean: Implications for circulation." *J. Mar. Sys.* 2 (1991): 241-255.
- Key, R. M., R. S. Stallard, W. S. Moore, and J. L. Sarmiento. "Distribution and flux of ^{226}Ra and ^{228}Ra in the Amazon River Estuary." *J. Geophys. Res.* 90 (1985): 6995-7004.
- Kinney, P., M. E. Arhelger, and D. C. Burrell. "Chemical characteristics of water masses in the Amerasian Basin of the Arctic Ocean." *J. Geophys. Res.* 75 (1970): 4097-4104.
- Klinkhammer, G. P., and L. H. Chan. "Determination of barium in marine waters by isotope dilution inductively coupled plasma mass spectrometry." *Analyt. Chim. Acta* 232 (1990): 323-329.
- Koch, S. E., M. DesJardins, and P. J. Kocin. "An interactive Barnes objective map analysis scheme for use with satellite and conventional data." *J. Climate Appl. Meteor.* 22, no. 9 (1983): 1487-1503.
- Lea, D. W. "Foraminiferal and coralline barium as paleoceanographic tracers." PhD, MIT/WHOI, WHOI-90-06, 1990.
- Létolle, R., J. M. Martin, A. J. Thomas, V. V. Gordeev, S. Gusarova, and I. Sidorov. " ^{18}O abundance and dissolved silicate in the Lena delta and Laptev Sea (Russia)." *Mar. Chem.* 43 (1993): 47-64.

Li, Y-H., and L. H. Chan. "Desorption of Ba and ^{226}Ra from riverborne sediments in the Hudson Estuary." *Earth Planet. Sci. Lett.* 43 (1979): 343-350.

Martin, J-M., and M. Meybeck. "Elemental mass-balance of material carried by major world rivers." *Mar. Chem.* 7 (1979): 173-206.

Macdonald, R. W. and J. M. Bowers. "Contaminants in the arctic marine environment: priorities for protection." *ICES J. Mar Sci.* 53 (1996): 537-563.

Mackenzie River Basin Committee, *Mackenzie River basin study report*, 1981.

McCrossan, R. G., and R. D. Glaister, eds. *Geological History of Western Canada*. 2nd ed. Alberta: Alberta Society of Petroleum Geologists, 1966.

McLaughlin, F. A., E. C. Carmack, R. W. Macdonald, and J. K. B. Bishop. "Physical and geochemical properties across the Atlantic/Pacific water mass front in the southern Canadian Basin." *J. Geophys. Res.* 101, no. C1 (1996): 1183-1197.

Milliman, J. D., and R. H. Meade. "World-Wide Delivery of River Sediment to the Oceans." *J. Geology* 91, no. 1 (1983): 1-21.

Milliman, J. D., and P. M. Syvitski. "Geomorphic/Tectonic Control of Sediment Discharge to the Ocean: The Importance of Small Mountainous Rivers." *J. Geology* 100 (1992): 525-544.

Moore, R. M., M. G. Lowings, and F. C. Tan. "Geochemical profiles in the Central Arctic Ocean: Their relation to freezing and shallow circulation." *J. Geophys. Res.* 88 (1983): 2667-2674.

Moore, W. S. "The effects of groundwater input at the mouth of the Ganges-Brahmaputra rivers on barium and radium fluxes to the Bay of Bengal." *Geochemica et Cosmochemica Acta* in press (1996).

Morison, J., M. Steele, and R. Anderson. "Hydrography of the upper Arctic Ocean measured from the nuclear submarine USS Pargo." *Deep-Sea Res.* (1997): in press.

Morrow, D. W., H. R. Krouse, E. D. Ghent, G. C. Taylor, and K. R. Dawson. "A hypothesis concerning the origin of barite in Devonian carbonate rocks of northeastern British Columbia." *Canadian Journal of Earth Sciences* 15, no. 9 (1978): 1391-1406.

Muench, R. D. *The physical oceanography of the northern Baffin Bay region*. Vol. 1, *Baffin Bay North Water Proj. Sci. Rep.* Montreal: Arctic Inst. of N. America, 1971.

Nalivkin. *The Geology of the U.S.S.R.: A Short Outline*. Translated by Tomkeieff, S. I. New York: Pergamon Press, 1960.

Östlund, H. G. "The residence time of the freshwater component in the Arctic Ocean." *J. Geophys. Res.* 87, no. C3 (1982): 2035-2043.

Östlund, H. G., and G. Hut. "Arctic Ocean water mass balance from isotope data." *J. Geophys. Res.* 89, no. C4 (1984): 6373-6381.

- Östlund, H. G., and G. Hut. "Arctic Ocean water mass balance from isotope data." *J. Geophys. Res.* 89 (1984): 6373-6381.
- Parfenov, L. M. "Accretionary History of Northeast Asia." Paper presented at the 1992 International Conference on Arctic Margins, Anchorage, AK 1994.
- Pavlov, V. K., L. A. Timokhov, G. A. Baskakov, M. Yu. Kulakov, V. K. Kurazhov, P. V. Pavlov, S. V. Pivovarov, and V. V. Stanovoy. "Hydrometeorological Regime of the Kara, Laptev, and East-Siberian Seas." . Seattle: Applied Physics Laboratory, University of Washington, 1996.
- Reeder, S. W., B. Hitchon, and A. A. Levinson. "Hydrogeochemistry of the surface waters of the Mackenzie River drainage basin, Canada-I. Factors controlling the inorganic composition." *Geochim. Cosmochim. Acta* 36 (1972): 825-865.
- Revelle, R. R. *Marine bottom samples collected in the Pacific Ocean by the Carnegie on its seventh cruise*. Vol. 556. Washington, D.C.: Publ. Carn. Inst., 1944.
- Revelle, R. R., M. Bramlette, G. Arrhenius, and E. D. Goldberg. "Pelagic sediments in the Pacific." *Spec. Paper Geol. Soc. America* 62 (1955): 221-236.
- Rigor, I. "Arctic ocean buoy program." *ARCOS Newslett.* 44 (1992): 1-3.
- Roach, A. T., K. Aagaard, C. H. Pease, S. A. Salo, T. Weingartner, V. Pavlov, and M. Kulakov. "Direct measurements of transport and water properties through the Bering Strait." *J. Geophys. Res.* 100, no. C9 (1995): 18,443-18,457.
- Rudels, B. "The outflow of polar water through the Arctic Arcipelago and the oceanographic conditions in Baffin Bay." *Polar Res.* 4 (1986): 161-180.
- Rudels, B., L. G. Anderson, and E. P. Jones. "Formation and evolution of the surface mixed layer and halocline of the Arctic Ocean." *J. Geophys. Res.* 101, no. C4 (1996): 8807-8821.
- Rundkvist, D. V., and F. P. Mitrofanov, eds. *Precambrian Geology of the USSR*. Elsevier: Amsterdam, 1993.
- Salmon, D. K., and C. P. McRoy. "Nutrient-based tracers in the Western Arctic: A new lower halocline water defined." In *The Polar Oceans and Their Role in Shaping the Global Environment*, edited by O. M. Johannessen, R. D. Muench and J. E. Overland, 47-62. Washington DC: AGU, 1994.
- Schlosser, P., D. Bauch, R. Fairbanks, and G. Bönisch. "Arctic river runoff: mean residence time on the shelves and in the halocline." *Deep-Sea Res.* I 41 (1994): 1053-1068.
- Schlosser, p., G. Bonisch, B. Kromer, K. O. Munnich, and K. P. Koltermann. "Ventilation rates of the waters in the Nansen Basin of the Arctic Ocean derived by a multi-tracer approach." *J. Geophys. Res.* 95 (1990): 3265-3272.
- Schlosser, P., J. H. Swift, D. Lewis, and S. L. Pfirman. "The role of the large-scale Arctic Ocean circulation in the transport of contaminants." *Deep-Sea Res. II* 42, no. 6 (1995): 1341-1367.

Select Committee on Intelligence, *Radioactive and other environmental threats to the United States and the Arctic resulting from past Soviet activities*. Washington, United States Senate, 1993.

Steele, M., and J. H. Morison. "Halocline water formation in the Barents Sea." *J. Geophys. Res.* 100, no. C1 (1995): 881-894.

Steele, M., D. Thomas, and D. Rothrock. "A simple model study of the Arctic Ocean freshwater balance, 1979-1985." *J. Geophys. Res.* 101, no. C9 (1996): 20,833-20,848.

Stone, D. B., S. C. Crumley, and L. M. Parfenov. "Paleomagnetism and the Kolyma Structural Loop." 1992 International Conference on Arctic Margins, Anchorage, AK 1994.

Telang, S. A., R. Pocklington, A. S. Naidu, E. A. Romankevich, I. I. Gitelson, and M. I. Gladyshev. "Carbon and Mineral Transport in Major North American, Russian Arctic, and Siberian Rivers: the St. Lawrence, the Mackenzie, the Yukon, the Arctic Alaskan Rivers, the Arctic Basin Rivers in the Soviet Union, and the Yenisei." In *Biogeochemistry of Major World Rivers*, edited by E. T. Degens, S. Kempe and J. E. Richey, 356. Chichester: John Wiley & Sons, 1991.

Thorndike, A. S., and R. Colony. "Sea ice motion in response to geostrophic winds." *J. Geophys. Res.* 87, no. C8 (1982): 5845-5852.

Treshnikov, A. F. *Atlas Arktiki*. Moscow: Arkt.-Antarkt. Nauch.-Issled. Inst., 1985.

Turekian, K. K., and E. H. Tausch. "Barium in deep sediments of the Atlantic Ocean." *Nature* 201 (1964): 696-697.

UNESCO. "World water balance and water resources of the Earth." Stud. Rep. Hydrol., No. 25, 1978.

UNESCO. "Algorithms for computation of fundamental properties of seawater." UNESCO technical papers in marine science, 1983.

Von Damm, K. L. "Seafloor hydrothermal activity: Black smoker chemistry and chimneys." *Annu. Rev. Earth Planet. Sci.* 18 (1990): 173-204.

Von Damm, K. L., J. M. Edmond, B. Grant, C. I. Measures, B. Walden, and R. F. Weiss. "Chemistry of submarine hydrothermal solutions at 21°N, East Pacific Rise." *Geochim. Cosmochim. Acta* 49 (1985): 2197-2220.

Wallace, D. W. R., R. M. Moore, and E. P. Jones. "Ventilation of the Arctic Ocean cold halocline; Rates of diapycnal and isopycnal transport, oxygen utilization and primary production inferred using chlorofluoromethane distributions." *Deep-Sea Res.* 34 (1987): 1957-1979.

Wallace, D. W. R., P. Schlosser, M. Krysell, and G. Bönisch. "Halocarbon and tritium/³He dating of water masses in the Nansen Basin of the Arctic Ocean." *Deep-Sea Res.* 39 (1992): S435-S458.

Weingartner, T. J., D. J. Cavalieri, K. Aagaard, and Y. Sasaki. "Circulation, dense water formation, and outflow on the northeast Chukchi shelf." *J. Geophys. Res.* submitted (1997).

Wheeler, P. A., J. M. Watkins, and R. L. Hansing. "Distributions of nutrients and organic carbon and nitrogen in the Arctic Ocean: Implications for the sources of dissolved organic carbon." *Deep-Sea Res.* submitted (1996).

Wilson, C., and D. W. R. Wallace. "Using the nutrient ratio NO/PO as a tracer of continental shelf waters in the central Arctic Ocean." *J. Geophys. Res.* 95, no. C12 (1990): 22,193-22,208.